

The Role of Innate Lymphoid Cells in Pulmonary Viral Infection and Allergic Inflammation

By

Matthew T. Stier

Dissertation

Submitted to the Faculty of the
Graduate School of Vanderbilt University
in partial fulfillment of the requirements
for the degree of

DOCTOR OF PHILOSOPHY

in

Microbiology and Immunology

August 31, 2017

Nashville, Tennessee

Approved:

R. Stokes Peebles Jr., M.D. (Thesis Advisor)

Mark Boothby, M.D. Ph.D. (Chair)

William Lawson, M.D.

Peggy Kendall, M.D.

John Williams, M.D.

Eric Sebzda, Ph.D.

Copyright © 2017 by Matthew T. Stier
All Rights Reserved

ACKNOWLEDGMENTS

Significant investment by my mentors, colleagues, and collaborators has been essential to the advancement of my education, the progression of my scientific investigations, and the composition of this dissertation.

Foremost, I am incredibly grateful for the mentorship of my dissertation advisor, Dr. R. Stokes Peebles, Jr. Over the past four years, his scientific curiosity, deep knowledge, and enthusiasm have molded my own passions and pursuits. He has provided extensive intellectual support, career guidance, and technical assistance that have bolstered my scientific development. It is with great pleasure that I consider Dr. Peebles among my most significant mentors, and I am thankful for all of his contributions. The work contained herein is a testament to his guidance.

My Thesis Advisory Committee has also been essential to my professional development. I am grateful to Dr. Mark Boothby (Chair), Dr. Eric Sebzda, Dr. John Williams, Dr. Peggy Kendall, and Dr. William Lawson for their expertise, critical analysis, and support. Their fingerprints can be found all throughout my dissertation.

Moreover, many collaborators have made the work in this dissertation possible. I am sincerely thankful for the intellectual, technical, and material support provided by the following: Dr. Martin Moore for productive discussions and RSV clinical isolates; Dr. Tina Hartert for scientific mentorship and the collection of RSV clinical isolates; Dr. Kelli Boyd for scoring our histopathology; Dr. Lan Wu for assistance with parabiosis experiments; Dr. Baohua Zhou for providing us with *Tslpr*^{-/-} mice; Dr. Andrew McKenzie for helpful commentary and for providing us with *Il33*^{-/-} and *St2*^{-/-} mice; and Dr. Jay Kolls and Dr. Kong Chen for assistance in performing

in vivo IL-23 depletions; and to all of the rest who have made contributions large or small, I am incredibly appreciative.

Thank you to my colleagues in the Peebles lab, past and present. Shinji, Kasia, Mark, Jian, Melissa, Weisong, Marc, Sara, and Dan—I am grateful for all of your support and encouragement. I have countless meaningful memories from my time in lab spent with you all; you have challenged me to grow personally and professionally, and for that I am thankful. I am similarly grateful to my colleagues across the hall—Dr. Dawn Newcomb, who has been a driving intellectual force behind and a consistent supporter of my work, as well as the rest of the Newcomb lab—Hubaida and Jacky.

I am also grateful for my scientific families over the years, dating back to my first experiences in the lab of Dr. Gurjit Hershey that helped stimulate my passion for science to my evolution as a scientist in the lab of Dr. Kathy Spindler during my undergraduate education. You both continue to be gracious supporters of my career, and I will always be thankful for what you have done for me.

Finally, thank you to all of my friends and family who have supported me over the years and have helped me advance towards my goals. Mom and Dad, you have championed my dreams and thrown all of your effort behind helping me to achieve them, and the work presented herein is the direct realization of your investment in me. I am truly grateful for everything you have done. To my dearest friends, and to Rachel—you have all stood beside me when experiments have gone my way, but also when they haven't. You have supported me, challenged me, and helped me grow as a person and a scientist. I am forever thankful.

TABLE OF CONTENTS

	Page
ACKNOWLEDGMENTS	iii
LIST OF TABLES	viii
LIST OF FIGURES	ix
Chapter	
1. Introduction.....	1
1.1. Overview	1
1.2. Scope and Rationale	1
2. Background.....	4
2.1. Allergy, Asthma, and Viral Infections	4
2.1.1. Epidemiology.....	5
2.1.2. Viral Infections and Asthma.....	6
2.1.3. Immunologic Response in Asthma and Allergy.....	8
2.2. Overview of Innate Lymphoid Cells	10
2.3. ILC Development and Tissue Composition	10
2.4. ILC2 Function, Homeostasis, and Disease.....	13
2.4.1. Activators and Inhibitors of ILC2	13
2.4.2. ILC2 Tissue Maintenance and Trafficking.....	15
2.4.3. ILC2 Mechanisms of Pathogenesis in Allergic Disease.....	19
2.4.4. ILC2 in Human Disease	25
2.5. ILC1 Function, Homeostasis, and Disease.....	28
2.6. ILC3 Function, Homeostasis, and Disease.....	30
2.7. ILC Plasticity.....	32
2.8. Summary	33
3. RSV Infection Activates IL-13-producing ILC2 via TSLP	34
3.1. Introduction	34
3.2. Methods	36
3.2.1. Virus and Mice	36
3.2.2. ELISA	37
3.2.3. Flow Cytometry	38
3.2.4. <i>In Vivo</i> TSLP Neutralization	39
3.2.5. BAL and PAS Staining.....	39
3.2.6. Corticosteroid Treatment.....	40
3.2.7. Airway Reactivity	40
3.2.8. Viral Load.....	41

3.2.9. Statistical Analysis	41
3.3. Results	42
3.3.1. RSV Infection Increases Lung IL-13 and the Number of IL-13 ⁺ ILC2 at Day 4 Post-Infection.....	42
3.3.2. TSLP is necessary for the RSV-induced ILC2 response.....	48
3.3.3. TSLPR-deficient mice have increased IL-13, mucus, and reactivity in the airways following RSV infection	55
3.3.4. Multiple pathogenic clinical isolates of RSV induce IL-13-producing ILC2 TSLP...	61
3.4. Discussion	64
4. STAT1 Represses ILC2 and ILC3 during Respiratory Viral Infection	69
4.1. Introduction	69
4.2. Methods.....	71
4.2.1. Mice.....	71
4.2.2. RSV Infection and Viral Titer	72
4.2.3. Flow Cytometry.....	72
4.2.4. ELISA.....	75
4.2.5. Quantitative PCR.....	75
4.2.6. Bronchoalveolar Lavage (BAL)	76
4.2.7. Periodic acid-Schiff (PAS) Staining.....	76
4.2.8. Bone Marrow Chimeras.....	77
4.2.9. IL-23p19 Neutralization	77
4.2.10. Statistics.....	77
4.3. Results	79
4.3.1. ILC and their Cytokine Products are Dysregulated in <i>Stat1</i> ^{-/-} Mice During Viral Infection.....	79
4.3.2. Cell-Intrinsic and Cell-Extrinsic Factors Contributed to ILC Dysregulation in <i>Stat1</i> ^{-/-} Mice	86
4.3.3. Expression of IL-33 and IL-23 is Increased During Viral Infection in <i>Stat1</i> ^{-/-} Mice	89
4.3.4. Disruption of IL-33 and IL-23 Signaling Inhibits ILC2 and ILC3 Activation in <i>Stat1</i> ^{-/-} Mice	92
4.3.5. IL-17A ⁺ ILC3 Express Receptors for Type I and II Interferons and IL-27	94
4.4. Discussion	96
5. IL-33 Promotes the Egress of ILC2 from the Bone Marrow	101
5.1. Introduction	101
5.2. Methods.....	103
5.2.1. Mice.....	104
5.2.2. Flow cytometry.....	104
5.2.3. <i>In vitro</i> ILC2P culture.....	108
5.2.4. Protein Measurements	108
5.2.5. BrdU Assay.....	108

5.2.6. Bone marrow chimeras	109
5.2.7. mRNA Quantification.....	109
5.2.8. <i>In vivo</i> AMD3100 and IL-33 treatments	112
5.2.9. <i>In vivo</i> <i>Alternaria alternata</i> extract challenge.....	112
5.2.10. Parabiosis.....	112
5.2.11. Statistics.....	113
5.3. Results	113
5.3.1. Deficiency in IL-33 Signaling Promotes Accumulation of ILC2P in the Bone Marrow	113
5.3.2. IL-33 Deficiency Does Not Appreciably Alter the Hallmark Functional Capacities of ILC2.....	118
5.3.3. Lack of IL-33 Signaling Does Not Alter the Rate of <i>De Novo</i> ILC2P Generation in the Bone Marrow	121
5.3.4. ILC2P/ILC2 Frequencies in <i>St2^{-/-}</i> mice are Established by an ILC2P/ILC2 Cell-Intrinsic Mechanism	124
5.3.5. <i>St2^{-/-}</i> ILC2P Differentially Express Multiple Chemokine Receptors.....	126
5.3.6. IL-33 is a Direct Negative Regulator of CXCR4 on ILC2P <i>In Vitro</i>	126
5.3.7. Blockade of CXCR4 Reduces Bone Marrow ILC2P Frequency in <i>St2^{-/-}</i> mice	127
5.3.8. Intravenously-Delivered IL-33 Drives the Egress of ILC2P from the Bone Marrow	129
5.3.9. Allergic Airway Inflammation Drives the Egress of ILC2P from the Bone Marrow	131
5.3.10. Hematogenous Reseeding of Peripheral Tissues by ILC2 Occurs in the Context of Disrupted Tissue Homeostasis.....	134
5.4. Discussion	136
6. Summary and Conclusion	140
6.1. Synopsis of Findings	140
6.2. Limitations in the Investigation of ILC	143
6.2.1. Identification and Visualization of ILC	143
6.2.2. Modeling the Role of ILC2 in Allergic Disease.....	145
6.3. Implications and Future Directions	147
6.3.1. Targeting ILC2 in Allergic Disease.....	147
6.3.2. Coordination of ILC Responses	149
6.3.3. Establishment and Maintenance of the Type 2 Immunologic Niche.....	150
6.3.4. Functional Significance of ILC	154
6.4. Closing	155
REFERENCES	156

LIST OF TABLES

Table	Page
4-1. Antibodies for Flow Cytometry.....	74
5-1. Flow Cytometry and FACS Antibodies.....	107
5-2. Quantitative PCR Primers.	111

LIST OF FIGURES

Figure	Page
2-1. ILC Development and Effector Function	18
2-2. The Role of ILC2 in Allergic Inflammation.....	24
3-1. RSV infection induced whole lung IL-13 accumulation and IL-13-producing ILC2 at day 4 post-infection.....	44
3-2. Flow cytometry gating strategies.....	45
3-3. RSV does not induce IL-5-producing ILC2.....	46
3-4. RSV stimulated ILC2 proliferation at day 4 post-infection.....	47
3-5. RSV-induced TSLP signaling is required for ILC2 activation.....	50
3-6. TSLPR expression in Ki67+ and Ki67- subsets of ILC at day 4 post-RSV infection.....	51
3-7. Pre-treatment of mice with dexamethasone decreases TSLP expression and ILC2 activation.....	52
3-8. RSV-induced IL-33 and ILC2.....	54
3-9. TSLPR-deficiency attenuated RSV-induced IL-13 production, airway mucus accumulation, airway reactivity, and weight loss without negative effects on viral load....	57
3-10. Lung IL-13 with TSLP neutralization.....	58
3-11. Analysis of ILC and T cells at day 6 post-infection.....	59
3-12. Supplementary histopathologic sections from WT and TSLPR-deficient mice at day 6 post-infection.....	60
3-13. Pathogenic clinical isolates of RSV induce IL-13+ ILC2 via TSLP.....	62
3-14. RSV-induced weight loss with 2012 clinical isolates.....	63
4-1. Gating strategies for cNK and ILC1.....	80
4-2. Gating strategies for ILC2 and ILC3.....	81
4-3. ILC are dysregulated in <i>Stat1</i> ^{-/-} mice.....	82
4-4. <i>Stat1</i> ^{-/-} ILC2 and ILC3 proliferate robustly during RSV infection.....	83
4-5. <i>Stat1</i> ^{-/-} mice displayed enhanced type 2 and type 17 immunity and poor viral clearance during RSV infection.....	85
4-6. ILC cell-intrinsic and cell-extrinsic factors contribute to the dysregulation of <i>Stat1</i> ^{-/-} ILC.....	88
4-7. Pro-ILC2 and ILC3 stimulatory cytokines are increased in <i>Stat1</i> ^{-/-} mice during viral infection.....	91
4-8. IL-33 and IL-23 are cell-extrinsic regulators of ILC that are dysregulated in <i>Stat1</i> ^{-/-} mice and promote enhanced ILC2 and ILC3 responsiveness.....	93
4-9. ILC3 express receptors for type I and type II IFNs and IL-27.....	95
5-1. ILC2P surface phenotyping.....	106
5-2. Deficiency in IL-33 signaling lead to an accumulation of ILC2P in the bone marrow.....	115
5-3. Deficiency in IL-33 signaling decreased the number of ILC2 in peripheral tissues.....	116
5-4. Deficiency in TSLP signaling reduced the number of ILC2P/ILC2 in the bone marrow and peripheral tissues.....	117

5-5. IL-33-deficient ILC2P were comparably functional to WT ILC2P.	120
5-6. Gating strategy for LMPP, CLP, CHILP, and ILCP in the bone marrow.	122
5-7. Lymphopoiesis of ILC2P <i>in vivo</i> did not require IL-33.	123
5-8. Tissue frequencies of ILC2/ILC2P were established by a cell-intrinsic, ST2-dependent mechanism.	125
5-9. CXCR4 on ILC2P promoted their bone marrow retention and was negatively regulated by IL-33 signaling.	128
5-10. Direct intravenous administration of IL-33 promoted ILC2P egress from the bone marrow.	130
5-11. Allergic airway inflammation induced by the fungal aeroallergen <i>Alternaria alternata</i> promoted increased serum IL-33 and ILC2P egress from the bone marrow. ..	132
5-12. Allergic airway inflammation induced by the fungal aeroallergen <i>Alternaria alternata</i>	133
5-13. ILC2 reseeded peripheral tissues by hematogenous spread in the context of disrupted homeostasis.	135
6-1. Graphical Summary of Dissertation Results	142

CHAPTER 1

INTRODUCTION

1.1. Overview

The ability to treat allergic disease including asthma, and the respiratory viral infections that predispose to and exacerbate asthma, is of paramount importance. The contents contained within this dissertation seek to expand our mechanistic understanding of the factors that influence allergic disease and respiratory viral infection. It begins with an outline of the scope and rationale for the work, followed by a synopsis of the literature upon which these studies were founded. Next, the data for three research aims are presented and a final commentary is provided about the significance of this work.

1.2. Scope and Rationale

Allergic diseases—including asthma, atopic dermatitis, and allergic rhinitis—are substantial causes of morbidity and mortality with a particularly high prevalence in developed countries. While considerable effort has been invested in developing therapeutics to treat allergic disease, many individuals remain refractory to treatment. Further mechanistic insight into the causes of allergy as well as the pathways that enhance or restrict disease will provide opportunities for better prevention and treatment strategies.

Over the last decade, critical insights into non-T cell sources of classical T cell cytokines

associated with allergy, such as IL-5 and IL-13, have led to the identification and characterization of group 2 innate lymphoid cells (ILC2). An extensive literature has accumulated (reviewed in Chapter 2) describing a necessary and sufficient role for ILC2 in mediating pathologic responses to allergens. However, key gaps in knowledge remain and provide the basis for the studies within this dissertation. Respiratory viral infections are recognized as a major cause of asthma exacerbations and infections with certain pathogens in infancy strongly correlates with the subsequent development of asthma. The contributions of ILC2 to allergic-like inflammation in the context of respiratory viral infections are still poorly defined. Notably, ILC2 involvement in the immune response to the pathogen respiratory syncytial virus (RSV) has not been established despite RSV representing the most common respiratory pathogen in early infants and severe RSV infection in infancy being strongly associated with a later diagnosis of asthma. Furthermore, it is largely unclear how the ILC2 compartment within the lungs and other mucosal sites is established and maintained throughout life. A more mechanistic understanding of the pathways that establish and maintain ILC2 cells in tissue will provide additional therapeutic targets for the treatment of allergic disease.

These gaps in knowledge provide the rationale for the aims of this dissertation:

Aim 1: Determine the effect of TSLP signaling on ILC2 activation and associated changes in airway physiology in a mouse model of RSV infection.

Aim 2: Characterize the effect of interferons (IFNs), a major antiviral defense pathway, and their signaling through signal transducer and activator of transcription 1 (STAT1) in

orchestrating the balance of group 1, 2, and 3 innate lymphoid cells during respiratory viral infection.

Aim 3: Interrogate the role of the major ILC2-activating cytokine IL-33 in regulating the egress of newly developed ILC2 from the bone marrow for hematogenous trafficking to peripheral tissues.

CHAPTER 2

BACKGROUND

2.1. Allergy, Asthma, and Viral Infections

Allergic reactions are inappropriate immune hypersensitivities to otherwise inert or non-pathogenic environmental antigens. Several common allergic conditions include allergic asthma, atopic dermatitis, allergic rhinitis, allergic conjunctivitis, and anaphylaxis. The severity of disease and the extent of tissue involvement vary widely by condition and between people. Common symptoms of allergic reactions include rhinorrhea, nasal congestion, conjunctivitis, pruritis, mucus production, urticaria, and difficulty breathing. Anaphylaxis is the most severe form of allergic reaction and may result in widespread hemodynamic instability and bronchospasm that is life-threatening.

Asthma represents an important component of allergic disease. Clinically, asthma is a disease of chronic airway inflammation. Severe exacerbations of asthma lead to luminal mucus accumulation and constriction of the airway smooth muscle, leading to compromised ventilation, resulting in respiratory accessory muscle use, coughing, and wheezing. In such severe cases, airway obstruction requires emergent medical intervention.

Below is a review of the epidemiology of allergy as well as the immunologic mechanisms that drive allergic disease, with a focus on asthma and the role of viral infections.

2.1.1. Epidemiology

Clinically apparent allergic diseases are estimated to affect 50 million individuals within the United States, and allergen sensitization as measured by serum IgE levels demonstrates that 30-50% of all individuals depending upon their age have been allergically sensitized.^{1,2}

Globally, the prevalence of allergic disease is staggering. Nearly 300 million individuals are diagnosed with asthma and over 200 million individuals suffer from food allergies, with the most common allergens being milk, eggs, peanuts, tree nuts, wheat, soybeans, fish, and shellfish.^{1,3} The prevalence of allergic disease has increased over the last several decades, particularly in developed countries, heightening the urgency for better therapeutic intervention strategies.⁴ The explanations for this are varied, but significant attention has been paid to the hygiene hypothesis. The premise for the hygiene hypothesis is that exposure to a diverse set of natural antigens trains the immune system to respond appropriately and with deference to tolerance when otherwise inert antigens are encountered. Because of changing living patterns (i.e. less contact with farm animals), medical interventions (i.e. antibiotics and vaccines), and increased use of soaps and hygiene techniques, it is hypothesized that our immune system is not properly trained during early life, thus leading to inappropriate reactions to otherwise inert antigens precipitating allergic disease.⁵ However, the specific antigen profile is likely important as to whether these exposures protect from or enhance allergic disease.^{6,7}

Asthma prevalence is estimated to be 7% in the United States and varies between 1-18% worldwide.⁸ Age, sex, and geographic location all contribute to asthma prevalence.⁹⁻¹¹ For instance, children are more likely to have asthma than adults. Prior to puberty, boys have a higher incidence of asthma but following puberty that inverts with women having a higher

incidence of asthma than men.^{9,11} Patients in the United States with uncontrolled asthma have more frequent hospitalizations, higher utilization of emergency departments, and more missed days from work with an increased cost burden of thousands of dollars per patient per year.¹² The total cost of illness associated with asthma in the United States was estimated to be over \$6 billion annually, with the largest expenditures associated with emergency room visits, hospitalizations, and death.¹³ Several risk factors in the prenatal period and in childhood influence asthma incidence and severity. Prenatal tobacco smoke exposure is consistently associated with episodes of childhood wheezing. Maternal antibiotic use also predisposes to persistent wheeze and childhood asthma in a dose-dependent manner. Finally, emergency caesarian sections are associated with a 2-3 fold increased risk of allergic disease compared to vaginal births, possibly reflecting microbiome-associated effects.¹⁴ Both childhood airborne tobacco exposure and antibiotics also increase the risk of asthma, while exposure to farm animals reduces allergic disease.¹⁴ Exposure to airborne pollutants such as ozone and diesel exhaust particulate can exacerbate asthma.^{15,16} Importantly, respiratory viral infections are a major cause of asthma exacerbations, and early life exposure to certain respiratory infections strongly correlates with the subsequent development of asthma.

2.1.2. Viral Infections and Asthma

An estimated 80% of asthma exacerbations in children are associated with respiratory viral infection.¹⁷⁻¹⁹ Of these, about two thirds represent infections with rhinovirus (RV). The remaining fraction represents a mixture of respiratory syncytial virus (RSV), influenza virus,

parainfluenza virus, and coronavirus. Of note, age is a major determinant of viral species and association with active wheezing or asthma exacerbations.²⁰ In patients less than 2 years old, RSV is the predominant virus associated with wheezing. In patients 3-18 years old, RV becomes the principal wheeze-inducing virus. Wheezing episodes also tracked with seasonal prevalence of RV and RSV in the fall and winter, further suggesting causality for asthma exacerbations.²⁰

As noted, RSV is the major respiratory pathogen in infants and is associated with wheezing episodes. The incidence of RSV infections in the first year of life is approximately 70%, and nearly all children have been infected at least once by the age of two.²¹ Numerous studies have shown an association between early life severe RSV infection and the subsequent development of asthma.⁶ In a retrospective birth cohort study, infants who were hospitalized with bronchiolitis had an higher odds of developing asthma compared to infants with no hospitalization.²² Dose-dependent effects of RSV in the first year of life comparing outpatient encounters, uncomplicated hospitalizations, and prolonged hospitalizations showed a severity-dependent association with the subsequent development of asthma.²³

Two key lines of evidence support a causal role for severe RSV infection in the initiation of asthma. First, birth month strongly correlates with the development of asthma. RSV circulates heavily in the late fall and early winter months. In a retrospective birth cohort, birth month was compared relative to peak viral circulation in the first year of life and asthma prevalence was assessed at ages 5-6. Despite annual variance in the winter viral season, the highest prevalence of asthma was observed in infants born almost exactly 4 months prior to the winter viral peak.²⁴ However, this study did not specifically evaluate the viral etiology, and

therefore does not definitively implicate RSV. Second, a randomized control trial evaluated the effect of palivizumab on the number of wheezing episodes within the first year of life.²⁵

Palivizumab is a monoclonal antibody against the RSV fusion protein that reduces hospitalizations by approximately 50% when given prophylactically. Compared to patients receiving placebo, there was a significant reduction in the burden of wheezing illness in patients receiving palivizumab. While wheezing does not necessarily indicate asthma, and asthma diagnoses could not be made in this population because they were too young, early life persistent wheezing correlate with a diagnosis of asthma later in life.²⁶ Similar results were obtained in a case-control study that evaluated palivizumab prophylaxis in infancy and wheezing at age three.²⁷ It is important to note that susceptibility to asthma is likely multifactorial, and host genetics may play a significant role independent of exposure. Patients may be susceptible to severe RSV infection and asthma by the same molecular mechanisms. Polymorphisms conferring susceptibility to both RSV and asthma have been identified in genes such as IL-4, IL-13, IL-8, IL-10, and TLR4.⁶ Collectively, these data demonstrate the critical importance of viral infections in exacerbations of asthma, and suggest a potential initiating role for RSV infection in the development of asthma.

2.1.3. Immunologic Response in Asthma and Allergy

Multiple immune cells and mechanisms are involved in mediating allergic reactions. The classical paradigm for allergic responses involves sensitization of the immune system to antigen followed by an exuberant response upon re-exposure to the same antigen. Upon encountering certain environmental antigens, dendritic cells mobilize to secondary lymphoid organs to

polarize CD4⁺ T cells via OX40L:OX40 signaling towards CD4⁺ T helper type 2 (Th2) cells.²⁸ CD4⁺ Th2 cells release IL-4 in an autocrine fashion to reinforce this polarization. CD4⁺ Th2 cells' expression of IL-4 in conjunction with CD40L signaling onto B cells induces antibody class switching to the IgE isotype. IgE circulate and binds to Fcε receptors on mast cells embedded within mucosal tissue. Re-exposure to the same antigen induces cross linking of antigen-specific IgE on the surface of the mast cell, immediately releasing pre-formed pro-inflammatory mediators such as tryptase and histamine, while leukotrienes and prostaglandin D₂ are newly formed, resulting in the generation of an acute allergic response. As the reaction progresses, memory CD4⁺ Th2 cells are activated to produce type 2 cytokines including IL-4, IL-5, and IL-13. In the lung, for instance, these cytokines mediate pathophysiologic changes in the airway including eosinophilia, mucus metaplasia and release in the airways, smooth muscle hyperreactivity, and airway remodeling.

Additional cell types of the innate immune system can mediate allergic disease, including antigen-specific IgE-mediated activation of basophils which express type 2 cytokines. Dendritic cells, endothelial cells, keratinocytes, and fibroblasts may produce chemokines such as CCL17 (also known as TARC) which preferentially recruits Th2 cells into tissue in which antigen is present. Recruitment of eosinophils, basophils, and CD4⁺ Th2 cells into the inflamed tissue is significantly induced by eotaxin/eotaxin-2/eotaxin-3 signaling via CCR3, with eotaxin-3 being a salient mediator of inflammation in eosinophilic esophagitis.²⁹⁻³¹ Type 2 cytokines such as IL-4 and IL-13 may differentiate macrophages into a collection of phenotypes that have been termed M2-like macrophages, which can produce TGF-β that may cause airway remodeling.³² More recently, the identification of innate lymphoid cells (ILC) with similar functional properties as

CD4⁺ T cells has led to an explosion of research in understanding their contributions to allergic disease.

2.2. Overview of Innate Lymphoid Cells

ILC are a broad class of cells embedded at mucosal sites that are involved in tissue homeostasis and response to diverse environmental insults. Derived from common lymphoid progenitors, ILC develop into three major cell subsets—group 1, 2, and 3 ILC. These cells have unique transcriptional signatures and effector functions, described in detail below. Briefly, ILC1, ILC2, and ILC3 are driven by T-bet, GATA3, and RORγt and produce IFN-γ; IL-5 and IL-13; and IL-17 and IL-22, respectively.³³ These gene signatures and effector functions mirror CD4⁺ Th1, Th2, and Th17 cells. However, ILC exhibit several key differences that make them distinct from their CD4⁺ Th cell counterparts. In contrast to CD4⁺ T cells, ILC are primarily at mucosal sites even at baseline and are only found in low numbers in secondary lymphoid organs such as lymph nodes and the spleen.³⁴ Moreover, even in ILC-rich tissues, ILC are found in significantly fewer numbers than CD4⁺ T cells. ILC do not depend on antigen presentation and can be activated immediately from stimuli in the tissue milieu, positioning them as innate counterparts to CD4⁺ T cells.^{35–37} ILC have been studied in a number of diseases in both pre-clinical models and in humans, the details of which are discussed below and summarized in graphically in **Error! Not a valid bookmark self-reference..**

2.3. ILC Development and Tissue Composition

Our understanding of ILC development comes largely from studies in mice, with the verification of key stepwise progenitors in humans. In mice, ILC derive from common lymphoid progenitors (CLP).³⁸ The expression of the transcriptional regulator Id2 halts T and B cell development and promotes the differentiation of CLP to alpha lymphoid precursor (α LP) cells and common helper innate lymphoid progenitor cells (CHILP).^{37,39-41} α LP/CHILP have multi-lineage potential, with the capability to form all ILC helper subsets as well as classical natural killer (NK) cells and lymphoid tissue inducer (LTi) cells.⁴¹ The expression of NFIL3 is also critical for differentiation of lymphoid progenitors to α LP/CHILP.⁴² CHILP depend upon the transcription factor ETS1 for appropriate fitness.⁴³ CHILP cells no longer maintain NK cell potential, but can differentiate into all helper ILC lineages as well as LTi cells. Expression of promyelocytic leukemia zinc finger (PLZF) protein and the upregulation of the cell surface receptor programmed death 1 (PD-1) marks the differentiation of CHILP into ILCP, which can repopulate all helper ILC lineages but not LTi cells.^{44,45}

The lineage specification of ILCP into committed precursors of ILC1, ILC2, and ILC3 remains an area of ongoing investigation. The expression of Bcl11b, Gfi1, and ROR α are vital for the generation of ILC2 precursors (ILC2P)^{46,47}, though Bcl11b-deficiency was dispensable for bone marrow ILC2P but not mature peripheral ILC2 numbers in one study.⁴⁸ Absence of Gfi1 and ROR α in mice leads to the loss of peripheral ILC2 populations and a deficit of bone marrow ILC2P. GATA3 is also a critical marker of ILC2-committed cells, though GATA3-deficient mice lack all ILC subsets.⁴⁹⁻⁵² It is thought that GATA3 expression in early progenitor cells is required for advancement towards all ILC development, but within the mature ILC compartment that high GATA3 expression demarcates the ILC2 fraction.⁴⁹

Recombination-activating genes 1 and 2 (RAG1 and RAG2) are dispensable for ILC development.³⁵⁻³⁷ Broadly, RAG-deficient mice have mostly normal ILC numbers and RAG gene expression is not detected in ILC precursors.⁵³ The mild reduction in ILC numbers may result for a lack of supportive T cell-derived IL-2.⁵⁴ Accordingly, RAG-deficient mice have been used extensively to understand ILC biology without T cell confounding.

Multiple environmental signals are known to guide ILC development. Mice lacking the IL-7 receptor (IL-7R α , also known as CD127) or the IL-2 receptor (IL-2R α , also known as CD25) have broad deficiencies in ILC, suggesting a critical role for these signals in ILC development.^{37,38} Interesting, the IL-7R α is a shared subunit between the receptors for IL-7 and TSLP. Yet, deficiencies in IL-7 and TSLP offer only modest reductions in the number of ILC in mice, suggesting potential redundancy in these cytokines for ILC development.⁴⁰ Both the IL-2 and IL-7 receptor complexes utilize the common γ chain. Consistent with these data, mice double-deficient in RAG and the common γ chain lack T cells, B cells, and ILC and these mice have been used to understand the extent of ILC contribution to pathophysiology. Notch-notch ligand signaling is also a critical pathway for ILC development, and disruption of this pathway leads to reduced ILC2 differentiation *in vitro*³⁸ and *in vivo*.⁵⁵⁻⁵⁸

Significant attention has been paid to ILC development in the bone marrow, though evidence suggests that ILC lymphopoiesis may happen outside of primary lymphoid tissues including in the fetal gut in mice.⁵⁹ In addition, in humans circulating ILC progenitor cells have been identified in the peripheral blood.⁶⁰ The establishment and maintenance of ILC populations in tissue is further detailed below.

2.4. ILC2 Function, Homeostasis, and Disease

ILC2 are a major type 2 immune effector cell and play pathologic, protective, and homeostatic roles, especially in the context of allergic disease. IL-5 and IL-13 are the major cytokine products of ILC2, though they are also sources of IL-9, IL-4, and amphiregulin under the appropriate circumstances. ILC2 effector cytokines imparts significant and diverse functional potential to the ILC2 lineage.

2.4.1. Activators and Inhibitors of ILC2

A variety of environmental stimuli are known to activate ILC2. The three canonical activators of ILC2 are IL-33, IL-25, and TSLP.^{36,37,61} ILC2 express the receptors for all three of these cytokines in both mice and humans^{36,62}, though different tissues may depend more critically on one cytokine over the others.⁶²⁻⁶⁴ IL-33 is a pro-inflammatory IL-1 family member. Epithelial cells, including type II pneumocytes within the lung and keratinocytes within the skin, and endothelial cells are major sources of IL-33.^{65,66} Macrophages and mast cells can also express IL-33. IL-33 is stored pre-formed within the nucleus of these cells, serving as a readily available inflammatory mediator.⁶⁷ *In vitro*, IL-33 robustly activates ILC2 increasing proliferation and expression of IL-5 and IL-13.^{36,37} IL-33 signaling deficiency or blockade of the IL-33 receptor attenuates ILC2 activation and associated physiologic responses in murine models of influenza infection⁶⁸, *Nippostrongylus brasiliensis* infection³⁶, atopic dermatitis⁶⁴, among others. Exogenous delivery of recombinant IL-33 elicits strong ILC2 responses in tissues such

as the lungs and gastrointestinal tract.^{36,37,69} Maximal ILC2 responses to IL-33 require a second signal that potentiates NFAT signaling, such as leukotrienes.⁷⁰

While neither activates ILC2 to any substantial effect in isolation *in vitro*, both IL-25 and TSLP have been shown to significantly enhance ILC2 proliferation and cytokine expression in combination with IL-33.^{36,37} Mice deficient in the IL-25 receptor (also known as IL-17RB) have impaired ILC2-mediated immunity to intestinal helminth infection while exogenous delivery of IL-25 enhances ILC2 activity.³⁷ Furthermore, deficiency in TSLP signaling attenuates ILC2 responses in the skin while overexpression of TSLP activates ILC2.⁶² TSLP and IL-25 are both expressed by epithelial cells, with a major source of IL-25 being tuft cells in the small intestine.^{71,72}

Several other ILC2 activators have been characterized. The lipid mediators leukotriene D₄ (LTD₄), LTE₄, and prostaglandin D₂ (PGD₂) induce cytokine expression from ILC2.^{73,74} Interestingly, LTD₄ extends ILC2 cytokine producing capacity to include IL-4 and PGD₂ is a potent chemoattractant of ILC2. Additional activators of ILC2 include IL-1 β and TL1A.^{75,76}

Conversely, there is intense interest in understanding inhibitors of ILC2 that may serve as therapeutic targets in allergic disease. Endogenous inhibitors of ILC2 include Spred1, a suppressor for the Ras-ERK pathway, and the cell surface receptor programmed death 1 (PD-1).^{77,78} Lipoxin A₄ and the cyclooxygenase product PGI₂ also negatively regulate ILC2 proliferation and cytokine production⁷⁹, and type I and II interferons negatively regulate ILC2 viability and function including in a model of allergic airway disease.^{69,80,81} Signaling through the α 7-nicotinic acetylcholine receptor similarly attenuates ILC2 function.⁸² ILC2 are also attenuated by the T regulatory cells and their products IL-10 and TGF- β .⁸³⁻⁸⁵ Therapeutics targeting IL-25, IL-33, and TSLP are of significant interest to the field.⁸⁶

2.4.2. ILC2 Tissue Maintenance and Trafficking

Tissue seeding by ILC2 occurs in the perinatal period. Prior to birth, ILC2 are virtually absent in the lungs.^{53,87,88} Across the first two weeks of life, ILC2 rapidly accumulate in the lungs and reach levels comparable to adult mice.^{53,87-89} This accumulation of ILC2 coincides with a wave of IL-33 expression in the lungs, primarily from CD45⁻ EpCam⁺ type II pneumocytes.⁸⁸ Conceptually, this IL-33 expression and ILC2 accumulation occurs during the alveolarization period of murine lung development with expansion and maturation of type II pneumocytes. Mice lacking IL-33 signaling had reduced numbers of ILC2 in the lungs at post-natal days 7, 10, and 14 consistent with a critical role for IL-33 in establishing the ILC2 compartment within the lungs.⁸⁷⁻⁸⁹ In the lungs during the post-natal period, ILC2 are the major source of type 2 cytokines, and the recruitment of type 2-associated effector cells such as eosinophils and anti-inflammatory M2 macrophages critically depends upon ILC2.^{88,89} Collectively, these changes promote type 2 immune skewing in the post-natal period that can be exacerbated with exposure to allergen and persist into adulthood. While ILC accumulation has been well characterized in the lungs, substantially less is known about ILC2 accumulation in other tissues.

An ample population of ILC progenitors exists in the bone marrow that may serve as the source of early ILC tissue seeding and as a reservoir for repopulation of tissues throughout life.⁹⁰ Additional progenitor cell sources in peripheral sites may contribute to tissue accumulation of ILC. Fetal ILC progenitors (fILCPs) expressing CD127, integrin $\alpha_4\beta_7$, and Arginase-1 and negative for ROR γ t, NK1.1, and ST2 were identified in the small intestine at embryonic day

15.5.⁵⁹ These ftILCPs had the potential to differentiate into mature ILC1, ILC2, and ILC3 *in vitro* and may serve as a progenitor cell source for populating the gastrointestinal tract with ILC. A similar population of progenitor cells that lacked expression of lineage markers and was positive for CD127, c-Kit, and PLZF has been identified in the fetal liver and can give rise to all helper ILC lineages.⁴⁴

ILC lineages are generally considered tissue resident under steady-state conditions. Pulse-chase experiments demonstrate that ILC2 are long-lived cells that exhibit self-renewing capacity *in situ* within tissues.⁵³ Parabiosis studies of naïve mice demonstrate that ILC2 are minimally replenished from hematogenous sources across short-term (40 day) or long term (130 day) experiments, with recovery of approximately 2-5% of donor ILC2 in the lung, small intestine, salivary gland, and adipose tissue of the opposing parabiont.^{91,92} However, in the context of infection with the helminth *Nippostrongylus brasiliensis*, which induces a strong type 2 immune response, ILC2 but not other ILC lineages are recruited to the lung in higher quantities than in mice receiving a mock inoculum.⁹² The signals that support and maintain ILC2 in tissue at steady-state are largely unknown. T cell-derived IL-2 is posited to support ILC2 in tissues via an MHCII mediated dialogue⁵⁴, though a separate study suggests IL-2 may be dispensable for ILC2 maintenance at baseline.⁹² Rag-deficient mice that lack mature T cells show variable effects on ILC2 number, with different studies identifying more⁹³ or equal⁵³ numbers of ILC2 at mucosal sites compared to WT controls providing equivocal evidence for T cell-derived IL-2 supporting ILC2 at baseline. ILC2 express ICOS, and ICOS-deficient mice have reduced numbers of ILC2 in the lungs and small intestine at baseline, suggesting a homeostatic role for ICOS signaling in supporting ILC2 populations at mucosal sites.^{94,95} While metabolic processes tied to Arginase-1 and fatty acid processing support ILC2 responses to environmental challenge,

disruptions of these systems have no effect on ILC2 at baseline.^{96,97} These data collectively demonstrate that ILC2 are primarily tissue-resident cells in adult mice and that recruitment of cells from the bloodstream may occur in response to disrupted homeostasis and inflammation.

A limited number of signaling pathways have been identified that influence ILC2 trafficking. Germline CCR9-deficiency reduced the trafficking of ILC2 to the small intestine, suggesting a possible defect in early ILC2 seeding of the gastrointestinal tract dependent upon CCR9.⁹⁸ Using Kaede transgenic mice that express a photoconvertible fluorescent protein allowing for cell tracking, ILC2 were found to traffic from the small intestinal lamina propria to the mesenteric lymph node rapidly within a 24 hour period.⁹⁹ Additionally, PGD₂ and via its receptor CRTH2 and the integrin β 2 both promote accumulation of ILC2 in the inflamed lung.^{100,101} Collectively, these data suggest ILC2 may transit dynamically within local regions or systemically during development or upon inflammatory stress.

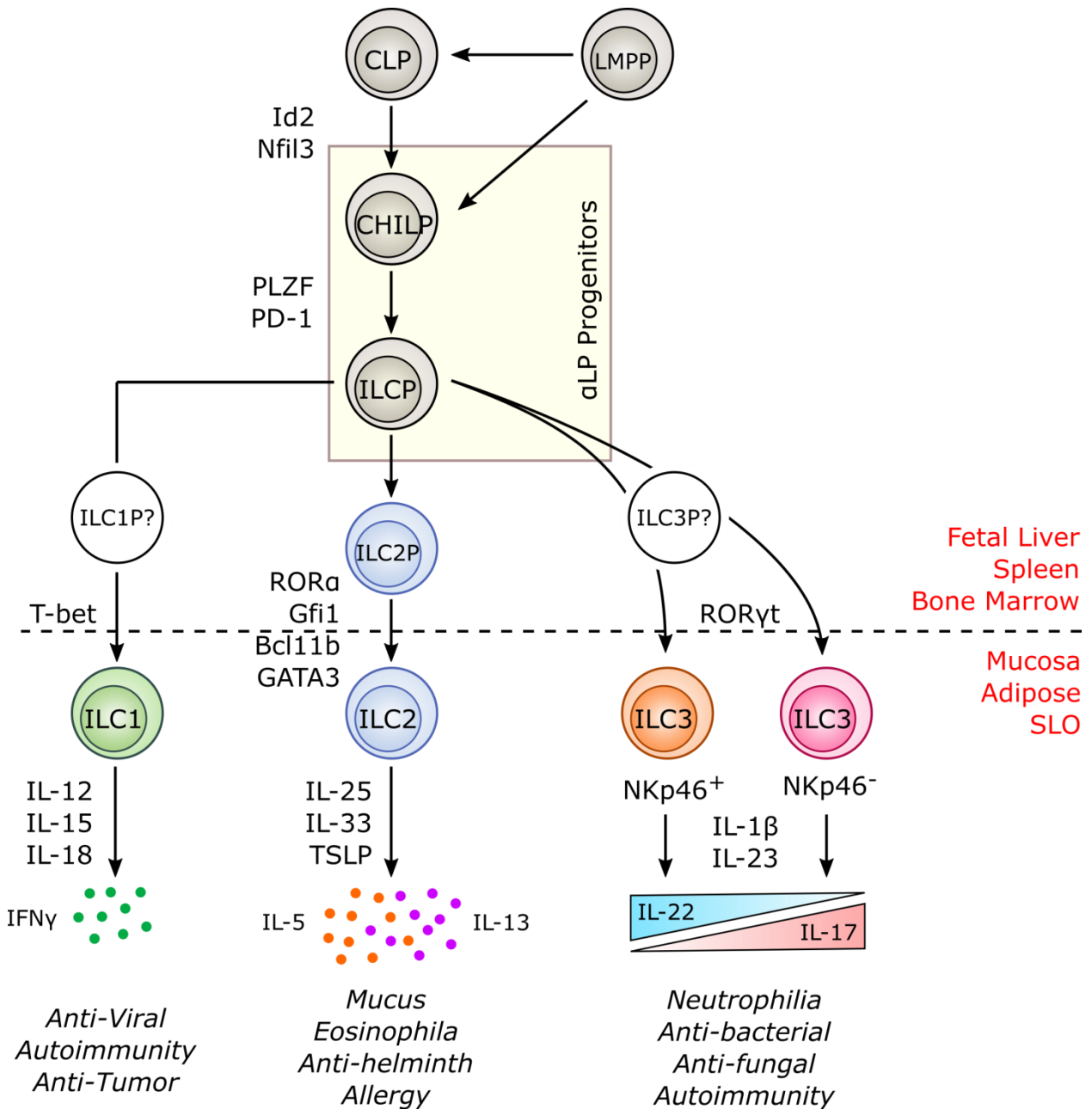


Figure 2-1. ILC Development and Effector Function

ILC develop from CLP and LMPP. CLP and LMPP differentiate into CHILP via expression of Id2 and Nfil3. The expression of PLZF initiates the differentiation into ILCP that are restricted to developing into the three main helper ILC lineages. PD-1 expression correlates with ILCP differentiation. The transcription factors T-Bet, GATA3, and ROR γ t guide the development of ILC1, ILC2, and ILC3 lineages. ILC2 lineage development also requires ROR α , Gfi1, and Bcl11b. ILC1, ILC2, and ILC3 have unique activation signals, express distinct cytokines, and are involved in non-redundant immune responses. P = progenitor; SLO = secondary lymphoid organ.

2.4.3. ILC2 Mechanisms of Pathogenesis in Allergic Disease

ILC2 are important mediators of allergic disease, and a significant literature sheds light on the mechanistic importance of ILC2 in response to allergens (summarized graphically in Figure 2-2). The initial reports describing ILC2 all demonstrated their physiologic importance in type 2 immune responses using a mouse model of infection with the helminth *Nippostrongylus brasiliensis*.³⁵⁻³⁷ These data suggested an important role for ILC2 in type 2 immune responses and by extension posited a potential role in allergic reactions. Subsequent work implicated ILC2 as important type 2 immune effector cells in mouse models of aeroallergen exposure to *Alternaria alternata* and papain, and adoptive transfer studies into lymphocyte-deficient mice demonstrated ILC2 to be sufficient to induce airway mucus accumulation and eosinophilia independent of the adaptive immune system.^{61,102} In comparison to CD4⁺ Th2 cells, ILC2 were found to be considerable independent expressers of IL-5 and IL-13 in house dust mite-induced allergic inflammation, and ILC2 have greater than 10 fold the per-cell cytokine producing capacity compared to CD4⁺ Th2 cells.¹⁰³

Related work employing murine models of atopic dermatitis have shed additional light on the role of ILC2 in allergic disease. Depletion of ILC2 in the skin of *Rag*^{-/-} mice ablated skin inflammation and thickening in a vitamin D analogue-induced model of atopic dermatitis.⁶² The activation of ILC2 within the skin may involve multiple circuits. While much attention has been focused on IL-33-induced activation of ILC2 in the lungs, all three of IL-25, IL-33, and TSLP have been implicated in ILC2-driven allergic reactions within the skin.^{62,64,104}

Activation of ILC2 in tissues profoundly changes their surface phenotype consistent with several feed-forward loops that may promote the allergic response. Notably, the high-affinity

subunit of the IL-2 receptor complex, CD25, is significantly upregulated in the setting of inflammation in both the lungs and skin.^{93,102} Increased CD25 expression positions ILC2 to better respond to IL-2, a potent IL-33-synergistic signal for ILC2 in mice and humans. Inflammation in the skin and lung also upregulates the IL-33 receptor.^{93,105,106} *In vitro* stimulation of human ILC2 increases the expression of the receptors for IL-25, IL-33, and TSLP, suggesting similar feed-forward loops may boost ILC2 responses in humans.¹⁰⁷ In addition, ILC2 but not CD4⁺ Th2 cells exhibit corticosteroid resistance in both mice and humans, particularly when they are stimulated by TSLP, positing these cells as pathophysiologic mediators in corticosteroid-resistant asthma.^{108–111}

Several transcriptional regulators maintain ILC2 identity and enhance ILC2 activity during allergic inflammation. GATA3 is a hallmark transcriptional regulator of ILC2 that defines the ILC2 lineage and when phosphorylated binds to the IL-5 and IL-13 promoters to drive cytokine production.^{40,51} Transgenic mice overexpressing GATA3 displayed significantly increased IL-5 and IL-13 production as well as ST2 and IL-25R expression in lung ILC2 compared to WT ILC2 or GATA3 hemizygous ILC2.⁵² GATA3 overexpressing ILC2 also had upregulated ST2 expression and cytokine production in a murine model of house dust mite induced allergic airway inflammation.¹¹² Whole transcriptome analysis of mature ILC2 with or without a conditional deletion of GATA3 demonstrates substantial changes in the overall ILC2 program reinforcing the importance of GATA3 in ILC2 function.⁴⁹ Similarly, overexpression of GATA3 increased ST2 and TSLPR expression as well as IL-5 and IL-13 cytokine production from human ILC2 stimulated *in vitro*.⁵⁰ Additionally, Gfi1 promotes ILC2 activity by increasing the expression of the IL-33 receptor, stabilizing GATA3, and blocking IL-17A production.¹⁰⁶ Mice with a conditional deletion of Gfi1 fail to respond effectively to aeroallergen challenge and

exhibit a hybrid ILC2-ILC3 effector state. Bcl11b critically stabilizes GATA3 and Gfi1 to promote the ILC2 program and functionality. Bcl11b-deficient mice fail to respond appropriately to IL-33 stimulation or *Nippostrongylus brasiliensis* infection, shifting towards an ILC3-like phenotype.^{46,48} Moreover, PLZF enhances IL-5 and IL-13 expression during allergen challenge from ILC2 but not CD4⁺ Th2 cells.¹¹³

Additional ILC2-intrinsic signals enhance ILC2 contribution to allergic disease. In addition to playing a role in ILC2 homeostasis, signaling via ICOS on ILC2 enhances cytokine production during IL-33-induced airway inflammation.⁹⁵ MicroRNAs may also play a role in shaping ILC2 responses, with miR-155 upregulated following IL-33 stimulation of ILC2 and contributing to ILC2 proliferation, IL-13 expression, and stabilization of GATA3.¹¹⁴

While ILC2 have sufficient capacity to induce pathophysiologically significant responses in isolation, ILC2 responses to allergens in intact organisms and humans occur in the context of a broader type 2 immune response. Several key interactions have been described between ILC2 and other cells of the immune system that have potential relevance in allergic disease. ILC2:T cell crosstalk appears to be a vital circuit for promoting robust innate and adaptive type 2 immune responses. ILC2 are competent for antigen uptake, processing, and presentation on MHC class II to T cells via interaction with the T cell receptor. ILC2 interact with antigen-specific T cells via antigen-loaded MHC II, triggering T cell expression of IL-2 that signals back onto the ILC2 to promote ILC2 proliferation and IL-13 production.⁵⁴ Conversely, mice lacking ILC2 have severe impairments in the number of CD4⁺ Th2 cells in lymph nodes of *Nippostrongylus brasiliensis*-infected mice.^{54,115} Effective CD4⁺ Th2 cell differentiation and responses require ILC2-derived IL-13 to mobilize dendritic cells to migrate to the lymph nodes for Th2 cell priming during both primary and memory responses in both adult and early postnatal

mice.^{87,116,117} Transfer of ILC2 and CD4⁺ T cells, but not either individually, into *Il7ra*^{-/-} mice was required for a robust antigen-specific allergic response.¹¹⁸ Furthermore, ILC2-derived IL-4 promotes mast cell sensitivity to degranulation and inhibits Treg cell induction, contributing to a shift away from tolerance that may predispose to food allergy. Similarly, ILC2 function alongside CD4⁺ Th2 cells to promote food allergy via IL-13 production.¹¹⁹ These data suggest a key collaboration between ILC2 and adaptive CD4⁺ T cells in promoting allergic type 2 immune responses.⁸⁵

With regard to other arms of the adaptive immune system, ILC2 may also promote B cell extrafollicular responses as evidence by increased B cell expression of EB12 in human ILC2:B cell co-culture.¹²⁰ In mice, co-culture of ILC2 and B1 or B2-type B cells enhanced B cell proliferation and antibody production, and adoptive transfer of ILC2 into *Il7r*^{-/-} mice enhanced B1 cell antigen-specific IgM production.¹²¹ These data suggest ILC2 may influence the B cell and/or IgE compartments in allergic disease.¹²² ILC2 also coordinate with cells of the innate immune system. Specifically, basophil derived IL-4 is required for ILC2 responses in a mouse model of atopic dermatitis.¹²³

A significant proportion of asthma exacerbations are triggered by viral infections, most notably with rhinovirus (RV), respiratory syncytial virus (RSV), and metapneumovirus (MPV). Emerging evidence suggests that ILC2 may play an important role in the pathophysiology of respiratory viral infection with consequence for allergic airway disease. The general paradigm is that viral infections particularly of the respiratory tract infect epithelial cells, leading to the expression of ILC2-activating cytokines such as IL-33 (later in these infections, macrophages become the predominant source of IL-33) that stimulate ILC2. Influenza infection triggers IL-5 and IL-13 production from ILC2 with concomitant eosinophilia and airway hyperreactivity in

both the presence and absence of an adaptive immune response.^{124,125} RV infection in neonatal mice activates ILC2 via IL-25 to expand and express IL-13, contributing to airway mucus accumulation and airway hyperactivity.¹²⁶ In a murine model of RV-exacerbated asthma, RV infection increased the expression of IL-25 in the lungs leading to an increase in ILC2 within the lungs that correlated with increased IL-5 and IL-13 cytokines in the BAL fluid.¹²⁷ Of note, ILC2 responses in the late stages of influenza infection are characterized by amphiregulin production from ILC2 that promotes tissue repair, suggesting that ILC2 may play both pathologic and beneficial roles at different points during viral infection.⁶⁸

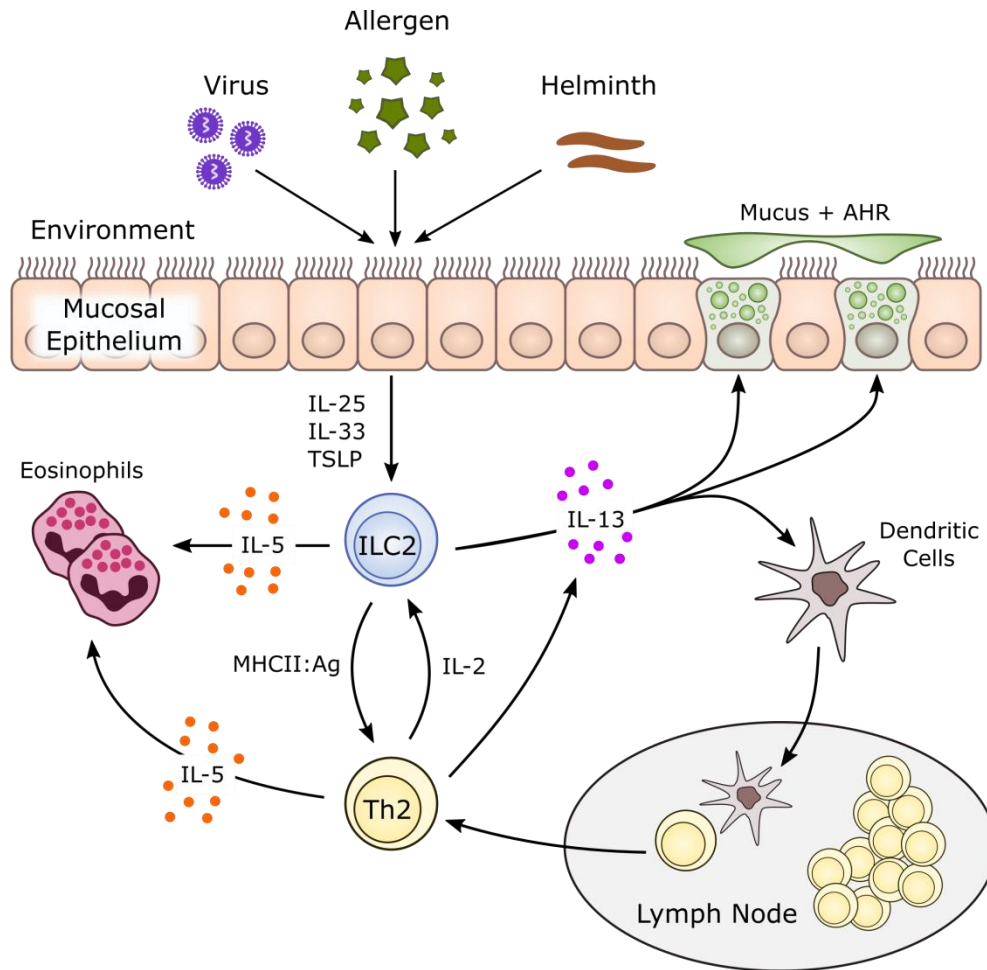


Figure 2-2. The Role of ILC2 in Allergic Inflammation.

Environmental stimuli activate or damage the epithelium leading to a release of IL-25, IL-33, and/or TSLP. These cytokines activate ILC2 to mediated an early type 2 response with eosinophilia and mucus production via the production of IL-5 and IL-13. ILC2-derived IL-13 also activates dendritic cells and induces their mobilization of draining lymph nodes where they prime CD4+ T h2 cells. These Th2 cells return to the inflamed tissue, and via signaling form MHC II loaded with antigen these cells produce IL-2 that further potentiates ILC2.

2.4.4. ILC2 in Human Disease

Enhancements in ILC2 number and/or function have been observed in humans in the setting of allergic disease including asthma, allergic rhinitis, chronic rhinosinusitis (CRS), and atopic dermatitis. ILC2 are twice as frequent in the blood of patients with allergic asthma as compared to healthy controls. These ILC2 were also significantly more responsive to IL-33 and IL-25 *ex vivo*, expressing higher levels of IL-5 and IL-13 as compared to healthy controls.¹²⁸ Increases in the number of ILC2 in the peripheral blood were substantially greater in patients with severe eosinophilic asthma compared to milder asthmatics or non-eosinophilic asthmatics, with a strong positive correlation between the severity of eosinophilia in the sputum and ILC2 frequency of the peripheral blood.^{129,130} Similar observations were made within the lung itself, with both the total number of ILC2 and the number of IL-13-producing ILC2 increased in the BAL fluid of asthmatics compared to non-asthmatic controls.^{131,132} Induction of airway inflammation in asthmatics by respiratory allergen challenge similarly increased ILC2 numbers and cytokine production in the sputum¹³³, and ILC2 activation was found to inversely correlate with effectiveness of corticosteroid treatment.^{133,134}

Dynamic changes in ILC2 frequencies are also observed in patients with allergic rhinitis. In cat-allergic subjects, nasal challenge with cat antigen significantly increased the frequency of ILC2 in the peripheral blood as compared to diluent challenge.¹³⁵ ILC2 are hypothesized to play a key role as pro-inflammatory cells in allergic rhinitis as patients challenged with intranasal exposure to allergen has increases in the number of ILC2 in nasal secretions that strongly and positively correlated with airway eosinophilia.¹³⁶ Interestingly, the extent of ILC2 induction and cytokine production in allergic rhinitis patients varies by antigen, with house dust mite

monosensitized patients significantly more responsive than mugwort monosensitized patients.¹³⁷ Furthermore, in one study no significant increase in ILC2 or their cytokine production was observed in patients with allergic rhinitis compared to healthy controls.¹²⁸ Pollen grass subcutaneous immunotherapy (SCIT) was effective in preventing ILC2 accumulation in the blood of seasonal allergic rhinitis patients, demonstrating the potential for therapeutic intervention in attenuating ILC2 responses.¹³⁸ These data broadly support a role of ILC2 in the pathogenesis of allergic rhinitis, though factors such as specificity of the antigen may influence ILC2 reactivity.

Considerable effort has also been invested in understanding the role of ILC2 in chronic rhinosinusitis (CRS). ILC2 are found in significantly higher frequency in nasal polyps of patients with CRS compared to uninflamed tissue from healthy controls.^{139,140} Further studies have demonstrated that ILC2 induction is primarily restricted to CRS with nasal polyps (CRSwNP) compared to CRS without nasal polyps (CRSsNP) or healthy controls.¹⁴¹⁻¹⁴⁴ CRS polyp endotype greatly influenced ILC2 frequency with allergic, eosinophilic polyps containing the largest proportion of ILC2.^{141,142,145} ILC2 in CRSwNP also showed features of activation, with increased surface expression of inducible T cell co-stimulator (ICOS), enhanced cellular complexity as measured by side scatter properties using flow cytometry, and increased IL-5 and IL-13 expression *ex vivo*.¹⁴³ Systemic corticosteroid treatment correlated with a partial decrease in the number of ILC2 in CRSwNP.¹⁴⁵ The ILC2-activating IL-33 axis is also upregulated in CRSwNP, including elevated levels of IL-33 from polyp tissue and increased expression of the IL-33 receptor ST2 on ILC2 compared to CRSsNP.¹⁴⁴ Importantly, ILC2 number positively correlated with severity of nasal symptom score, a combined measure accounting for nasal

obstruction, need to expel nasal discharge, loss of smell or taste, thickness of nasal discharge, and sinus pain.¹⁴²

Atopic dermatitis in humans is also linked to dysregulation of ILC2. ILC2 are markedly increased in the skin of patients with atopic dermatitis compared to skin samples collected from healthy controls.^{62,64,123,146} Moreover, ILC2 in the setting of atopic dermatitis displayed features consistent with an activated phenotype, including the upregulation of CRTH2, CD161, ST2, TSLPR, IL-25R, and KLRG1.^{62,64} Within the dermis of inflamed atopic skin, ILC2 were found in close proximity to basophils or T cells, suggesting possible coordination between these pro-inflammatory cell types.¹²³ Induction of an inflammatory response in allergic patients via exogenous, intraepidermal injection of house dust mite antigen significantly increased the number of ILC2 and their cytokine products IL-4, IL-5, and IL-13 at the site of injection as compared to control saline instillation. Collectively, these data strongly suggest a pathologic role for ILC2 in the setting of atopic dermatitis.

Emerging evidence supports a potential role for ILC2 in the context of several other allergic diseases. Patients with aspirin-exacerbated respiratory disease (AERD) challenged intranasally with NSAIDs had increased ILC2 burdens in nasal scrapings collected during challenge as compared to ILC2 levels in nasal scrapings at baseline, and that this increase in ILC2 burden positively correlated with severity of symptoms.¹⁴⁷ Additionally, several eosinophilic disorders have been associated with ILC2 activation. Active eosinophilic esophagitis (EoE) promotes an increase in the percentage of ILC2 in the esophagus compared to patients with quiescent disease or healthy controls.¹⁴⁸ Eosinophilic pleural effusion (EPE) induces a marked increase in the number of ILC2 in the pleural fluid.¹⁴⁹

2.5. ILC1 Function, Homeostasis, and Disease

Helper-like ILC1 are a developmentally distinct class of cells that express the transcription factor T-bet and produce large quantities of IFN- γ . They are unique from other innate IFN- γ producing cells, namely classical NK cells, as they lack expression of CD49b (DX5) and do not depend on the transcription factor eomesodermin (EOMES).^{41,150} ILC1 are found throughout the body, but accumulate in particularly high levels in the liver and intraepithelial fraction of the intestine.^{151,152} Due to their expression of IFN- γ , these cells have been functionally implicated in many pro-inflammatory settings.

Because of this potent production of IFN- γ , ILC1 are generally considered anti-viral, though firm evidence for this role in humans is presently lacking. ILC1 were found in higher frequencies in the blood of patients with chronic hepatitis B infection and ILC1 frequencies were directly correlated with hepatitis B viral load.¹⁵³ These ILC1 from chronic hepatitis B patients also expressed higher levels of T-bet and IFN- γ compared to ILC1 from healthy controls, suggesting increased activity. However, chronicity of viral infection may paradoxically alter extrinsic factors affecting ILC1, complicating such analyses. For instance, decreases in IL-7 in HIV-infected patients correlated with significantly reduced number of ILC1 in the gastrointestinal tract compared to healthy controls.¹⁵⁴ Further characterization of ILC1 during human viral infection is imperative to firmly establish a role for ILC1, though given their potent expression of IFN- γ it is likely that such a connection exists.

ILC1 have been more robustly characterized in several other human inflammatory conditions. Specifically, ILC1 are recovered in significantly increased frequency from the inflamed intestines of individuals with Crohn's disease compared to healthy controls.¹⁵⁵

Intestinal ILC1 are also increased in patients with wheat sensitivity upon exposure to wheat, and return towards normal levels after initiation of a wheat-free diet.¹⁵⁶ ILC1 are also increased in the duodenum of patients with type 1 diabetes, though the role of ILC1 in this disease process remains unknown.¹⁵⁷ In patients recently diagnosed with rheumatoid arthritis, ILC1 were found in significantly higher frequency in inguinal lymph nodes compared to healthy controls.¹⁵⁸ Interestingly, increases in inguinal lymph node frequency of ILC1 were also observed in patients at-risk for rheumatoid arthritis as defined by serum IgM rheumatoid factor or anti-citrullinated antibody levels without clinical disease, suggesting a potential causative pro-inflammatory role of ILC1 in the establishment of rheumatoid arthritis.¹⁵⁸ Finally, ILC1 have been identified in other tissues in humans including the lung and decidua, though their potential role in disease has not been interrogated to date.¹⁵⁹

Our functional understanding of ILC1 comes largely from studies in mice. Immunity to influenza virus was significantly enhanced in the presence of ILC1 and depended upon T-bet expression.¹⁶⁰ Complementing this data, adoptive transfer of ILC1 into Rag2^{-/-} Il2rg^{-/-} mice significantly improved the clearance of the intracellular parasite *Toxoplasma gondii*.⁴¹ Therefore, ILC1 in mice, as expected based on their IFN- γ production, play a critical role in the clearance of viruses and intracellular pathogens. ILC1 also promote the clearance of extracellular pathogens including *Citrobacter rodentium* and *Clostridium difficile*, with IFN- γ and T-bet established as critical mediators in the latter.^{161,162}

Mirroring the increases in ILC1 seen in patients with Crohn's disease, ILC1-derived IFN- γ was critical for pathophysiologic changes observed in anti-CD40-induced colitis in mice.¹⁵¹ Additionally, ILC1 accumulated in subcutaneous adipose tissue of mice fed a high fat diet (HFD).⁹¹ Adoptive transfer of HFD-conditioned ILC1 into HFD-fed Rag2^{-/-} Il2rg^{-/-} mice

promoted insulin resistance by expression of IFN- γ and polarization of adipose tissue macrophages to a pro-inflammatory phenotype.⁹¹ ILC1 are also induced with COPD-associated triggers such as cigarette smoke exposure.¹⁶⁰ Collectively, human and murine data point to a key pro-inflammatory role for ILC1, particularly in the context of viral immunity, inflammatory bowel disease, and diabetes.

2.6. ILC3 Function, Homeostasis, and Disease

ILC3 are a heterogeneous subset of ILC that are activated by IL-23 and are major producers of IL-17 and IL-22. The transcription factor ROR γ t governs ILC3 fate and function.¹⁶³ Two distinct subsets of ILC3 exist and are separated based on their surface expression of NKp46 (mice) or NKp44 (humans). NKp46⁺ ILC3 are associated with increased IL-22 production, while NKp46⁻ ILC3 are more substantial producers of IL-17.^{163,164} ILC3 are populous throughout the gastrointestinal tract and localize within the lamina propria.¹⁵² ILC3 are implicated in homeostatic as well as pathologic roles.

Within the gastrointestinal tract in particular, the commensal microbiome critically influences the immune system. Commensal bacteria promote a tolerogenic immune response skewed towards T regulatory cells and anti-inflammatory mediators. This enhancement of the regulatory compartment within the gastrointestinal tract is necessary to protect against inappropriate immune activation in the context of innocuous luminal contents such as food.¹⁶⁵ Alterations in the microbiota that lead to overgrowth of pathogenic bacterial species or disruptions in the intestinal barrier integrity are believed to be initiating or exacerbating events in the pathogenesis of inflammatory bowel disease and celiac disease.¹⁶⁵

An ILC3-dependent axis contributes to the maintenance of the healthy tolerogenic phenotype within the gut. Commensal microbes induce IL-1 β , which promotes the expression of Csf2 (GM-CSF) by ILC3 that controlled dendritic cells leading to increased potential for T regulatory differentiation.¹⁶⁶ In this same study, ILC3-derived Csf2 was shown to promote a tolerance loop towards dietary antigens, providing *in vivo* evidence that ILC3 promote tissue homeostasis within the gastrointestinal tract. ILC3 also express MHC class II, which is used to present commensal antigens, identify T cells reactive to these antigens, and eliminate these T cells by starving them of the key lymphocyte growth factor IL-2.^{167,168} This mechanism of peripheral tolerance is dependent upon ILC3-specific expression of MHC II and prevents the development of lethal spontaneous inflammation directed against host commensals. However, this phenotype has not been observed in related mouse models, suggesting additional complexity to this interaction.¹⁶⁹

ILC3 elaborate IL-22, an IL-10 family member that acts on stromal cells to promote epithelial barrier integrity and defense against bacterial pathogens.^{170,171} ILC3-specific expression of IL-22 is required for protection against *Citrobacter rodentium* infection in the absence of an adaptive immune system, and exogenous delivery of IL-22 rescues this phenotype.^{163,172} These IL-22-associated effects are likely in part mediated by increased production of antimicrobial products as a result of IL-22 signaling.^{173,174} ILC3-derived IL-22 is also required for the maintenance of intestinal stem cells and activation of the epithelium in the context of tissue damage.¹⁷⁵ In the skin, ILC3 accumulate within wounds, express elevated levels of IL-22 and IL-17F, and promote healing.¹⁷⁶ Additionally, IL-17 is a major ILC3 cytokine product. Skewing of ILC3 responses towards IL-17 production was associated the development of innate intestinal pathology.¹⁶⁴ Moreover, IL-17A production by ILC3 induced

airway hyperreactivity in a mouse model of obesity-associated asthma.¹⁷⁷ NKp46/NKp44 expression may regulate the balance of IL-17A and IL-22 production, with NKp46/NKp44⁺ ILC3 skewed towards IL-22 production and NKp46/NKp44⁻ ILC3 skewed towards IL-17A production.^{163,164} These data highlight the heterogeneity of ILC3 function, with potential for both protective and pathologic roles.

In humans, ILC3 have been evaluated in the context of inflammatory bowel disease (IBD), including Crohn's disease and ulcerative colitis (UC). Crohn's disease patients have reduced numbers of IL-22-expressing ILC3 in the intestine, though similar changes were not observed in UC.¹⁵⁵ However, IL-17-expressing ILC3 may actually be increased in Crohn's disease, reflecting a shift in the balance from IL-22 production to the more inflammatory mediator IL-17.¹⁷⁸ In patients with IBD, colonic ILC3 expression of MHC II was diminished, suggesting reduced potential for elimination of commensal-reactive T cells that may drive inflammation.¹⁶⁸ In summary, these data from humans and mice suggest an important role for ILC3 in mucosal tissue homeostasis and defense against bacterial pathogens.

2.7. ILC Plasticity

While ILC are classically grouped into the three main classes described above, evidence suggest that certain stimuli can promote interconversion between ILC1, ILC2, and ILC3. Specifically, IL-12 and IL-18 promote the transition of ROR γ t⁺ ILC3 into T-bet⁺ ILC1 that express IFN- γ .¹⁷⁹ Conversely, signaling via IL-23 on ILC1 can upregulate ROR γ t⁺ and IL-17 expression consistent with an ILC3-like phenotype. Similarly, IL-12 promotes the conversion of ILC2 to IFN- γ -expressing ILC1 that upregulate T-bet.^{140,160} Ex-ILC2 that have converted to

ILC1 have the potential to revert back to an ILC2-like phenotype in the presence of IL-4. However, *de novo* generated ILC1 do not appear to have this capacity.¹⁴⁰

2.8. Summary

Allergic disease is a major cause of morbidity in the United States and globally. Respiratory viruses are strongly associated with the development and exacerbation of allergic asthma. ILC2 are at the center of these processes, and the data presented in Chapters 3, 4, and 5 aims to significantly advance the field of ILC biology and our understanding of allergic inflammation.

CHAPTER 3

RSV INFECTION ACTIVATES IL-13-PRODUCING ILC2 VIA TSLP

3.1. Introduction

Respiratory syncytial virus (RSV) is the leading cause of infant hospitalization in the United States.¹⁸⁰ RSV induces bronchiolitis and viral pneumonia, and in severe cases, can lead to death. Severe RSV infection in infancy is also linked to the subsequent development of asthma, and RSV can cause asthma exacerbations in older children and adults.⁶ Current therapeutic options are limited. Ribavirin, a nucleoside analog that inhibits viral replication, has shown poor effectiveness in treating RSV-induced disease.¹⁸¹ Corticosteroids have also proven ineffective during viral-induced bronchiolitis, failing to reduce the number of hospital admissions, length of stay, or disease severity.¹⁸²⁻¹⁸⁴ The majority of treatment strategies are supportive, focusing on fluid and respiratory maintenance. Widely-available, cost-effective preventative options are also lacking. The only FDA-approved preventative therapy is palivizumab, an antibody directed against the surface-exposed RSV fusion protein, which given as prophylaxis decreases the number of RSV-associated hospitalizations by up to 55%.^{185,186} While effective, palivizumab is prohibitively expensive for widespread use and is currently only recommended for infants in the first year of life with chronic lung disease, with hemodynamically significant congenital heart disease, or born significantly premature (< 29 weeks).¹⁸⁷ Moreover, decades of research have failed to yield a safe and effective RSV vaccine.

Our incomplete understanding of the immune response to RSV presents a major obstacle to the development of new therapeutics and a vaccine. It is unclear which aspects of the immune response are protective and which are detrimental. Severe RSV infection in infants is characterized by airway epithelial cell destruction and sloughing, mucus production, peribronchiolar inflammation, and pulmonary obstruction.¹⁸⁸ Classically, mucus production has been associated with the activation of CD4⁺ Th2 cells.¹⁸⁹ CD4⁺ Th2 cells mediate responses to certain viral, parasitic, bacterial, and allergen exposures and produce the cytokine interleukin 13 (IL-13), a central mediator of airway reactivity and mucus production.¹⁹⁰ However, no studies have evaluated early IL-13 production during RSV infection prior to CD4⁺ Th2 cell maturation. A better understanding of the host immune response to RSV will inform rational design of new clinical and pharmacologic interventions.

Group 2 innate lymphoid cells (ILC2) are an early, significant source of IL-13 in several other pulmonary diseases.^{61,63,68,102,124,126,191–194} Our understanding of lung ILC2 has largely come from investigations into their role in allergic asthma, where they have been characterized as important mediators of airway responsiveness, eosinophilia, and mucus production.^{61,63,102,192,193} Several studies have also shown that ILC2 can play a role in pathologic changes during influenza and rhinovirus infections via either IL-33 or IL-25, though the effect of TSLP on viral-induced ILC2 activation in the lungs remains unknown.^{68,124–126,194}

We hypothesized that RSV induces a robust IL-13-producing ILC2 response during the early phase of RSV infection in a murine model. To test this hypothesis, we used the RSV clinical strain 01/2-20 that was isolated from a patient with RSV bronchiolitis and potentiated IL-13 production in mice.¹⁹⁵ We identified a significant increase in the total lung IL-13 concentration and the number of IL-13⁺ ILC2 at day 4 post-infection. TSLP signaling was

required for this ILC2 enhancement. Moreover, RSV-infected TSLP receptor-deficient mice had reduced lung IL-13 protein concentration, decreased airway mucus and reactivity, were partially protected from RSV-induced weight loss, and had comparable viral loads to wild type mice. Finally, infection of mice with recent clinical isolates of RSV with known human pathogenic potential demonstrated a similar induction of IL-13⁺ ILC2 at day 4 post-infection that required TSLP. Collectively, these data demonstrate a critical role for TSLP in RSV-induced ILC2 activation, suggesting this cytokine as a potential therapeutic target to treat the immune-associated pathology of severe RSV illness.

3.2. Methods

3.2.1. Virus and Mice

Unless otherwise noted, all experiments were performed using RSV strain 01/2-20, which was isolated from a patient in 2001 in the Vanderbilt Vaccine Clinic (Nashville, TN).¹⁹⁵ The 01/2-20 strain was selected due to its recent isolation with limited *in vitro* passaging and its mucogenic potential. Where indicated, we performed experiments using RSV strains 12/11-19 and 12/12-6, which were isolated in 2012 from hospitalized patients with severe lower respiratory tract infection and bronchiolitis as part of the Infant Susceptibility to Pulmonary Infections and Asthma Following RSV Exposure (INSPIRE) study.¹⁹⁶ These viruses were propagated and titrated in HEp-2 cells as previously described.¹⁹⁷ Mock inoculum was prepared by collecting cell culture supernatant from lysed, uninfected HEp-2 cells. UV-inactivation was performed by exposing the virus directly to a 30 watt UV light for 40 minutes on ice. Female, 8-

12 week old IL-33 citrine reporter (IL-33-deficient; IL-33 KO) mice, TSLP receptor-deficient (TSLPR KO) mice, or wild type BALB/c (WT) mice were used in compliance with the revised 1996 Guide for the Care and Use of Laboratory Animals prepared by the Committee on Care and Use of Laboratory Animals of the Institute of Laboratory Animal Resources, National Research Council. IL-33 KO mice and TSLPR KO mice were generated on or backcrossed to a BALB/c background as previously described.^{65,198,199} Wild type BALB/c mice were purchased from the Jackson Laboratory. Mice were housed in microisolator cages under specific pathogen free conditions. For infection, mice were anesthetized with a ketamine/xylazine solution and inoculated via intranasal delivery with 3.0×10^6 PFU of RSV 01/2-20, 1.0×10^6 PFU of RSV 12/11-19, 9.0×10^5 PFU of RSV 12/12-6, or an equal volume of mock inoculum as previously described.¹⁹⁷ Illness severity was measured daily by weight loss.

3.2.2. ELISA

Lungs were snap-frozen in liquid nitrogen at the time of harvest. Lungs were mechanically disrupted using 1 mL of radioimmunoprecipitation assay buffer (RIPA buffer, Sigma-Aldrich, St. Louis, MO) with complete protease inhibitor (Roche Applied Science, Penzberg, Germany) in a BeadBeater (BioSpec Products, Bartlesville, OK). Protein measurements were performed as per manufacturer instructions using ELISA kits from R&D Systems (Minneapolis, MN) for IL-25 (DuoSet), IL-33 (DuoSet), TSLP (Quantikine), IL-4 (Quantikine), IL-5 (Quantikine), and IL-13 (Quantikine).

3.2.3. Flow Cytometry

Right and left lungs were digested in RPMI media with 5% FBS, 1 mg/mL collagenase, and 0.02 mg/mL DNase I for 60 minutes at 37°C. A single cell suspension was generated by straining these digestions through a 70 µm filter. RBC lysis (BioLegend, San Diego, CA) was performed as per manufacturer instructions. Cells were restimulated with 10 ng/mL of PMA and 1 µM ionomycin in the presence of 0.07% monensin in IMDM media supplemented with 10% FBS, 0.01 mM non-essential amino acids, penicillin/streptomycin, and 1 mM sodium pyruvate for 6 hours at 37°C. Cells were stained with Live/Dead Blue (Life Technologies, Carlsbad, CA) and combinations of the following surface markers: CD45 (30-F11) and CD25 (PC61.5) from eBioscience (San Diego, CA); CD127 (SB/199) and CD3 (17A2) from BioLegend (San Diego, CA); TSLPR (goat polyclonal) from R&D; and a surface marker cocktail containing CD5, CD45R (B220), CD11b, Gr-1 (Ly-6G/C), 7-4, and Ter-119 from Miltenyi (Bergisch Gladbach, Germany). Cells were fixed/permeabilized and stained for with combinations of the following intracellular markers: IL-13 (eBio13A) and Ki67 (SolA15) from eBioscience; IL-5 (TREK5) from BD Biosciences (San Jose, CA). All samples were run on a BD LSR II Flow Cytometer and analyzed using FlowJo Software Version 10. Total innate lymphocytes (ILC) were defined as Lineage⁻ CD45⁺ CD25⁺ CD127⁺ cells where Lineage (Lin) includes (CD3, CD5, CD45R [B220], CD11b, Gr-1 [Ly-6G/C], 7-4, and Ter-119). ILC2 were defined as ILC that expressed IL-5 and/or IL-13. T cells were defined as CD45⁺ CD3⁺ cells. MFI was determined as the geometric mean.

3.2.4. *In Vivo* TSLP Neutralization

The monoclonal hybridoma cell line 28F12 was grown and anti-TSLP antibodies were purified by the Vanderbilt Antibody and Protein Resource. The 28F12 hybridoma was developed by Dr. Andrew Farr and was obtained from the Developmental Studies Hybridoma Bank (DSHB). The DSHB was created by the NICHD of the NIH and maintained at The University of Iowa, Department of Biology, Iowa City, IA 52242. The 28F12 monoclonal antibody has demonstrated TSLP neutralizing activity with efficacy for *in vivo* depletion²⁰⁰⁻²⁰². Purified monoclonal rat IgG2aκ isotype control antibody was purchased from BioLegend (Cat. # 400544). At either 6 hours or 36 hours post RSV infection, mice received a single dose of 200 µg of 28F12 or isotype control antibody via intraperitoneal injection.

3.2.5. BAL and PAS Staining

An intratracheal tube was inserted and lungs were flushed with 0.8 mL of physiologic saline. An aliquot of BAL fluid was taken to determine total cells counts. For cell differentials, 0.1 mL of BAL fluid was spun onto slides and stained with Diff-Quik kit (American Scientific Products) to visualize macrophages, lymphocytes, eosinophils, and neutrophils. For PAS staining, lungs were perfused with 1x PBS, inflated with 10% neutral buffered formalin, and fixed in 20 mL of 10% neutral buffered formalin for 24 hours at room temperature. Lungs were then transferred to 70% ethanol, paraffin embedded, sectioned (5 µm), and stained with periodic acid-Schiff (PAS) to visualize mucus. Small and medium sized airways were scored for mucus by a trained pathologist blinded to the experimental information using the following scoring

scheme: (0) no PAS positive cells observed in cross sections of medium to small airways; (1) less than 10 PAS positive cells observed in cross sections of medium to small airways; (2) greater than 10 PAS positive cells observed in cross sections of medium to small airways; (3) greater than 10 PAS positive cells observed in cross sections of medium to small airways with mucous strands observed in air spaces; or (4) greater than 10 PAS positive cells observed in cross sections of medium to small airways with mucous plugging of airways.

3.2.6. Corticosteroid Treatment

Dexamethasone 21-phosphate disodium salt (Sigma-Aldrich) was prepared by dissolving in PBS. Mice were treated with 2.5 mg/kg dexamethasone or equivalent volume of PBS vehicle via intraperitoneal injection. Mice were treated 24 hours prior to infection, 1 hour prior to infection, and every 24 hours after infection until mice were euthanized.

3.2.7. Airway Reactivity

Airway reactivity was measured as previously described^{203,204}. Briefly, mice were anesthetized with an intraperitoneal injection of pentobarbital sodium (85 mg/kg). A tracheostomy tube was inserted for ventilation. The internal jugular vein was cannulated for intravenous delivery of acetyl- β -methacholine. The mice were then placed in a whole body plethysmography chamber and mechanically ventilated. Precision glass microsyringes were used to deliver increasing doses of acetyl- β -methacholine. Baseline airway resistance measurements were collected followed by measurements with 45, 137, 411, and 1233 $\mu\text{g}/\text{kg}$

body weight of acetyl- β -methacholine. Peak airway reactivity measurements for each dose were recorded.

3.2.8. Viral Load

Mice were infected with 3.0×10^6 PFU of RSV 01/2-20 as described above. On days 2, 4, and 6 post-infection, lungs were collected, weighed, and snap-frozen. Thawed lungs were resuspended in 1 mL of sterile MEM media and homogenized via BeadBeater. Lung homogenates were serially diluted and used to infect subconfluent HEp-2 cells in 12 well plates for 1 hour at room temperature while shaking. Cells were subsequently overlaid with MEM supplemented with 10% FBS, penicillin G, streptomycin, gentamicin, amphotericin B, and 0.75% methylcellulose and incubated at 37°C. After 6 days, cells were fixed for 1 hour with 10% neutral buffered formalin and stained with hematoxylin and eosin to visualize plaques.

3.2.9. Statistical Analysis

Data were analyzed using GraphPad Prism version 5. Differences between groups were evaluated by unpaired t-test, one-way analysis of variance (ANOVA) with Bonferroni post test, or two-way ANOVA with Dunn's multiple comparison test, as appropriate. Measurements below the limit of detection were assigned half of the value of the limit of detection to allow for statistical analyses.

3.3. Results

3.3.1. RSV Infection Increases Lung IL-13 and the Number of IL-13⁺ ILC2 at Day 4 Post-Infection

We first determined the kinetics of IL-13 expression in the lungs of RSV-infected mice. 8 week old WT mice were infected with 3×10^6 PFU of RSV clinical isolate 01/2-20 and lungs were harvested on days 0, 2, 4, 6, 8, and 10 for measurement of IL-13 by ELISA. There was a significant induction of IL-13 protein in the lungs of RSV-infected mice compared to mock-infected mice beginning at day 4 post-infection and continuing through day 8 post-infection (Figure 3-1 A). We hypothesized that ILC2 rather than T cells were the predominant source of the early IL-13 observed at day 4 post-infection, as this time point precedes the adaptive immune response during RSV infection.²⁰⁵ No unique surface marker(s) is presently known to identify ILC2 exclusively. We defined innate lymphocytes (ILC) by flow cytometry as hematopoietic lineage marker (CD3, CD5, B220, CD11b, Gr-1, 7-4, and Ter-119) negative CD45⁺ CD25⁺ CD127⁺ and ILC2 as ILC that are IL-5⁺ and/or IL-13⁺ (Figure 3-2).³³

At day 4 post-infection, we noted a significant increase in the total number of cells in the lung, the percentage of live cells that were ILC and IL-13⁺ ILC2, and the total number of ILC and IL-13⁺ ILC2 in RSV-infected mice relative to mock-infected mice (Figure 3-1 B-E and G-H). Moreover, viral replication was required for this phenomenon as inoculation with UV-inactivated virus did not increase the number of ILC or IL-13⁺ ILC2 compared to mock inoculum (Figure 3-1 B-E and G-H). Additionally, the ILC compartment had an increased side-scatter MFI, consistent with an activate state (Figure 3-1 F).^{102,206} Finally, the MFI of IL-13 in

ILC2 was higher in the RSV-infected group compared to inoculation with mock preparation or UV-inactivated virus, suggesting increased production of IL-13 on a per ILC2 basis following RSV infection (Figure 3-1 I). As expected at day 4 post-infection, IL-13⁺ T cells were not detected as staining for IL-13 in the CD3⁺ T cell compartment was comparable to isotype signal (Figure 3-1 B).

ILC2 also have the potential to express considerable amounts of IL-5 in addition to IL-13. We did not identify appreciable concentrations of IL-4 or IL-5 by ELISA in RSV-infected mice compared to mock-infected mice during the first 10 days after RSV infection, with only IL-4 being statistically significant but just slightly above the limit of detection at day 6 post-infection (Figure 3-3 A-B). Consistent with this finding, we did not identify a significant difference in the total number of IL-5⁺ ILC2 or in the MFI of IL-5 at day 4 post-infection between mock and RSV-infected mice (Figure 3-3 C-F). Furthermore, RSV-infection did not increase the percent or total number of eosinophils in the BAL at day 4 post-infection compared to mock-infected mice (Figure 3-3 G-H). These data suggest that the predominant functional capacity of ILC2 induced during RSV infection is the expression of IL-13.

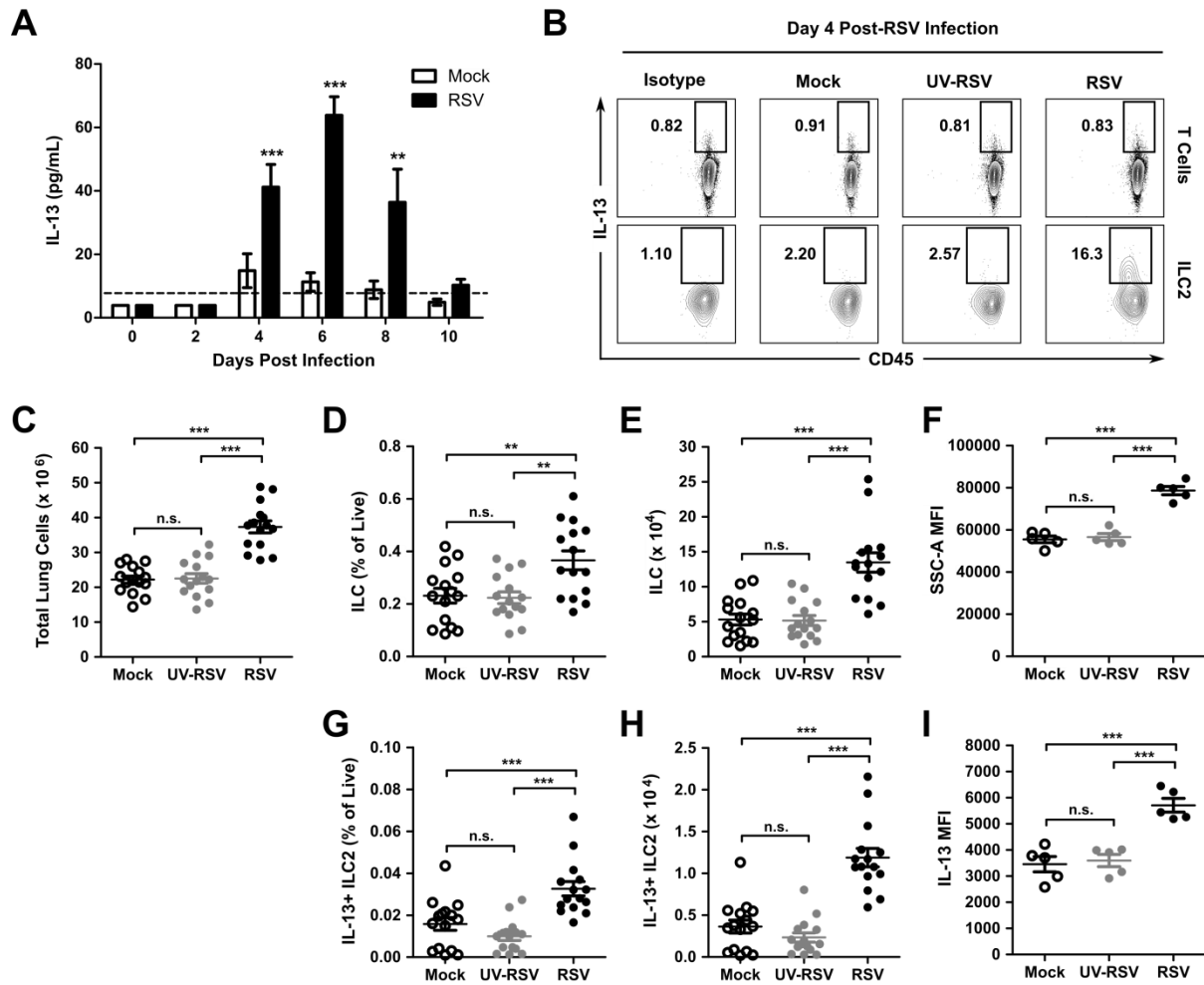


Figure 3-1. RSV infection induced whole lung IL-13 accumulation and IL-13-producing ILC2 at day 4 post-infection.

WT mice were infected with 3×10^6 PFU of RSV strain 01/2-20 and harvested on days 0-10 post-infection. (A) ELISA for IL-13 in whole lung homogenate (right lung only). (B) Representative IL-13 expression measured by flow cytometry in ILC2 ($\text{Lin}^- \text{CD45}^+ \text{CD25}^+ \text{CD127}^+ \text{IL-13}^+$) and T cells ($\text{CD45}^+ \text{CD3}^+ \text{IL-13}^+$) compared to isotype control staining at day 4 post-infection; numbers indicate the percent of T cells or ILC2 within the gated region. (C) Total number of live cells, (D) percent of live cells that are ILC, (E) total number of ILC, (F) MFI of side-scatter area in ILC, (G) percent of live cells that are IL-13⁺ ILC2, (H) total number of IL-13⁺ ILC2, and (I) MFI of IL-13 in IL-13⁺ ILC2 measured at day 4 post-infection. Data plotted as mean + SEM. For A, $n = 8-14$ mice per group combined from 3 independent experiments. For B, F, and I, data are representative of 3 independent experiments. For C-E and G-H, $n = 15$ mice per group combined from 3 independent experiments. ** $p < 0.01$ and *** $p < 0.001$ by one-way (C-F) or two-way (A) ANOVA; n.s. = not significant. Dashed line is the limit of detection of the assay.

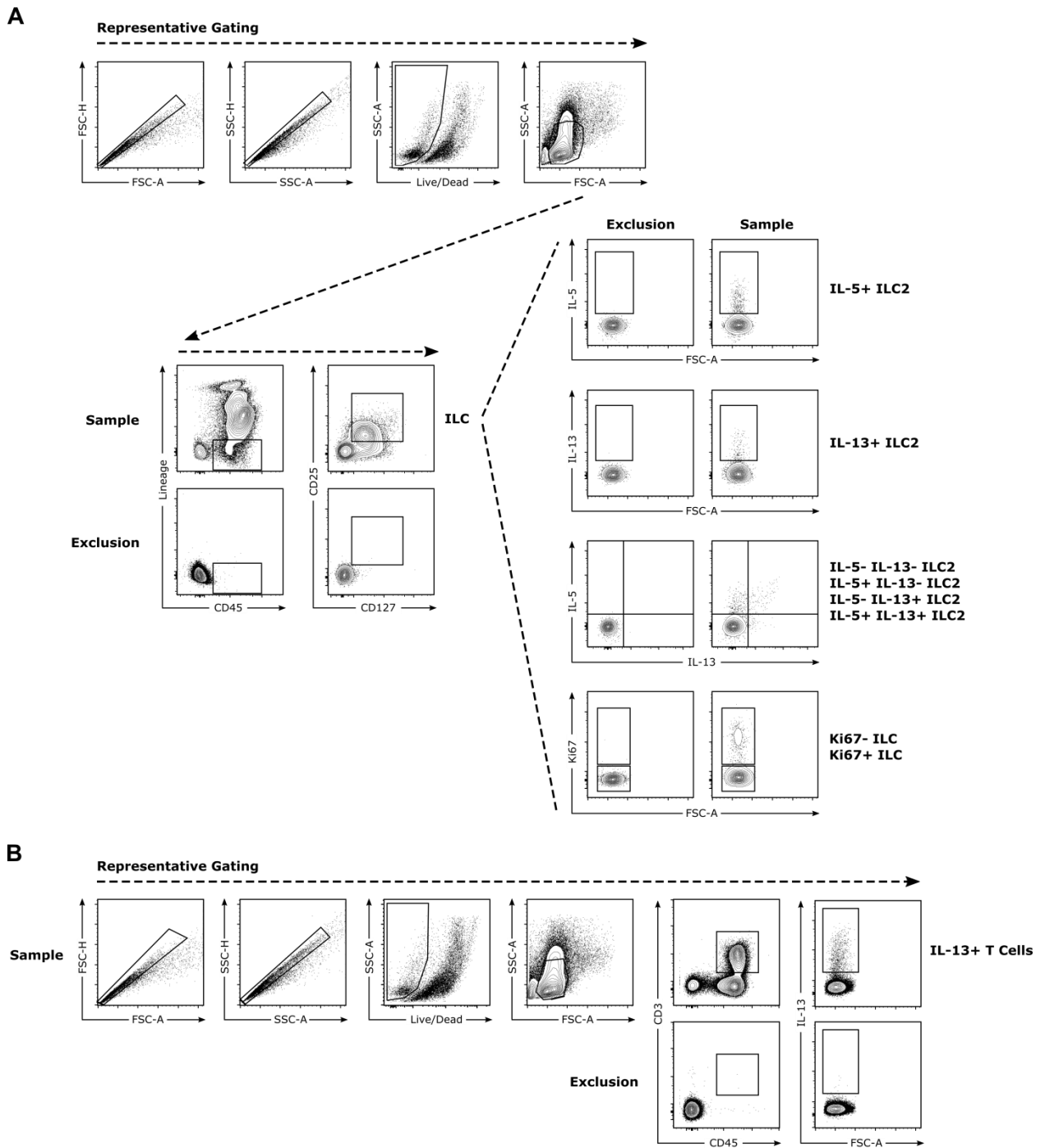


Figure 3-2. Flow cytometry gating strategies.

(A) ILC were defined as viable Lin⁻ CD45⁺ CD25⁺ CD127⁺. ILC2 were defined as ILC that were positive for either IL-5 or IL-13. (B) T cells were defined as viable CD45⁺ CD3⁺ cells.

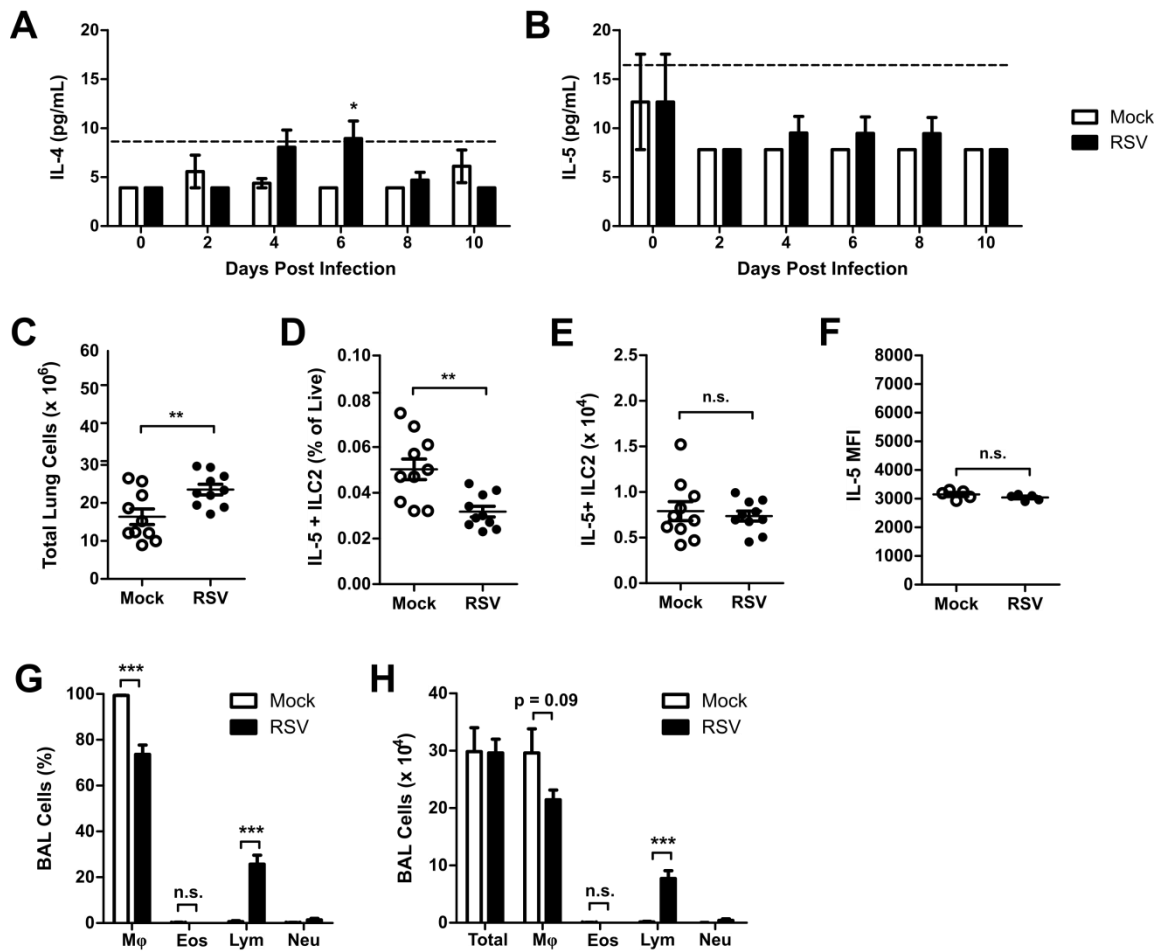


Figure 3-3. RSV does not induce IL-5-producing ILC2.

WT mice were infected with 3×10^6 PFU of RSV strain 01/2-20 and harvested on days 0-10 post-infection. ELISA for (A) IL-4 and (B) IL-5 in whole lung homogenate. (C) Total number of live cells in the lungs at day 4 post-infection. (D) IL-5⁺ ILC2 as a percentage of viable cells as measured by flow cytometry at day 4 post-infection. (E) Total number of IL-5⁺ ILC2 as measured by flow cytometry at day 4 post-infection. (F) MFI of IL-5 staining in ILC2 as measured by flow cytometry at day 4 post-infection. (G) Percent of cells in the BAL at day 4 post-infection. (H) Total number of cells in the BAL at day 4 post-infection. Data plotted as mean + SEM. For A and B, n = 8-14 mice per group combined from 2 independent experiments. For C-E, G, and H, n = 10 mice per group combined from 2 independent experiments. For F, n = 5 mice per group representative of 2 independent experiments. *p < 0.05, **p < 0.01 and ***p < 0.001 by unpaired t test (C-H) or two-way ANOVA (A, B); n.s. = not significant. Dashed line is the limit of detection of the assay.

Moreover, there was a significant increase in the number of total ILC and IL-13⁺ ILC2 that stained for Ki67, a marker of cellular proliferation, at day 4 post-infection in the RSV-infected group compared to mock infection (Figure 3-4). These data suggest that local proliferation of ILC2 within the lungs contributes to the increase in the total number of ILC and IL-13⁺ ILC2 as a result of RSV infection. Collectively, these data suggest that ILC2 are a source of early IL-13 production following RSV infection.

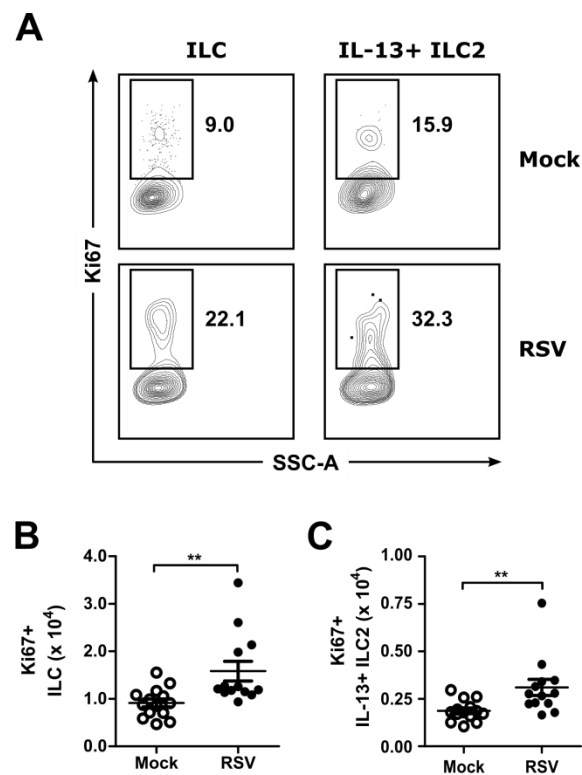


Figure 3-4. RSV stimulated ILC2 proliferation at day 4 post-infection.

WT mice were infected with 3×10^6 PFU of RSV strain 01/2-20 and lungs were harvested for flow cytometry at day 4 post-infection. Cells were gated for viable IL-13⁺ ILC2 and analyzed for Ki67. (A) Representative plots for Ki67 staining; numbers indicate the percent of Ki67⁺ ILC or Ki67⁺ IL-13⁺ ILC2 within the gated region. (B) Total number of Ki67⁺ ILC and (C) Ki67⁺ IL-13⁺ ILC2. Data plotted as mean + SEM. n = 13-14 mice per group combined from 2 independent experiments. **p < 0.01 and ***p < 0.001 by unpaired t test.

3.3.2. TSLP is necessary for the RSV-induced ILC2 response

We next sought to understand the mechanism by which RSV drives ILC2 accumulation in the lungs. TSLP has not previously been recognized to affect ILC2 during respiratory viral infection; however it is a known stimulus of ILC2 in other disease models and can be released from epithelial cells similar to IL-33 and IL-25. Moreover, previous studies have shown that infections with RSV strains A2 and Line 19 provoke TSLP expression in murine lungs, though these studies focused on the effect of TSLP on dendritic cells and Th2 cells.^{207,208} To determine if TSLP is required for the RSV-induced ILC2 response, we first measured the concentration of TSLP by ELISA in the lungs of mock- and RSV-infected mice. We identified a significant increase in the total concentration of TSLP in the lungs of RSV-infected mice compared to mock-infected mice at 12 hours post-infection (Figure 3-5 A). Measurements of TSLP by ELISA between 24 and 96 hours post-infection were all below the limit of detection (data not shown). Consistent with a role for TSLP in lung ILC2 activation during RSV infection, we identified that lung ILC2 in naïve mice express the TSLPR and are thus poised to respond directly to TSLP (Figure 3-5 B). To determine the role of TSLP during RSV-induced ILC2 activation, we assayed the total number of ILC and IL-13⁺ ILC2 in TSLPR KO mice at day 4 post-infection. Both wild type and TSLPR KO mice displayed a substantial inflammatory response to RSV infection (Figure 3-5 C). However, RSV-infected TSLPR KO mice had significantly reduced numbers of total ILC compared to WT RSV-infected mice (Figure 3-5 D). Among these ILC, RSV-infected TSLPR KO mice had similar numbers of IL-13⁺ ILC2 compared to mock-infected TSLPR KO mice and significantly reduced numbers of IL-13⁺ ILC2

compared to RSV-infected wild type mice (Figure 3-5 E). TSLPR expression was also upregulated on total ILC following RSV infection (Figure 3-5 F), and was selectively enhanced on IL-5⁻ IL-13⁺ ILC2 (Figure 3-5 G). Similarly, TSLPR expression was upregulated on Ki67⁺ ILC compared to Ki67⁻ ILC (Figure 3-6 A) and high levels of expression were restricted to Ki67⁺ IL-5⁻ IL-13⁺ ILC2 (Figure 3-6 B).

To determine the plausibility of exogenously targeting TSLP signaling during RSV infection, we tested the effect of a TSLP neutralizing antibody (clone 28F12) on RSV-driven ILC2 induction (Figure 3-5 H). RSV-infected mice treated either 6 hours or 36 hours post-infection with a single 200 µg dose of TSLP neutralizing antibody had a trend for a decrease in the total numbers of ILC compared to RSV-infected mice treated with isotype control antibody, but this was not statistically significant (Figure 3-5 I). Importantly, there was a statistically significant decrease in the number of IL-13⁺ ILC2 in the groups receiving TSLP neutralizing antibody at either 6 hours or 36 hours post-infection compared to RSV-infected mice treated with isotype control antibody (Figure 3-5 J). Consistent with these data, we found that treatment of mice every 24 hours with dexamethasone beginning 24 hours prior to infection decreased lung TSLP expression and the total number of IL-13⁺ ILC2 at day 4 post-infection compared to vehicle treated mice, further highlighting the importance of TSLP during RSV-induced ILC2 activation (Figure 3-7). Of note, dexamethasone was given prophylactically in our model, a key distinction from human trials of corticosteroids in which administration has been post-infection and demonstrated to be ineffective. Collectively, these data strongly suggest a TSLP-dependent mechanism for the induction of IL-13-producing ILC2 following RSV infection that could be potentially exploited therapeutically.

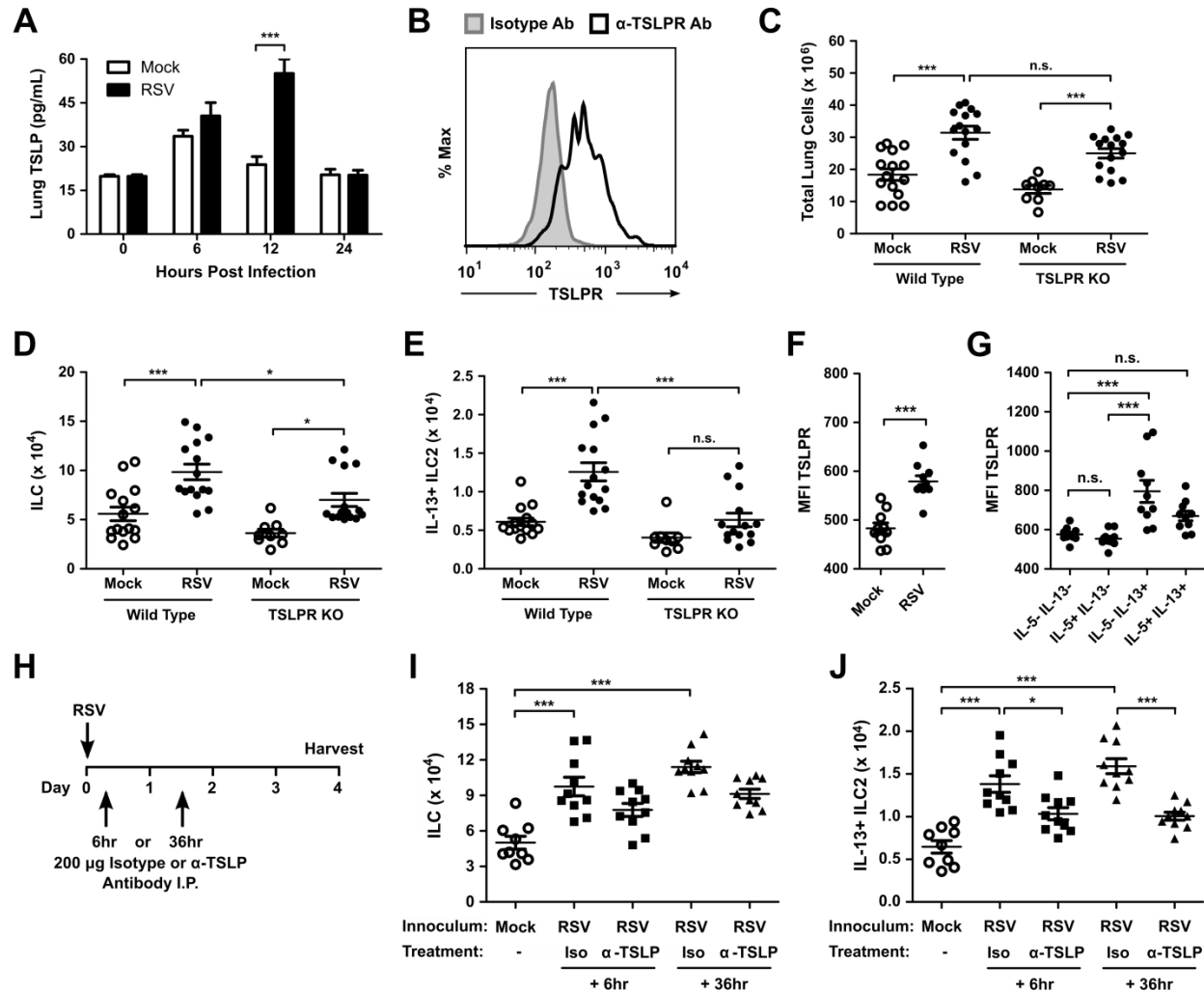


Figure 3-5. RSV-induced TSLP signaling is required for ILC2 activation.

WT or TSLPR KO mice were infected 3×10^6 PFU of RSV strain 01/2-20 and lungs were harvested for ELISA or flow cytometry. (A) ELISA for TSLP in the whole lung homogenate. (B) TSLPR expression by flow cytometry in IL-13⁺ ILC2 from naïve mice. (C) Total number of live cells, (D) ILC, and (E) IL-13⁺ ILC2 as measured by flow cytometry at day 4 post-infection. (F) MFI of TSLPR on ILC from mock and RSV-infected mice. (G) MFI of TSLPR on ILC subsets in RSV-infected mice. (H) Protocol for *in vivo* neutralization of TSLP. (I) Total number of ILC and (J) IL-13⁺ ILC2 as measured by flow cytometry at day 4 post-infection. Data plotted as mean + SEM. For A, n = 5-10 mice per group combined from 2 independent experiments. For B, data are representative of 2 independent experiments. For C-E, n = 9-15 mice per group combined from 3 independent experiments. For F-G, n = 10 mice per group. For I-J, n = 9-10 mice per group combined from 2 independent experiments. *p < 0.05 and ***p < 0.001 by unpaired t test (F), one-way (C-E, G, I-J), or two-way (A) ANOVA; n.s. = not significant.

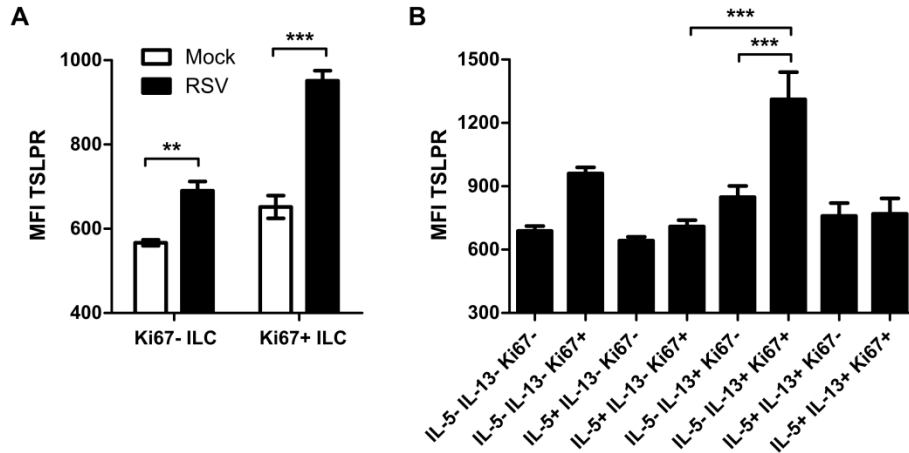


Figure 3-6. TSLPR expression in Ki67+ and Ki67- subsets of ILC at day 4 post-RSV infection.

WT mice were infected with 3×10^6 PFU of RSV strain 01/2-20 and lungs were harvested for flow cytometry. (A) MFI of TSLPR expression by flow cytometry at day 4 post-RSV infection stratified by Ki67 expression status. (B) Subset analysis of ILC stratified by Ki67 expression status in RSV-infected mice at day 4 post-infection. Data plotted as mean + SEM. For A and B, n = 5 mice per group. ***p < 0.001 by one way ANOVA.

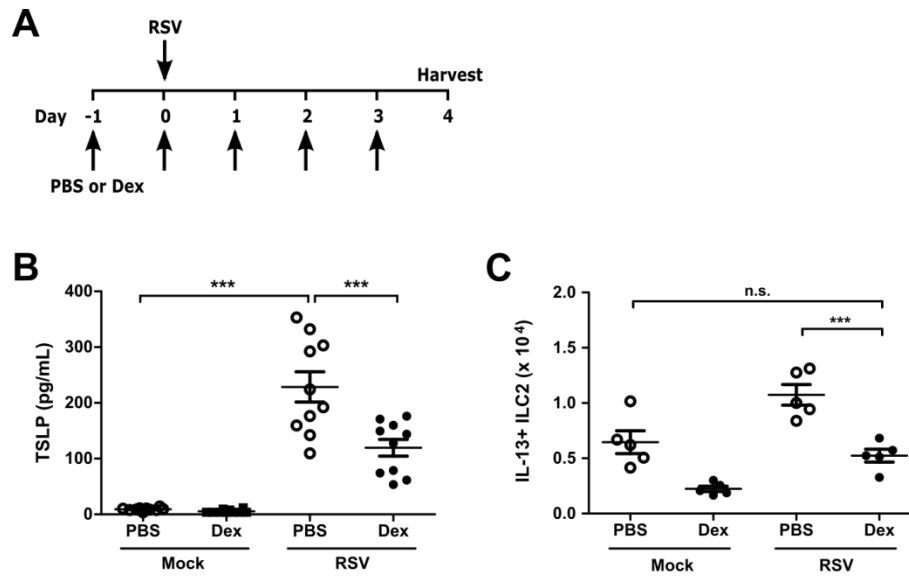


Figure 3-7. Pre-treatment of mice with dexamethasone decreases TSLP expression and ILC2 activation.

WT mice were treated every 24 hours with 2.5 mg/kg of dexamethasone beginning 1 day prior to infection and up until harvest. Mice were infected on day 0 with 3×10^6 PFU of RSV strain 01/2-20 and lungs were harvested for flow cytometry at day 4 post-infection. (A) Protocol for dexamethasone administration. (B) ELISA for TSLP in the whole lung homogenate at 12 hours post-infection. (C) Total numbers of IL-13⁺ ILC2 as measured by flow cytometry at day 4 post-infection. Data plotted as mean + SEM. For B, n = 10 mice per group combined from 2 independent experiments. For C, n = 5 mice per group representative of 3 similar experiments. ***p < 0.001 by one-way ANOVA; n.s. = not significant.

IL-33 and IL-25 have been implicated as activators of ILC2 during infection with other respiratory viruses^{68,124,126,194}, and RSV strain Line 19 has been shown to induce transcription of IL-25.²⁰⁹ To determine the importance of these cytokines during RSV infection, we measured the whole lung concentration of IL-33 and IL-25 protein by ELISA following RSV infection. We identified a significant increase in lung IL-33 protein in RSV-infected mice compared to mock-infected mice at 12 hours post-infection (Figure 3-8 A). IL-25 was below the limit of detection by ELISA across the first 96 hours after infection (data not shown). To determine if IL-33 was required for activating ILC2 during RSV infection, we measured the total number of IL-13⁺ ILC2 in the lungs at day 4 post-infection in wild type and IL-33 KO mice. Both wild type and IL-33 KO mice showed a significant inflammatory response to RSV as measured by total lung cell numbers compared to mock infection (Figure 3-8 B). RSV infection induced a significant increase in the number of IL-13⁺ ILC2 compared to mock infection in both wild type and IL-33 KO mice, and there was no statistically significant difference in the total number of IL-13⁺ ILC2 between RSV-infected wild type and IL-33 KO mice (Figure 3-8 C). There was, however, a significant decrease in the total lung concentration of IL-13 in the RSV-infected IL-33 KO mice compared to RSV-infected WT mice (Figure 3-8 D), highlighting an equivocal role for IL-33 during RSV-induced ILC2 activation in our murine model of infection.

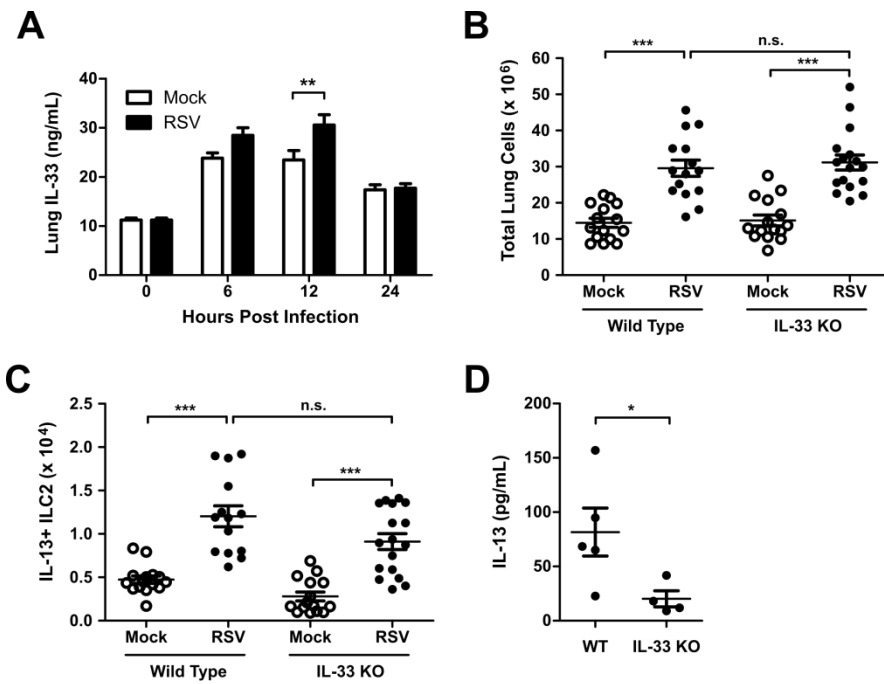


Figure 3-8. RSV-induced IL-33 and ILC2.

WT or IL-33 KO mice were infected with 3×10^6 PFU of RSV strain 01/2-20 and lungs were harvested for ELISA or flow cytometry. (A) ELISA for IL-33 in the whole lung homogenate. (B) Total number of live cells in the lungs at day 4 post-infection. (C) Total numbers of IL-13⁺ ILC2 as measured by flow cytometry at day 4 post-infection. (D) ELISA for IL-13 in the whole lung homogenate (right and left lung) at day 4 post-infection. Data plotted as mean + SEM. For A, n = 5-10 mice per group combined from 2 independent experiments. For B and C, n = 13-17 mice per group combined from 3 independent experiments. For D, n = 4-5 mice per group from 1 independent experiment. *p < 0.05, **p < 0.01, and ***p < 0.001 by one-way (B-C) or two-way (A) ANOVA; n.s. = not significant.

3.3.3. TSLPR-deficient mice have increased IL-13, mucus, and reactivity in the airways following RSV infection

To consider the efficacy of targeting TSLP for the attenuation of ILC2 responses during RSV infection, we considered the effect of TSLPR-deficiency on RSV disease severity. Notably, RSV-infected TSLPR KO mice had significantly decreased levels of whole lung IL-13 compared to RSV-infected WT mice at day 4 post-infection (Figure 3-9 A). TSLP neutralization also had a trend for a decrease in IL-13 whole lung concentration at day 4 post-infection, though this was not statistically significant (Figure 3-10). We next sought to determine the physiologic effect of early RSV-induced IL-13 on mucous cell metaplasia and airway mucus accumulation. To allow time for this early IL-13 to induce physiologic changes in the airways, we evaluated PAS-stained sections of lungs from mock and RSV-infected WT and TSLPR KO mice at day 6 post-infection. Importantly, at day 6 post-infection, there remained a significant increase in the total number of ILC as well as IL-13⁺ ILC2, but not IL-5⁺ ILC2 (Figure 3-11 A-C). Additionally, there was an increase in the total numbers of CD3⁺ T cells but no significant increase in the number of IL-5⁺ or IL-13⁺ T cells, though a trend for an increase was seen with IL-13⁺ T cells (Figure 3-11 D-F). These data suggest that ILC2 remain a major component of the type 2 immune response at day 6 post-infection. In mock-infected WT and TSLPR KO mice, there was minimal or absent mucous cell metaplasia (Figure 3-9 B). In RSV-infected WT mice, we identified moderate mucous cell metaplasia and significant airway mucus accumulation with both intraluminal mucus strands and overt mucous plugging. RSV-infected TSLPR KO mice also exhibited moderate mucous cell metaplasia but they had no substantial intraluminal mucus accumulation. Collective scoring of airways from multiple mice showed a significant decrease

in mucus severity score in RSV-infected TSLPR KO mice compared to RSV-infected WT mice (Figure 3-9 C and Figure 3-12). The primary difference between these groups of mice was related to the amount of intraluminal, obstructing mucus, which was never observed in the RSV-infected TSLPR KO mice. To evaluate airway obstruction and reactivity, we performed a methacholine challenge experiment at day 6 post-infection on mock or RSV-infected WT and TSLPR KO mice. We saw a significant increase in airway reactivity in the RSV-infected WT group compared to the RSV-infected TSLPR KO mice with increasing methacholine concentration (Figure 3-9 D). No significant differences were observed between mock and RSV-infected TSLPR KO mice.

Within the first four days after infection, both RSV-infected WT and TSLPR KO mice had significant weight loss relative to mock-infected controls. However, RSV-infected TSLPR KO mice had significantly less weight loss compared to RSV-infected WT mice (Figure 3-9 E). Next, we sought to determine whether TSLPR-deficiency altered viral load. We did not observe any significant differences in the viral load at days 2, 4, or 6 after RSV infection between TSLPR KO and WT mice (Figure 3-9 F). Together, these data suggest that the absence of TSLP signaling is unlikely to exacerbate disease or increase viral load and implicate TSLP as a potential therapeutic target for attenuating ILC2-associated immunopathology during RSV infection.

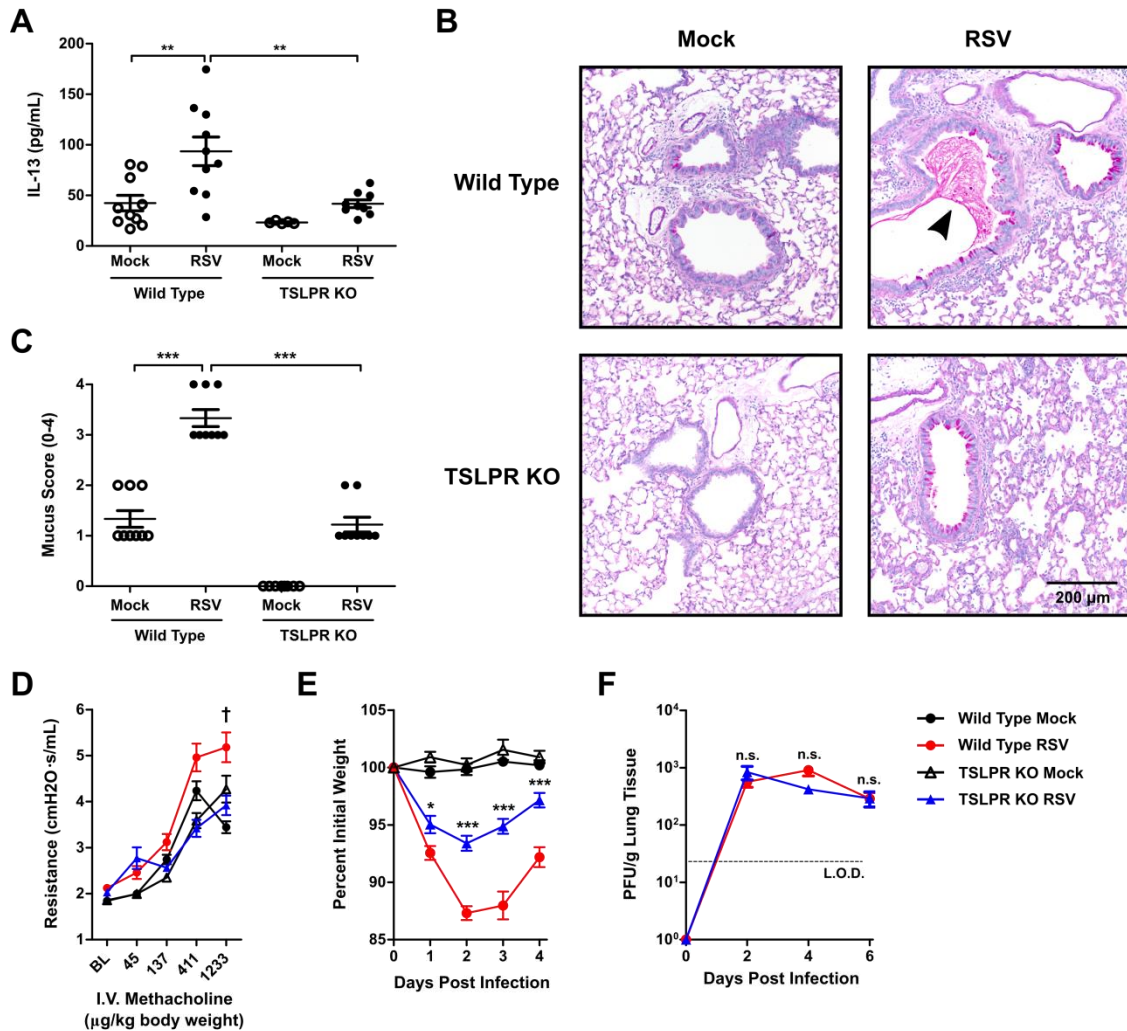


Figure 3-9. TSLPR-deficiency attenuated RSV-induced IL-13 production, airway mucus accumulation, airway reactivity, and weight loss without negative effects on viral load.

WT or TSLPR KO mice were infected with 3×10^6 PFU of RSV strain 01/2-20. (A) IL-13 measured by ELISA from whole lung homogenate (right and left lung) at day 4 post-infection. (B) Representative PAS-stained sections of mucus-containing airways in the lungs on day 6 post-infection (20x magnification); arrowhead (\blacktriangleright) denotes intraluminal mucus plugging. (C) Quantification of airway mucus from the experiment in B; each dot represent a combined airway mucus score for an individual mouse. (D) Airway reactivity measured at baseline and increasing doses of methacholine at day 6 post-infection. (E) Daily weight loss displayed as percentage of original body weight prior to infection. (F) Lung viral titers determined at days 2, 4, and 6 post-infection by plaque assay. For A, $n = 5-10$ mice combined from 2 independent experiments. For B-C, $n = 8-9$ mice per group combined from 2 independent experiments. For D, $n = 5-10$ mice per group. For E, $n = 12-15$ mice per group combined from 3 independent experiments. For F, $n = 6-8$ mice per group combined from 2 independent experiments. All data plotted as mean + SEM. * $p < 0.05$, ** $p < 0.01$, and *** $p < 0.001$ by one-way (A, C) or two-way (D-F) ANOVA; n.s. = not significant. For D-F, statistical comparisons indicated are between Wild Type RSV and TSLPR KO RSV. Dashed line is the limit of detection of the assay. BL = baseline.

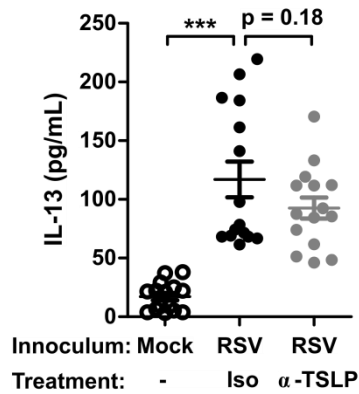


Figure 3-10. Lung IL-13 with TSLP neutralization.

WT mice were infected 3×10^6 PFU of RSV strain 01/2-20, treated with 200 μ g of anti-TSLP antibody or isotype control at 6 hours post-infection, and lungs were harvested for ELISA at day 4 post-infection. ELISA data is shown for measurements of IL-13 in the whole lung homogenate (right and left lung). Data plotted as mean + SEM. For A, n = 15 mice per group combined from 3 independent experiments. ***p < 0.001 by one-way ANOVA.

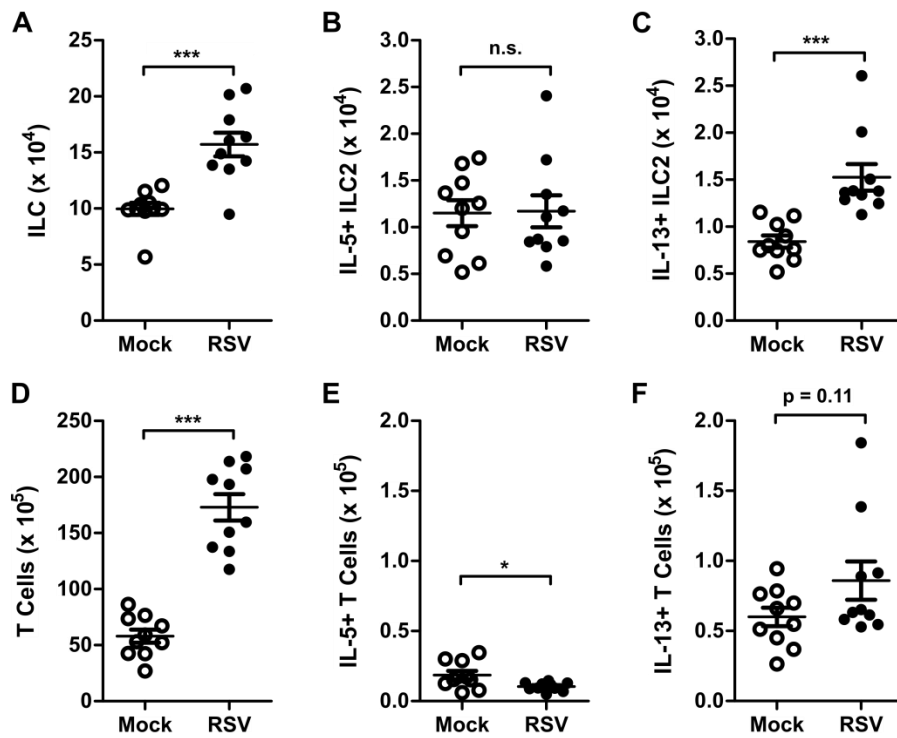


Figure 3-11. Analysis of ILC and T cells at day 6 post-infection.

WT mice were infected with 3×10^6 PFU of RSV strain 01/2-20 and harvested on day 6 post-infection for flow cytometry. Total numbers of (A) ILC, (B) IL-5⁺ ILC2, (C) IL-13⁺ ILC2, (D) T cells, (E) IL-5⁺ T cells, and (F) IL-13⁺ T cells were determined. Data plotted as mean + SEM. For A-E, n = 10 mice per group from 2 independent experiments. *p < 0.05 and ***p < 0.001 by unpaired t test.; n.s. = not significant.

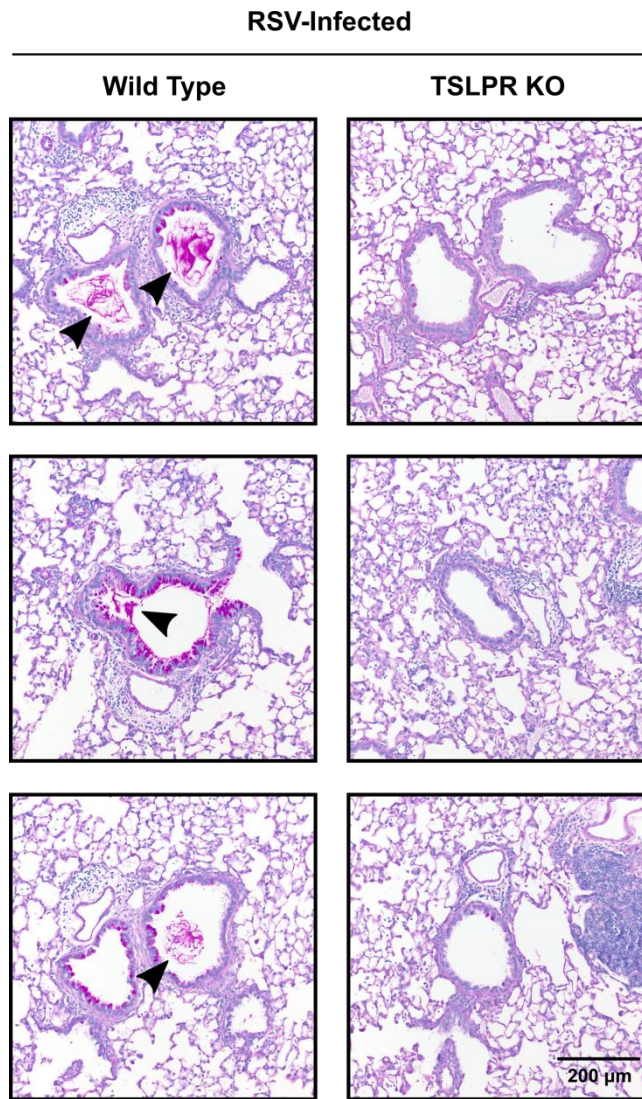


Figure 3-12. Supplementary histopathologic sections from WT and TSLPR-deficient mice at day 6 post-infection.

WT or TSLPR KO mice were infected with 3×10^6 PFU of RSV strain 01/2-20. Additional representative PAS-stained sections of mucus-containing airways in the lungs on day 6 post-infection (20x magnification); arrowhead (►) denotes intraluminal mucus plugging.

3.3.4. Multiple pathogenic clinical isolates of RSV induce IL-13-producing ILC2 via TSLP

To determine the generalizability of our results and their clinical relevance to strains of RSV with known human pathogenic potential, we evaluated the ability of two recently collected clinical isolates of RSV to induce ILC and IL-13⁺ ILC2 and the necessity of TSLP in this process. RSV strains 12/11-19 and 12/12-6 were both isolated in 2012 as part of the Infant Susceptibility to Pulmonary Infections and Asthma Following RSV Exposure (INSPIRE) study from two different patients who were hospitalized with severe lower respiratory tract infection and bronchiolitis.¹⁹⁶ Mice were infected with 1.0×10^6 or 9.0×10^5 PFU of 12/11-19 or 12/12-6, respectively, and the number of ILC and IL-13⁺ ILC2 was determined at day 4 post-infection. Consistent with our results obtained with RSV strain 01/2-20, both 12/11-19 and 12/12-6 induced a significant expansion of total ILC and IL-13⁺ ILC2 by day 4 post-infection (Figure 3-13 A-B). Moreover, anti-TSLP neutralizing antibody was able to significantly attenuate the RSV-induced IL-13⁺ ILC2 response for both 12/11-19 and 12/12-6 (Figure 3-13 A-B). Importantly, both of these clinical isolates induced the accumulation of IL-13 in the whole lung homogenate at day 4 post-infection and airway mucus at 6 post-infection (Figure 3-13 C-E), though significant weight loss was only observed with 12/11-19 (Figure 3-14). Collectively, these data demonstrate that the TSLP-dependent activation of ILC2 is a conserved feature among RSV strains with known human pathogenic potential that have recently circulated in the human population.

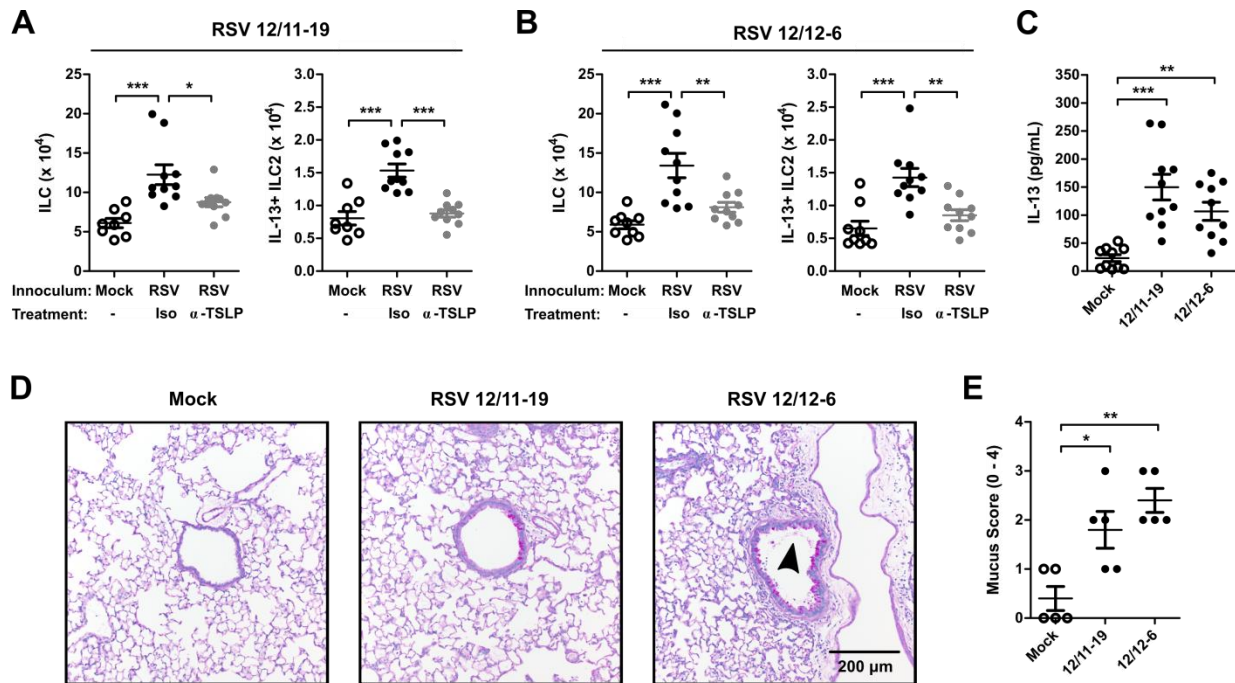


Figure 3-13. Pathogenic clinical isolates of RSV induce IL-13+ ILC2 via TSLP.

WT mice were infected with RSV strains 12/11-19 (1.0×10^6 PFU) or 12/12-6 (9.0×10^5 PFU), treated with either 200 μ g of isotype or anti-TSLP antibody at 6 hours post-infection, and harvested on day 4 or 6 post-infection. Total numbers of ILC and IL-13⁺ ILC2 in mice infected with (A) RSV 12/11-19 and (B) RSV 12/12-6 at day 4 post-infection. (C) Whole lung IL-13 measured by ELISA (right and left lung) at day 4 post-infection. (D) Representative PAS-stained sections of mucus-containing airways in the lungs on day 6 post-infection (20x magnification); arrowhead (\blacktriangleright) denotes intraluminal airway mucus. (E) Quantification of airway mucus from the experiment in D; each dot represent a combined airway mucus score for an individual mouse. Data plotted as mean + SEM. For A and B, $n = 8-10$ mice per group combined from 2 independent experiments. For C, $n = 10$ mice per group combined from 2 independent experiments. For D-E, $n = 5$ mice per group. * $p < 0.05$, ** $p < 0.01$, and *** $p < 0.001$ by one-way ANOVA.

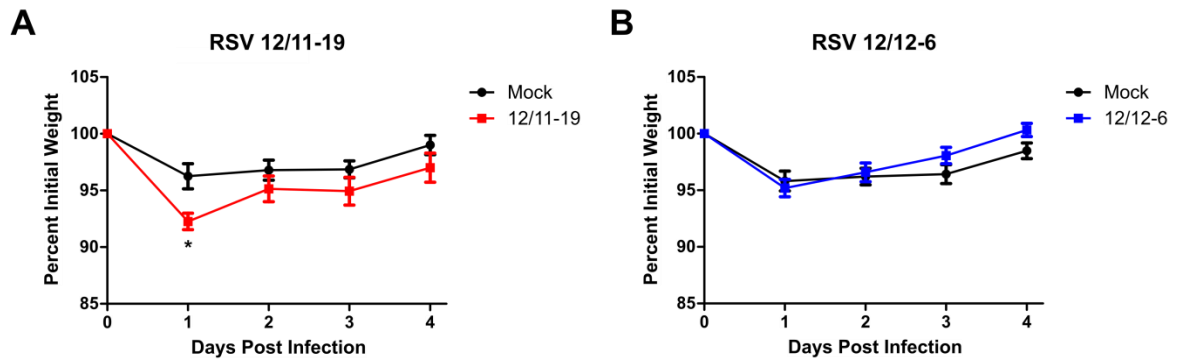


Figure 3-14. RSV-induced weight loss with 2012 clinical isolates.

WT mice were infected with RSV strains (A) 12/11-19 (1.0×10^6 PFU) or (B) 12/12-6 (9.0×10^5 PFU) and weight loss was measured daily for four days. Data are displayed as a percent of initial body weight and represent the mean + SEM. For A-B, $n = 8-10$ mice per group from 2 independent experiments. * $p < 0.05$ by two-way ANOVA.

3.4. Discussion

The immunologic contributions to the pathophysiology of severe RSV infection are incompletely understood. Our studies implicate the recently described group 2 innate lymphoid cells as a key source of IL-13 during the early stages of RSV infection in a murine model. We demonstrated that TSLP signaling was required for induction of ILC2 during RSV infection. Moreover, TSLPR-deficient mice had reduced airway mucus, airway reactivity, and weight loss and a similar viral load compared to wild type mice, suggesting that TSLP may be a potential therapeutic target for IL-13-driven immunopathology associated with RSV. Finally, we identified that multiple recently collected clinical isolates of RSV with known human pathogenic potential induced IL-13-producing ILC2 via a TSLP-dependent mechanism. Collectively, these data demonstrate the importance of ILC2 and TSLP during the early stages of RSV infection and are the first to link TSLP to the activation of ILC2 during a respiratory viral infection.

TSLP is primarily produced by epithelial cells, especially those in the lungs and gut as well as keratinocytes in the skin.^{210,211} Lung epithelial cells are the primary site of RSV infection in humans and mice^{188,195}, suggesting a means by which TSLP may be elaborated rapidly after infection. Interestingly, direct treatment of purified lung ILC with TSLP alone failed to induce cell proliferation or IL-5 and IL-13 cytokine production (data not shown; all values below the limit of detection). It is possible that TSLP is acting on non-ILC to produce further signals that activate ILC2. However, our data demonstrating that lung ILC2 express the TSLPR and that changes in TSLPR expression are restricted to the ILC2 subset that is increasing in number suggest that TSLP is likely having effects directly on ILC2. Previous studies have shown that TSLP acts synergistically with other stimuli, rather than individually, to potentiate murine and

human ILC2.^{50,212} Together, these data suggest that an additional collaborative partner(s) may play a role in conjunction with TSLP during the *in vivo* activation of ILC2 following RSV infection. IL-33 has been shown to be an important activator of ILC2 in mouse models of allergic airway inflammation, influenza infection, and rhinovirus infection.^{61,63,65,102,124,192,194,213} Interestingly, we found similar numbers of IL-13-producing ILC2 following RSV infection in IL-33-deficient mice, though there was a statistically significant decrease in the total lung concentration of IL-13 at day 4 post-infection. These incongruous results could be explained in the IL-33-deficient mice by potentially defective functionality of ILC2 despite similar numbers to wild type mice or different kinetics or localization of the ILC2 response. Also, we cannot exclude additional sources of IL-13 in these mice, including epithelial cells themselves²¹⁴, which could be susceptible to IL-33-deficiency leading to decreased total lung IL-13 concentrations despite stable numbers of IL-13-producing ILC2. Age-variable effects of IL-33 on ILC2 in the mouse model of RSV infection may also play a role.¹⁰⁵ Furthermore, ILC2 activation in the neonatal mouse model of rhinovirus infection requires IL-25.¹²⁶ Additionally, RSV strain Line 19 has been shown to induce IL-25 transcription in mice.²⁰⁹ However, we did not detect this cytokine by ELISA following RSV infection with strain 01/2-20, suggesting it is less likely to play a role in this model. Beyond IL-33 and IL-25, additional pro-inflammatory molecules including cysteinyl leukotrienes (notably LTD₄) and TNF family cytokines (notably TLA1) have recently been identified as activators of ILC2 and may play a role, in conjunction with TSLP, during RSV infection.^{75,215} Future studies will be required to precisely define the network of cytokines influencing ILC2 activation during RSV infection, though our data strongly suggest a critical role for TSLP in this milieu.

Importantly, the identification of TSLP as an activator of ILC2 is distinct from other respiratory viruses. These data highlight that different respiratory viruses induce ILC2 through unique mechanisms. Determination of the precise stimuli for ILC2 in each disease model will be necessary when conceptualizing and developing therapeutics, specifically with monotherapies targeting only IL-33, IL-25, or TSLP.

A recent Phase II randomized control trial evaluated the effectiveness of an anti-TSLP monoclonal antibody, AMG 157, in reducing disease severity in patients with mild allergic asthma.⁸⁶ Patients randomized to AMG 157 had reduced airway obstruction and inflammation relative to patients receiving placebo following aeroallergen challenge. Both airway obstruction and inflammation are associated with Th2 cytokines including IL-13. Given that RSV induces a TSLP-dependent, IL-13-producing ILC2 response in mice and that IL-13 promotes airway obstruction, it is intriguing to consider the therapeutic potential of an anti-TSLP monoclonal antibody for treating severe RSV infection. Our studies demonstrate that a neutralizing monoclonal antibody targeting TSLP was capable of reducing the number of IL-13-producing ILC2 in the lungs of mice following RSV infection, providing a small animal model proof of concept for this therapeutic approach. Critically, it has been demonstrated that RSV infection can stimulate the production of TSLP in primary human airway epithelial cells, supporting the translational significance of TSLP during RSV infection.²⁰⁷ In addition, TSLP has previously been shown to enhance the CD4⁺ Th2 compartment during the later stages of RSV infection.^{207,208} The use of an anti-TSLP monoclonal antibody may also have the dual benefit of decreasing both ILC2 and CD4⁺ Th2 contributions to immunopathology. Additional studies will be required to further assess the feasibility of an anti-TSLP monoclonal antibody during severe RSV infection in humans.

Interestingly, neutralization of TSLP significantly attenuated the IL-13⁺ ILC2 induction during RSV infection whether intervention occurred 6 or 36 hours post-infection. This was surprising given that the peak of TSLP in the lungs occurred 12 hours post-infection. One potential explanation for these data is the continued production of TSLP in the lungs beyond 12 hours post-infection that is physiologically significant but below the limit of detection of the ELISA. Dynamic changes in TSLPR expression on ILC2 may play a critical role in responsiveness to this sub-maximal TSLP. Specifically, we identified that TSLPR is increased in expression on ILC following RSV infection, and that the increased expression clusters most significantly with proliferating Ki67⁺ IL-5⁻ IL-13⁺ ILC2. Increased receptor expression in this subset may allow for continued responsiveness to levels of TSLP that are below the limit of detection of our ELISA.

Furthermore, our data suggest a deficiency in TSLP signaling is unlikely to affect viral load and may improve clinical illness as measured by weight loss, all while attenuating IL-13-producing ILC2, whole lung concentration of IL-13, airway mucus accumulation, and airway reactivity. While the human pathogenesis of RSV is multifaceted, inclusive of both viral and host contributions, several lines of evidence suggest that immunopathology and airway mucus hypersecretion promote disease severity in infants.^{188,216} Importantly, we did not identify any significant increase in viral load in TSLPR-deficient mice, suggesting that the targeting of the TSLP axis is unlikely to exacerbate virally-associated disease metrics while still providing relief to immunopathologic changes in the airways. It is relevant to note that while weight loss is a common measure of illness severity in mice, the direct implications of this murine observation to prognosis or disease course in humans remain unclear.

Respiratory viral infections, including RSV, are an important cause of asthma exacerbations in both children and adults.²¹⁷ Atopic asthma is associated with elevated levels of Th2 cytokines in the airways, including IL-4^{218–220}. Several studies demonstrate that IL-4 enhances the capacity of human airway epithelial cells to produce TSLP.^{221,222} Moreover, the combination of IL-4 plus dsRNA synergistically enhanced the production of TSLP from human airway epithelial cells.²²¹ Together, it is intriguing to consider whether a mechanism exists for RSV-induced asthma exacerbation whereby pre-existing allergic inflammation and IL-4 production may prime airway epithelial cells to produce augmented levels of TSLP upon infection with RSV, leading to an exaggerated ILC2 response with increased Th2 cytokine production. Consistent with this hypothesis, airway epithelial cells isolated from asthmatic children express greater levels of TSLP upon *in vitro* RSV infection than airway epithelial cells isolated from non-asthmatic children.²⁰⁷ Further studies will be needed to determine whether such a mechanism exists, and if so, to what degree it influences RSV-exacerbated asthma.

Our data demonstrate that ILC2 are an important source of IL-13 during the early stages of RSV infection in a murine model. This process required TSLP signaling and the lack of TSLP signaling did not negatively impact viral load but significantly reduced disease severity as measured by weight loss, airway mucus accumulation, and airway reactivity. Additionally, infection of mice with two recent clinical isolates of RSV with known human pathogenic potential similarly induced IL-13-producing ILC2 via a TSLP-dependent mechanism. These studies have significant and broad implications for the targeting of ILC2 during primary RSV infection, potentially via neutralization of TSLP, as well as during RSV-induced wheezing illnesses.

CHAPTER 4

STAT1 REPRESSES ILC2 AND ILC3 DURING RESPIRATORY VIRAL INFECTION

4.1. Introduction

A carefully orchestrated immune response is vital for effective host defense and tissue homeostasis. Both innate and adaptive immune responses are precisely regulated to respond productively to a variety of different environmental insults while simultaneously restricting detrimental host immunopathology. Lymphocytes, both innate and adaptive, exhibit the expected functional diversity to accomplish this arduous task.

Innate lymphoid cells (ILC) are an expansive class of cells that derive from the common lymphoid progenitor and respond rapidly to cytokine stimuli in an antigen-independent manner.²²³ ILC have been classified into three major subsets—ILC1, ILC2, and ILC3, which largely mirror adaptive CD4⁺ Th1, Th2, and Th17 cells, respectively, in both transcriptional regulation and cytokine production. Several endogenous signals have been identified as inhibitors of ILC including prostacyclin (PGI₂), 1,25-dihydroxyvitamin D3, and the natural Ras-ERK inhibitor Spred1.^{78,79,224} In particular, the activation of ILC2 induces detrimental immunopathology in the context of influenza and rhinovirus infection.^{124–126,194,225} Similarly, the activation of CD4⁺ Th2 and Th17 cells has previously been associated with maladaptive immunopathology and enhanced disease severity in the context of viral infection.^{226–230} Conversely, ILC1 have been shown to produce anti-viral mediators in the context of viral infection and/or enhance viral clearance.^{160,231,232}

In Chapter 3, we demonstrated that RSV induces the activation of ILC2 with potential pathophysiologic consequences. Considerations of pathways that repress ILC2 are likely to be of pharmacologic interest. If those pathways can also mediate beneficial changes in ILC1 or ILC3, it would be of particularly high value.

Coordinated responses to viral infection, namely the enhancement of anti-viral Th1 cells and the restriction of Th2 and Th17 cells, are accomplished by several mechanisms. Multiple, unique signals are integrated to either promote or inhibit Th1, Th2, or Th17 cells. Notably, type I, II, and/or III interferons are produced at high levels during viral infection and have convergent signaling through signal transducer and activator of transcription 1 (STAT1).²³³ The presence of interferons in the polarizing cytokine milieu strongly promotes the generation of Th1 cells and IFN- γ while restricting Th2 and Th17 polarization and their associated cytokine production.^{234–}
²⁴⁰ These data implicate interferons and STAT1 signaling as a principle coordinator of CD4⁺ T cell subset balance during viral infection.

While many discrete pathways for activation and inhibition of ILC have been defined, it remains unclear how ILC responses are orchestrated collectively to provide an effective anti-viral response. Given the central role of STAT1 signaling during viral infection and in the regulation of CD4⁺ T cell subset balance, we hypothesized that STAT1 signaling promotes ILC1 responses and restrains ILC2 and ILC3 responses to viral infection. To test this hypothesis, we evaluated cytokine-producing ILC responses in *Stat1*^{-/-} mice infected with RSV, a major pathogen of infants and the elderly with robust clinical morbidity in both developed and undeveloped countries and a particularly high mortality rate worldwide. ILC were significantly dysregulated in *Stat1*^{-/-} mice, with diminished IFN- γ ⁺ ILC1 and enhanced IL-5⁺ ILC2, IL-13⁺ ILC2, and IL-17A⁺ ILC3 populations. This dysregulation was associated with increased

production of ILC-associated cytokines in the lungs, pathophysiologic changes in the airways, and poor viral clearance. Concurrently, *Stat1*^{-/-} mice had significantly increased expression of IL-33 and IL-23, and abrogating IL-33 or IL-23 attenuated the cytokine-producing ILC2 and ILC3 responses in these mice, respectively. Together, these data demonstrate the critical role of STAT1 signaling in the proper regulation of ILC responses to viral infection.

4.2. Methods

4.2.1. Mice

Female 8-12 week old mice were used for all experiments. BALB/cJ and CByJ.SJL(B6)-Ptpcr^a/J CD45.1⁺ congenic mice were obtained from the Jackson Laboratory. *Stat1*^{-/-} and *Il33*^{-/-} mice on a BALB/c genetic background were generated as previously described.^{65,241,242} *Stat1*^{-/-} *Il33*^{-/-} double-deficient mice were bred from these strains. Mice were housed in microisolator cages under specific pathogen free conditions. All animal experiments were approved by the Vanderbilt University Medical Center Institutional Animal Care and Use Committee and were conducted in compliance with the 1996 “Guide for the Care and Use of Laboratory Animals” prepared by the Committee on Care and Use of Laboratory Animals of the Institute of Laboratory Animal Resources, National Research Council.

4.2.2. RSV Infection and Viral Titer

Respiratory syncytial virus strain 01/2-20 was isolated from a patient in the Vanderbilt Vaccine Clinic and propagated in HEp-2 cells as previously described.^{195,197} Mice were anesthetized with a ketamine/xylazine solution and inoculated with 3.0×10^6 PFU of RSV 01/2-20 by intranasal instillation with 100 μ l of viral preparation or mock preparation (lysed uninfected HEp-2 cells). Mice were sacrificed and harvested for tissue on days 0-9 post-infection. Viral titer was assessed by immunodetection plaque assay.²⁴³ Briefly, lungs were collected and homogenized in 1 mL of MEM media using a BeadBeater.¹⁹⁵ Debris was removed by centrifugation and serial dilutions of the homogenate were plated on 80% confluent HEp-2 cells for 1 hour while shaking. The cells were then overlaid with MEM supplemented with 10% FBS, penicillin G, streptomycin, gentamicin, amphotericin B, and 0.75% methylcellulose and incubated at 37°C for 6 days. Cells were subsequently fixed with methanol at -80°C for 2 hour, blocked with 5% non-fat milk/PBS buffer, incubated at 37°C for 1 hour each with primary goat anti-RSV (EMD Millipore Cat. # AB1128, 1:250 dilution) and secondary HRP-conjugated donkey anti-goat (Jackson Immuno Cat. # 705-035-147, 1:500 dilution) antibodies, and visualized with 4-chloronaphthol.

4.2.3. Flow Cytometry

Flow cytometric analysis was performed as previously described.²²⁵ Briefly, lungs were minced and enzymatically disrupted with 1 mg/mL collagenase IV and 50 U/mL of DNase I in RPMI with 5% FBS for 1 hour at 37°C. Enzymes were inactivated with EDTA and the disrupted

lungs were passed through 70 micron strainers to generate single cell suspensions. RBCs were lysed and cells were restimulated with 10 ng/mL phorbol 12-myristate 13-acetate and 1 μ mol/L ionomycin in the presence of 0.07% monensin in Iscove modified Dulbecco medium media supplemented with 10% FBS, 0.01 mmol/L nonessential amino acids, penicillin/streptomycin, and 1 mmol/L sodium pyruvate for 5 hours at 37°C. In some experiments, cells were treated during the restimulation one hour prior to collection with 0.1% BSA in PBS (vehicle) or 10 ng/mL of recombinant murine IFN- α (R&D Cat. #12100-1), IFN- β (R&D Cat. # 12400-1), IFN- γ (PeproTech Cat. # 50-813-664), IFN- λ 2 (R&D Cat. # 4635-ML-025), or IL-27 (R&D Cat. # 2799-ML-010). Restimulated cells were stained with a fixable viability dye (Tonbo Cat. # 13-0868) and combinations of cell surface markers. Cells were fixed and permeabilized (Tonbo Cat. # TNB-0607-KIT) per manufacturer instructions and stained for intracellular markers. All antibodies used for flow cytometric analysis are listed in Table 4-1. Cells were subsequently evaluated on a BD LSR II Flow Cytometer and analyzed using FlowJo Software Version 10. Classical NK cells (cNK) were defined as CD3⁻ CD19⁻ NKp46⁺ CD49b⁺ T-bet⁺ EOMES⁺ cells that produced IFN- γ . Non-NK cells ILC1 were defined as Lin⁻ CD127⁺ T-bet⁺ EOMES⁻ NKp46⁺ ROR γ t⁻ cells that produced IFN- γ . ILC2 were defined as Lin⁻ CD45⁺ CD25⁺ CD127⁺ cells that expressed either IL-5 or IL-13. ILC3 were defined as Lin⁻ CD90⁺ CD127⁺ ROR γ t⁺ cells that expressed either IL-17A or IL-22. Lineage markers (Lin) include CD3, CD5, B220, CD11b, Gr-1, 7-4, and Ter-119.

Table 4-1. Antibodies for Flow Cytometry

Epitope	Clone	Manufacturer	Fluorophore	Dilution^a
<i>CD3e</i>	145-2C11	BD	APC-Cy7	1:100
<i>CD19</i>	6D5	BioLegend	PE-Cy5	1:800
<i>CD49b</i>	DX5	eBioscience	APC	1:200
<i>NKp46</i>	29A1.4	eBioscience	PerCP-eFluor 710	1:200
<i>EOMES</i>	DAN11MAG	eBioscience	AF488	1:100
<i>T-bet</i>	eBio4B10	eBioscience	PE-Cy7	1:200
<i>IFN-γ</i>	XMG1.2	eBioscience	eFluor 450	1:200
<i>Lineage Cocktail</i>	130-092-613	Miltenyi	Biotin	1:25
<i>CD3</i>	17A2	eBioscience	Biotin	1:200
<i>CD45</i>	30-F11	Tonbo	rF710	1:400
<i>CD25</i>	PC61.5	eBioscience	AF488	1:50
<i>CD127^b</i>	SB/199	eBioscience	PE-Cy7	1:200
<i>CD127^c</i>	SB/199	BioLegend	APC	1:100
<i>CD127^d</i>	A7R34	eBioscience	PE-Cy5	1:200
<i>IL-5</i>	TRFK5	BD Biosciences	APC	1:200
<i>IL-13</i>	eBio13A	eBioscience	PE	1:200
<i>CD90.2</i>	30-H12	eBioscience	FITC	1:400
<i>RORγt</i>	B2D	eBioscience	PE	1:200
<i>RORγt</i>	Q31-378	BD Biosciences	BV786	1:50
<i>IL-17A</i>	eBio17B7	eBioscience	PE-Cy7	1:200
<i>IL-22</i>	1H8PWSR	eBioscience	PerCP-eFluor 710	1:200
<i>Ki67</i>	SolA15	eBioscience	eFluor 450	1:100
<i>IFN-αR1</i>	MAR1-5A3	eBioscience	PE	1:100
<i>IFN-γR1(CD119)</i>	200	eBioscience	PE	1:100
<i>IL-27Rα</i>	2918	BD Biosciences	PE	1:100
<i>Stat1 (pY701)</i>	4a	BD Biosciences	PE	1:5
<i>CD45.1</i>	A20	BioLegend	BV510	1:100
<i>CD45.2</i>	104	BioLegend	BV421	1:100
<i>Streptavidin</i>	405208	BioLegend	APC-Cy7	1:400

^a Stains were performed in a volume of 100 μl with 3-5 million total lung cells

^b Used in flow cytometric analysis of ILC2

^c Used in flow cytometric analysis of ILC3

^d Used in flow cytometric analysis of ILC1

4.2.4. ELISA

Lungs were isolated and homogenized in 1 mL of MEM media using a BeadBeater. Cell debris was removed by centrifugation and supernatants were plated for ELISA. ELISAs for IL-5 (Cat. # M5000), IL-13 (Cat. # M1300CB), IL-17A (Cat. # M1700), IL-22 (Cat. # M2200), IL-12 p70 (Cat. # M1270), IL-15 (Cat. # DY447), IL-18 (Cat. # 7625), IL-33 (Cat. # DY3626), TSLP (Cat. # MTLP00), IL-25 (Cat. # DY1399), IL-1beta (Cat. # MLB00C), and IL-12p40 (Cat. # DY2398) were obtained from R&D and performed as per manufacturer instructions.

4.2.5. Quantitative PCR

Lungs were collected and homogenized in 1 mL of TRIzol reagent (Ambion Cat. # 15596018) using a BeadBeater. RNA was isolated per TRIzol manufacturer instructions. Samples were DNase treated (Invitrogen Cat. # 18068-015) and cDNA was generated using SuperScript III (Invitrogen Cat. # 18080-051) per manufacturer instructions. cDNA abundance was assessed using FAM-MGB TaqMan primers for *Il23p19* (Cat. # Mm01160011_g1), *Il33* (Cat. # Mm00505403_m1) and *Gapdh* (Cat. # Mm99999915_g1) from Applied Biosystems. Amplifications were carried out on an Applied Biosystems QuantStudio 12k Flex Real-Time PCR machine and data were analyzed using Applied Biosystems QuantStudio 12k Flex Software v1.2.2. *Il23p19* expression was normalized to *Gapdh* and expressed as a fold change calculated by comparing *Stat1*^{-/-} to WT samples by the $\Delta\Delta C_t$ method at each time point.

4.2.6. Bronchoalveolar Lavage (BAL)

Endotracheal tubes were placed into euthanized mice. Saline (0.8 mL) was instilled into the lungs and recovered with a syringe placed in the endotracheal tube. 0.1 mL of the recovered solution was spun onto slides and these cells stained (Richard-Allan Scientific Cat. # 22-050-272) to visualize macrophages, lymphocytes, neutrophils, and eosinophils. 200 cells on each slide were counted to assess cell type frequencies. Total numbers were determined by multiplying the cell frequencies by the total number of cells recovered from the BAL. In some experiments, BAL fluid was centrifuged to remove cells and the supernatants were plated for ELISA.

4.2.7. Periodic acid-Schiff (PAS) Staining

To evaluate mucus, lungs were instilled with 0.8 mL of 10% neutral buffered formalin and immersed in excess 10% neutral buffered formalin for 24 hours at room temperature. Lungs were subsequently paraffin embedded and sectioned (5 μ) for histologic analysis. Slides were stained with PAS. Small- and medium-sized airways were quantified for airway mucus by a trained pathologist blinded to the experimental conditions using the following scoring matrix: 0, no PAS+ cells observed in cross-sections of medium to small airways; 1, less than 10 PAS+ cells observed in cross-sections of medium to small airways; 2, greater than 10 PAS+ cells observed in cross-sections of medium to small airways; 3, greater than 10 PAS+ cells observed in cross-sections of medium to small airways with mucous strands observed in air spaces; or 4, greater

than 10 PAS+ cells observed in cross-sections of medium to small airways with mucous plugging of airways.

4.2.8. Bone Marrow Chimeras

Female 6 week-old BALB/cJ or *Stat1*^{-/-} mice were lethally irradiated with 10 Gy of Cs-137. A 1:1 mixture of whole bone marrow was prepared from 6 week-old CByJ.SJL(B6)-Ptpcr^a/J CD45.1⁺ congenic and *Stat1*^{-/-} CD45.2⁺ mice. This bone marrow mixture was transferred via retroorbital injection into irradiated mice and allowed to reconstitute for 6 weeks prior to RSV infection and analysis. Mice were maintained on antibiotic water (0.025% trimethoprim/0.125% sulfamethoxazole) for 2 weeks following transplant.

4.2.9. IL-23p19 Neutralization

Stat1^{-/-} mice were treated on day 0 and day 3 post-infection intraperitoneally with 250 µg of an anti-IL-23p19 subunit neutralizing monoclonal antibody (Amgen) or an isotype control (BioXCell clone MOPC-21). Lungs were isolated at day 6 post-infection for flow cytometric analysis.

4.2.10. Statistics

All data were collated and analyzed in GraphPad Prism Version 5. Whenever possible, data were pooled from multiple experiments for analysis. Statistical analyses including Student's

t-test, one-way ANOVA with Bonferroni post-test, or two-way ANOVA with Bonferroni post-tests were performed using GraphPad Prism Version 5 as appropriate and as documented throughout the text.

4.3. Results

4.3.1. ILC and their Cytokine Products are Dysregulated in *Stat1*^{-/-} Mice During Viral Infection

To test the role of STAT1 signaling on cytokine-producing ILC populations during viral infection, we infected *Stat1*^{-/-} mice intranasally with RSV or mock inoculum (uninfected HEp-2 cell lysate) and measured ILC1, ILC2, and ILC3 cell numbers throughout the course of infection. Gating for ILC1, ILC2, and ILC3 are described in the Methods section and representative gating is shown in Figure 4-1 (cNK and ILC1) and Figure 4-2 (ILC2 and ILC3). We defined ILC subsets by their cytokine production, as our primary interest in these studies was in understanding the balance of type 1, 2, and 17 cytokine production by ILC. Relative to WT mice, RSV-infected *Stat1*^{-/-} mice exhibited a significant decrease in the total number of IFN- γ ⁺ cNK cells at days 3 and 6 post-infection and a significant increase in the total number of IL-5⁺ ILC2, IL-13⁺ ILC2, and IL-17A⁺ ILC3 at days 6 and 9 post-infection (Figure 4-3 A-C). There were no significant increases throughout the course of infection in IFN- γ ⁺ non-NK ILC1 or IL-22⁺ ILC3 with RSV infection compared to mock infection in either WT or *Stat1*^{-/-} mice, except a very modest but statistically significant increase in IL-22⁺ ILC3 at day 9 post-infection in *Stat1*^{-/-} mice (Figure 4-3 A and C). The IL-17A⁺ ILC3 were exclusively NKp46⁻, consistent with previous reports of ILC3 in the lungs (data not shown).¹⁷⁷

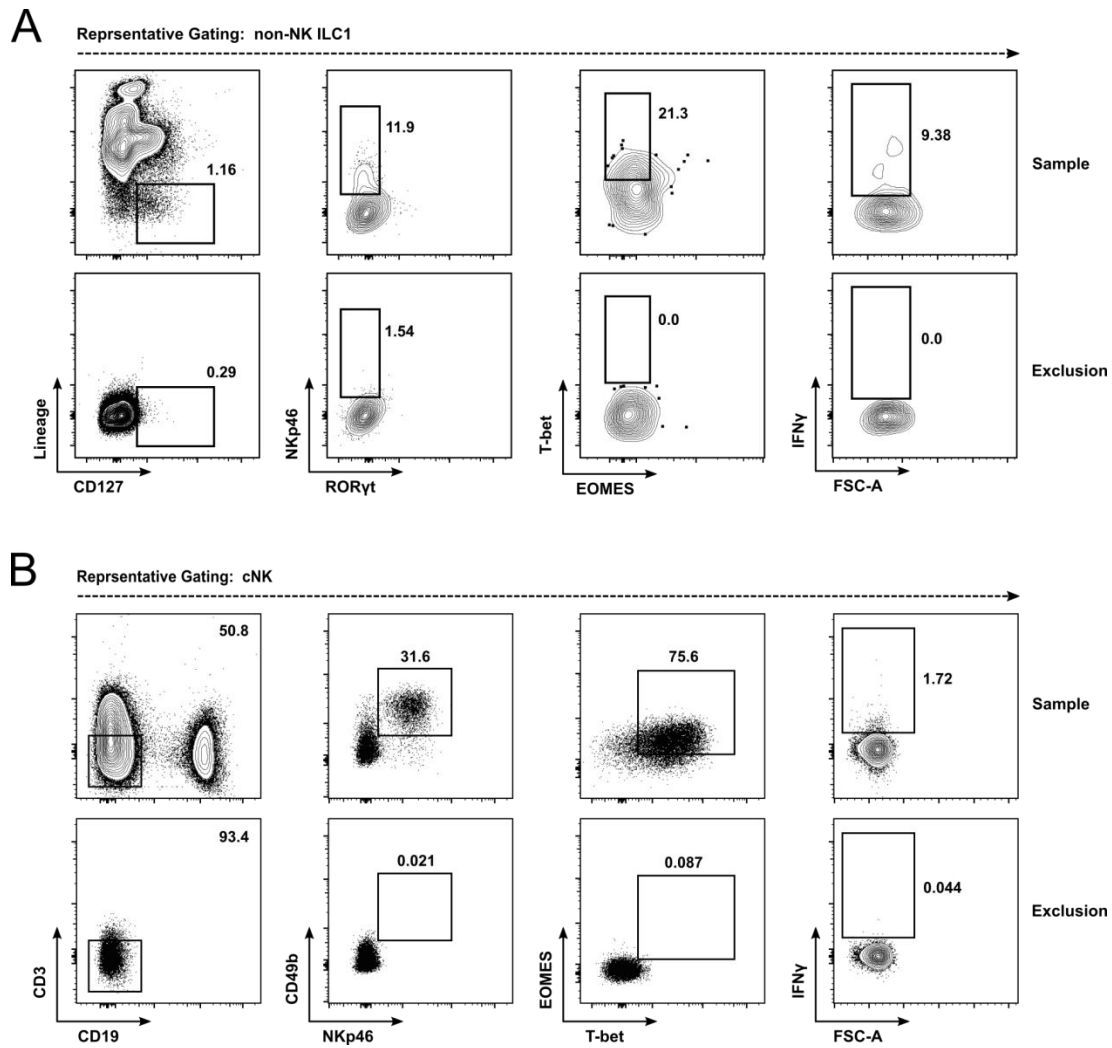


Figure 4-1. Gating strategies for cNK and ILC1.

Data are representative of the gating strategies used throughout the paper to measure cNK and non-NK ILC1. Samples shown were pre-gated for viable singlets with low to intermediate FSC-A and SSC-A properties consistent with resting and activated lymphocytes.

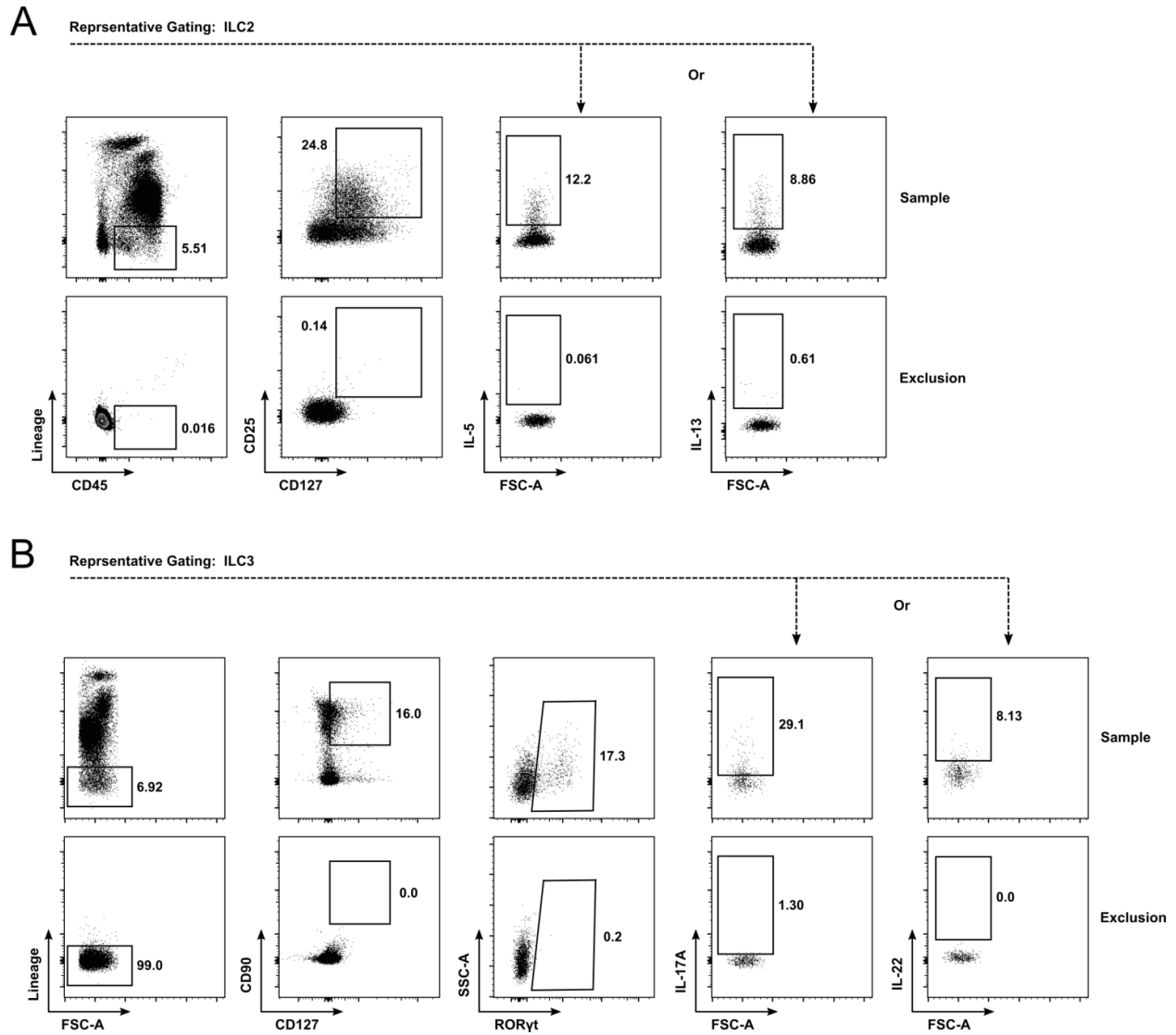


Figure 4-2. Gating strategies for ILC2 and ILC3.

Data are representative of the gating strategies used throughout the paper to measure ILC2 and ILC3. Samples shown were pre-gated for viable singlets with low to intermediate FSC-A and SSC-A properties consistent with resting and activated lymphocytes.

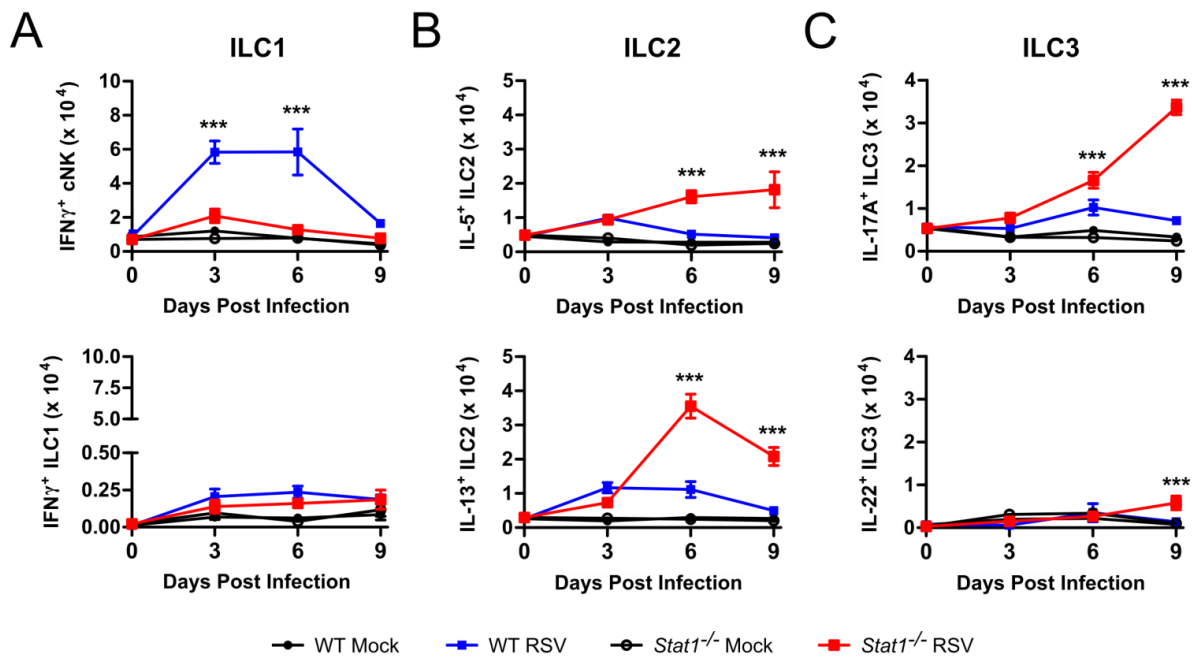


Figure 4-3. ILC are dysregulated in *Stat1*^{-/-} mice.

WT and *Stat1*^{-/-} mice were infected with RSV or mock infected with vehicle and lungs were harvested on days 0, 3, 6, and 9 post-infection for flow cytometry. The total number of functional cytokine-producing (A) ILC1, (B) ILC2, and (C) ILC3 as determined by flow cytometric analysis are shown. Data are pooled from 2 independent experiments comprising 5-7 mice per time point per group and evaluated by two-way ANOVA. **p<0.01 and ***p<0.001 between WT RSV and *Stat1*^{-/-} RSV.

Local proliferation of ILC populations is thought to be an important driver of inflammatory responses, including during RSV infection.^{69,92,225} To assess whether ILC were replicating *in situ*, we measured the expression of the cell cycle associated protein Ki67 in IL-5⁺ or IL-13⁺ ILC2 and IL-17A⁺ ILC3. RSV-infected *Stat1*^{-/-} mice had increased expression of Ki67 in the IL-13⁺ ILC2 and IL-17A⁺ ILC3 compartments, but not the IL-5⁺ ILC2 compartment, compared to RSV-infected WT mice (Figure 4-4). These data suggest that local proliferation of IL-13⁺ ILC2 and IL-17A⁺ ILC3 contribute to the increased numbers of these cells in *Stat1*^{-/-} mice during RSV infection.

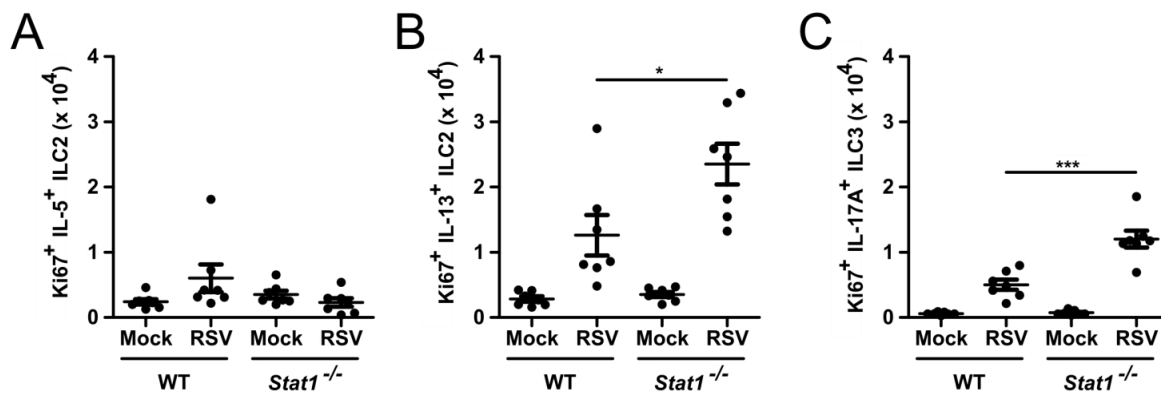


Figure 4-4. *Stat1*^{-/-} ILC2 and ILC3 proliferate robustly during RSV infection. WT and *Stat1*^{-/-} mice were infected with RSV or mock infected with vehicle and lungs were harvested on day 6 post-infection for flow cytometry. The total number of Ki67⁺ (A) IL-5⁺ ILC2, (B) IL-13⁺ ILC2, and (C) IL-17A⁺ ILC3 is shown. Data are pooled from 2 independent experiments and evaluated by one-way ANOVA. *p<0.05 and ***p<0.001.

Concurrent with the increases observed in cytokine-producing ILC2 and ILC3, we identified significantly increased expression of the cytokines IL-5, IL-13, and IL-17A at day 6 post-infection in RSV-infected *Stat1*^{-/-} mice compared to WT mice (Figure 4-5 A). While unlikely to be the exclusive source of these cytokines, the increased expression of IL-5, IL-13, and IL-17A correlates with an increase in the number of cytokine-expressing ILC. We also identified robust BAL eosinophilia and neutrophilia and airway mucus accumulation at day 6 post-infection in RSV-infected *Stat1*^{-/-} mice (Figure 4-5 B, D, and E). Importantly, *Stat1*^{-/-} mice exhibited poor viral control, as evidenced by both increased viral titers and delayed viral clearance compared to WT mice (Figure 4-5 C). These cytokine, BAL, and viral load data are broadly consistent with prior reports of a dysregulated Th2/Th17-skewed immune response in *Stat1*^{-/-} mice following RSV infection.²⁴⁴⁻²⁵¹ Collectively, these data demonstrate a critical role for STAT1 signaling in promoting IFN- γ ⁺ ILC1 and restraining IL-5⁺ ILC2, IL-13⁺ ILC2, and IL-17A⁺ ILC3 during RSV infection that largely parallels the ineffective, pathologic immune response occurring in the lungs.

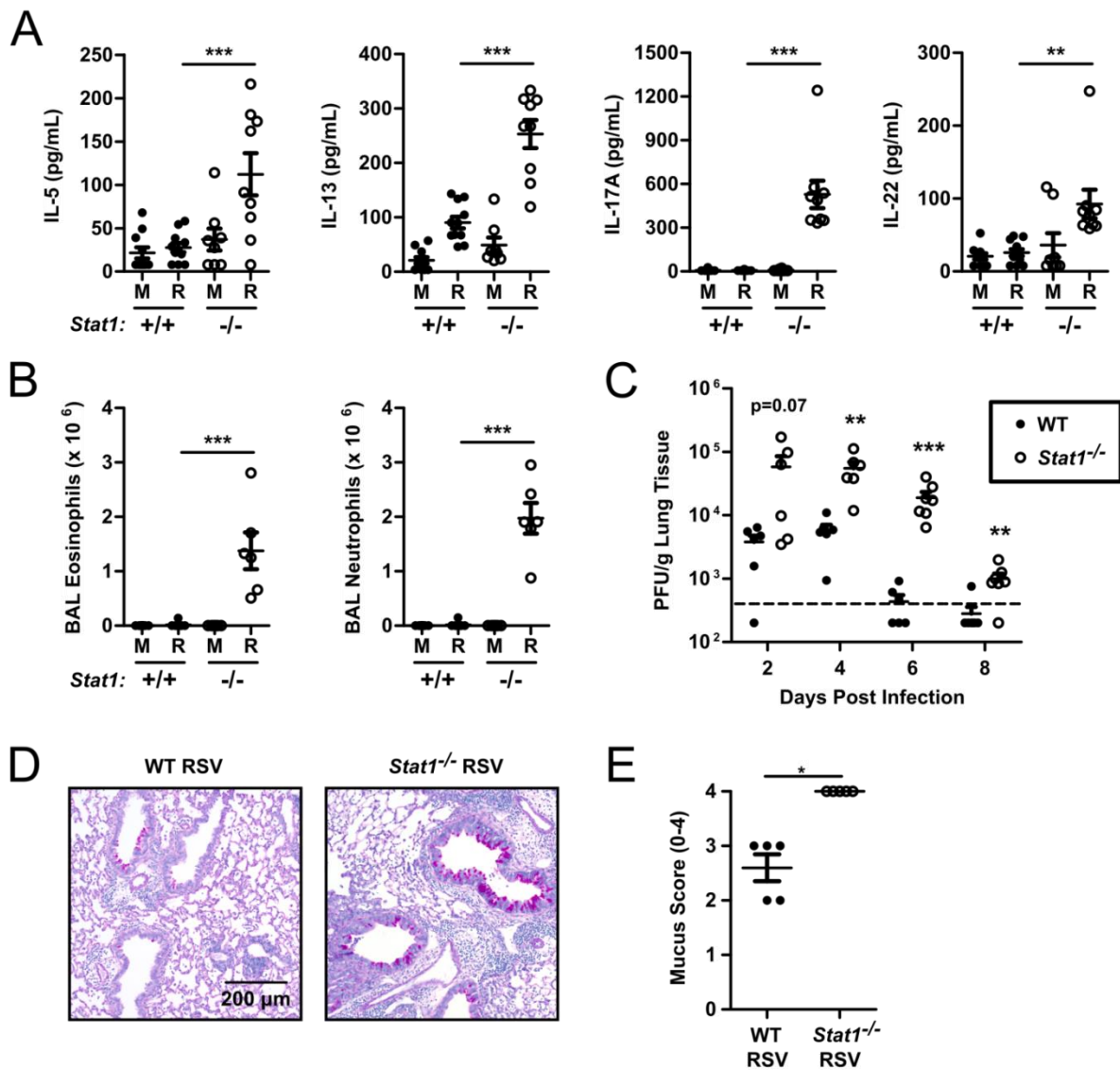


Figure 4-5. *Stat1*^{-/-} mice displayed enhanced type 2 and type 17 immunity and poor viral clearance during RSV infection.

WT and *Stat1*^{-/-} mice were infected with RSV or mock infected with vehicle and lungs were harvested on day 6 post-infection. (A) IL-5, IL-13, IL-17A, and IL-22 protein measured in the whole lung homogenate. (B) Total number of eosinophils and neutrophils in the bronchoalveolar lavage. (C) Viral load measured by plaque assay from lungs harvested on days 2, 4, 6, and 8 post-infection. (D) Representative airway sections stained with PAS and (E) quantification of PAS staining for multiple mice. Data are pooled from 2 independent experiments (A-C). Data were evaluated by one-way ANOVA (A, B) with the resultant comparisons shown or Student's *t*-test (C and E) comparing WT and *Stat1*^{-/-} mice on each day post-infection. ***p*<0.01 and ****p*<0.001. M = mock-infected. R = RSV-infected.

4.3.2. Cell-Intrinsic and Cell-Extrinsic Factors Contributed to ILC Dysregulation in *Stat1*^{-/-} Mice

To interrogate whether cell-extrinsic factors contribute to the skewed cytokine-producing ILC response in *Stat1*^{-/-} mice, we measured the number of WT and *Stat1*^{-/-} ILC following RSV infection in a mixed bone marrow chimera model. WT (BALB/cJ) or *Stat1*^{-/-} mice were lethally irradiated and reconstituted via retroorbital injection with a 1:1 mixture of WT CD45.1⁺ (CByJ.SJL[B6]-Ptprc^{a/J}) or *Stat1*^{-/-} CD45.2⁺ whole bone marrow. Six weeks after reconstitution, mice were inoculated with RSV and the total numbers of cytokine-producing WT and *Stat1*^{-/-} ILC were enumerated at day 6 post-infection (Figure 4-6). Mock-infected WT recipients had significantly more WT IL-5⁺ and IL-13⁺ ILC2 than *Stat1*^{-/-} IL-5⁺ and IL-13⁺ ILC2, suggesting a potential basal advantage of WT ILC2 in the WT recipient background (Figure 4-6 A-C). Upon infection, however, *Stat1*^{-/-} IL-5⁺ and IL-13⁺ ILC2 were significantly increased compared to WT IL-5⁺ and IL-13⁺ ILC2, demonstrating a cell-intrinsic advantage of IL-5⁺ and IL-13⁺ *Stat1*^{-/-} ILC2 during viral infection (Figure 4-6 A-C).

In *Stat1*^{-/-} recipient mice, both WT and *Stat1*^{-/-} IL-5⁺ and IL-13⁺ ILC2 were found in similar numbers with mock infection (Figure 4-6 A-C). Similar to WT recipient mice, *Stat1*^{-/-} IL-5⁺ and IL-13⁺ ILC2 were disproportionately activated upon RSV infection compared to WT IL-5⁺ and IL-13⁺ ILC2, though notably to a lesser degree than in the WT recipient, suggesting additional factors that may be present in the WT mouse that further potentiate cytokine-producing ILC2 responses (Figure 4-6 A-C). Collectively, these data indicate that cell-intrinsic differences are at least partially responsible for the enhanced responsiveness of *Stat1*^{-/-} ILC2 during RSV infection.

We similarly evaluated the number of IL-17A⁺ ILC3 in our mixed bone marrow chimera model (Figure 4-6 A and D). In WT recipients, we found equal numbers of WT and *Stat1*^{-/-} IL-17A⁺ ILC3 suggesting comparable fitness of these cells in the absence of a viral insult. Upon RSV infection, we identified significantly more *Stat1*^{-/-} IL-17A⁺ ILC3 than WT IL-17A⁺ ILC3, though the number of *Stat1*^{-/-} IL-17A⁺ ILC3 was comparable between mock and RSV infection in the WT recipient. In *Stat1*^{-/-} recipients, *Stat1*^{-/-} IL-17A⁺ ILC3 were found in higher frequencies in both mock and RSV-infected mice, with particularly robust expansion following RSV infection. In contrast, WT IL-17A⁺ ILC3 did not expand following RSV infection in the *Stat1*^{-/-} recipients (Figure 4-6 A and D). These data suggest that *Stat1*^{-/-} IL-17A⁺ ILC3 have a cell-intrinsic advantage over WT cells and that this at least partially contributes to the dysregulation of IL-17A⁺ ILC3 during RSV infection. Moreover, these data suggest that an additional cell-extrinsic factor(s) present in the *Stat1*^{-/-} recipient may be required for dysregulation of the ILC3 population.

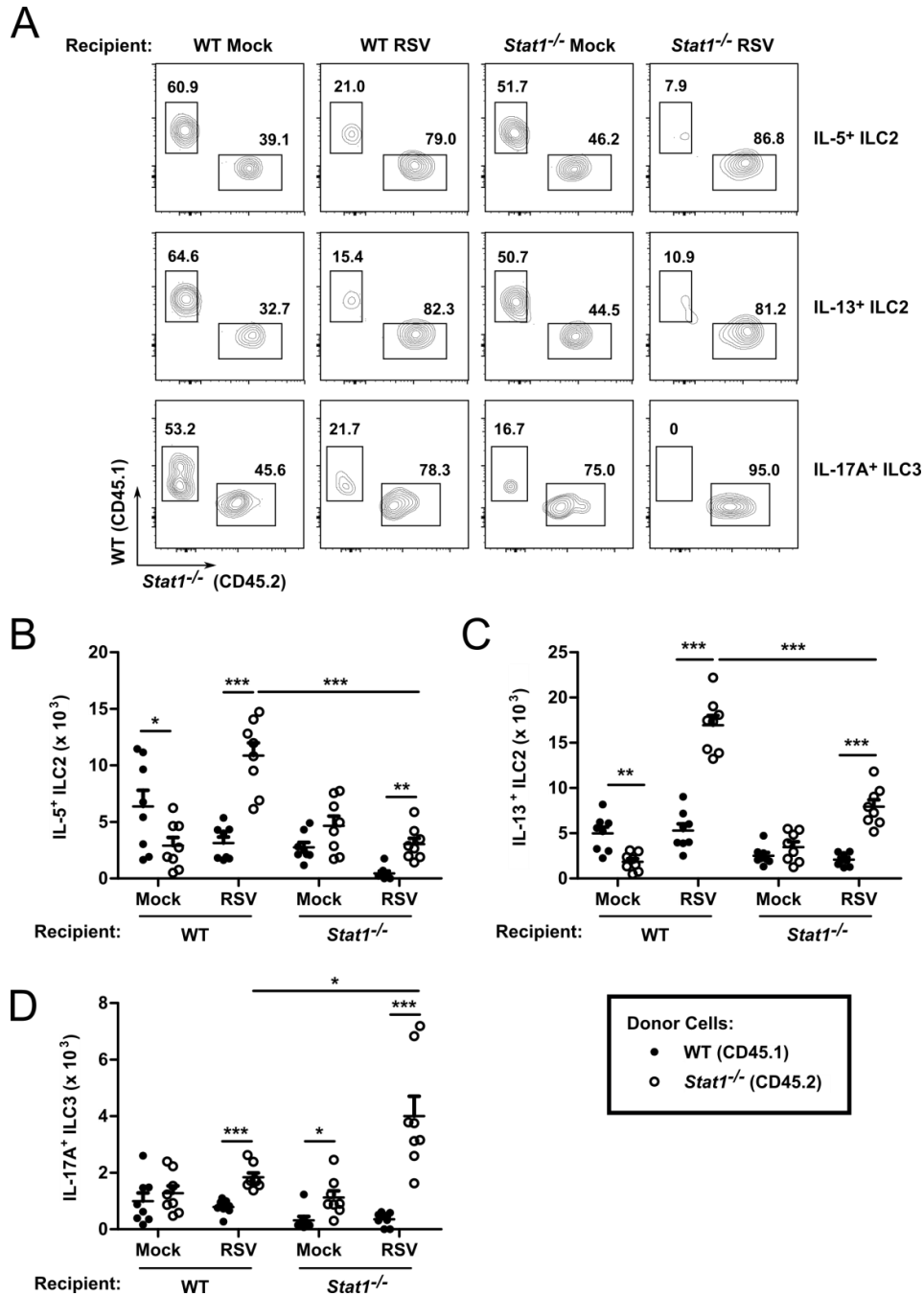


Figure 4-6. ILC cell-intrinsic and cell-extrinsic factors contribute to the dysregulation of *Stat1*^{-/-} ILC.

Six week old BALB/c mice were lethally irradiated and transplanted with a 1:1 mixture of WT Congenic (CD45.1) and *Stat1*^{-/-} (CD45.2) bone marrow. Mice were reconstituted for 6 weeks, infected with RSV or mock infected with vehicle, and harvested six days post-infection. (A) Representative flow plots with the percentages of the parent gates (IL-5⁺ ILC2, IL-13⁺ ILC2, or IL-17A⁺ ILC3) as indicated. Aggregated data for the total number of (B) IL-5⁺ ILC2, (C) IL-13⁺ ILC2, and (D) IL-17A⁺ ILC3. Data are pooled from 2 independent experiments and analyzed by two-way ANOVA. *p<0.05, **p<0.01, and ***p<0.001.

4.3.3. Expression of IL-33 and IL-23 is Increased During Viral Infection in *Stat1*^{-/-} Mice

Our bone marrow chimera experiments suggest that both cell-intrinsic and cell-extrinsic factors may play a role in the dysregulation of cytokine-producing ILC during viral infection. Prior reports suggest that ILC2 are intrinsically susceptible to inhibition to type I and II interferons, providing a likely explanation for the cell-intrinsic effect seen in our bone marrow chimeric mice.^{69,80,252-254} However, STAT1-dependent cell-extrinsic factors that regulate ILC frequencies have not been described. The cytokine milieu is critical for the activation of ILC. We hypothesized that pro-ILC stimulatory cytokines were differentially regulated in *Stat1*^{-/-} mice compared to WT mice. We infected WT and *Stat1*^{-/-} mice with RSV and measured the expression of IL-12, IL-15, IL-18, IL-33, TSLP, IL-25, IL-1 β , IL-23p19, and IL-12/IL-23p40 in the whole lung homogenate daily for 5 days beginning 12 hours post-infection. All cytokines were measured by ELISA except IL-23, which was measured by quantitative PCR due to lack of sensitive and specific protein-based reagents. Strikingly, there was a delayed but substantial increase in IL-33 protein and mRNA in the whole lung homogenates, beginning at day 4.5 post-infection and continuing through day 5.5 post-infection with a statistically significant nearly tenfold increase in *Stat1*^{-/-} mice compared to WT mice (Figure 4-7 D and E). IL-33 is stored as preformed cytokine in the nucleus of cells. To assess whether this increased expression of IL-33 in the whole lung homogenate led to an increase in the extracellularly-available IL-33, we measured IL-33 concentrations in the BAL. We identified a significantly increased concentration of IL-33 in the BAL of RSV-infected *Stat1*^{-/-} mice compared to RSV-infected WT mice at day 5.5 post-infection, when peak levels of IL-33 were observed in the whole lung homogenate, indicating that IL-33 was being released into the airways (Figure 4-7 F).

Similar to IL-33, we observed a statistically significant tenfold increase in *Il23p19* expression in *Stat1*^{-/-} mice compared to WT mice, peaking at day 4.5 post-infection (Figure 4-7 J). IL-23 is a heterodimer formed between the IL-23p19 subunit and the IL-12/IL-23p40 subunit. IL-12/IL-23p40 was found in significantly lower levels throughout infection in *Stat1*^{-/-} mice compared to WT mice, though levels post-infection in *Stat1*^{-/-} mice were universally higher than those at the time of infection suggesting an increased availability of the IL-12/IL-23p40 subunit for complexing with IL-23p19 and forming an active cytokine (Figure 4-7 K). IL-12, TSLP, and IL-1 β were marginally, but statistically significantly, higher in WT mice at days 3.5, 0.5, and 0.5, respectively (Figure 4-7 A, G, and I). Expression of IL-15, IL-18, and IL-25 was absent or only detected at very low levels (Figure 4-7 B, C, and H). Given the central role of IL-33 and IL-23 in the activation of ILC2 and ILC3, respectively, these data suggest an ILC cell-extrinsic mechanism for their dysregulation during viral infection in *Stat1*^{-/-} mice. Importantly, the expression of IL-33 and IL-23 coincided with the onset of ILC dysregulation in *Stat1*^{-/-} mice, which occurred between days 3 and 6 post-infection (Figure 4-3 A-C).

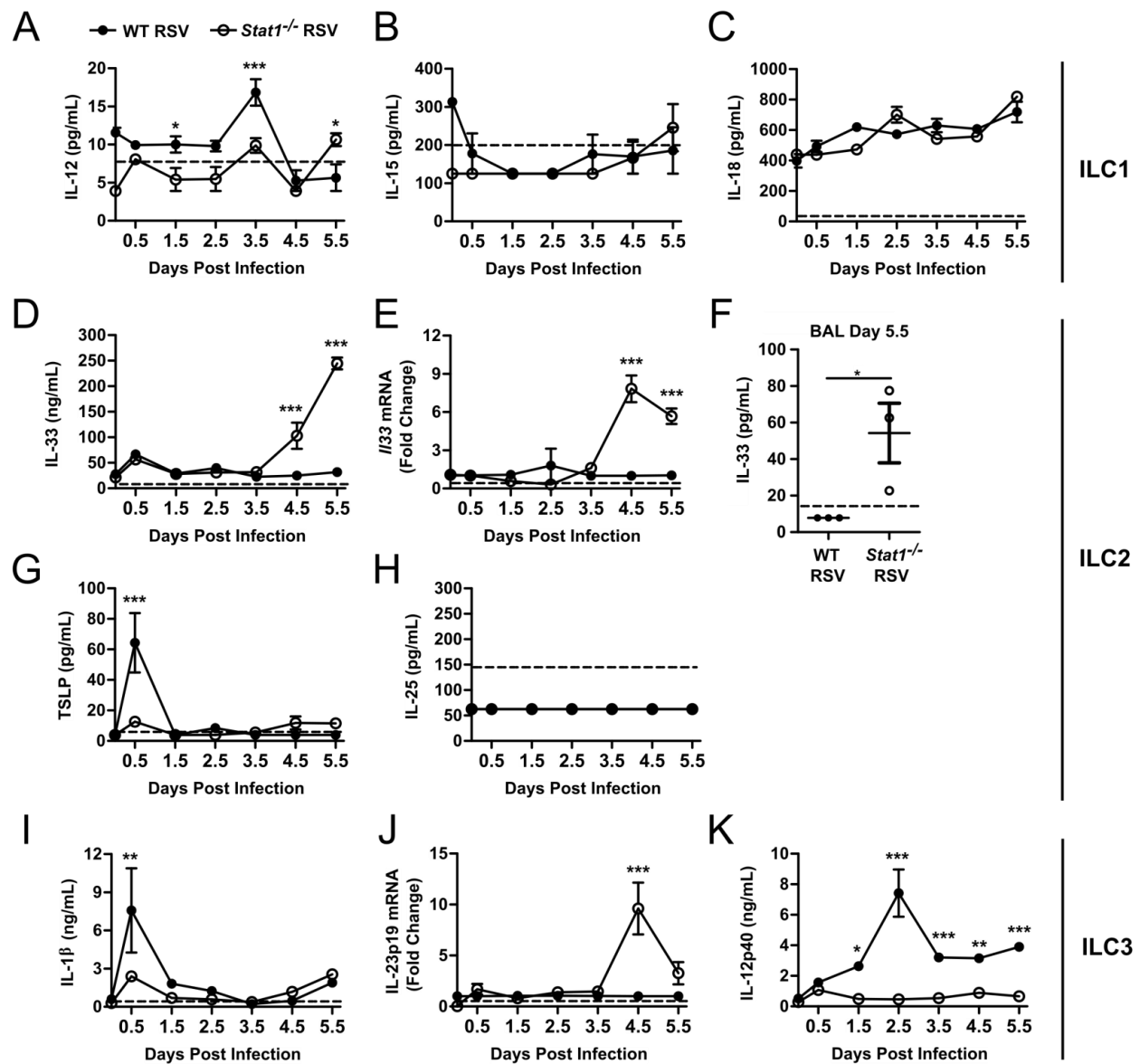


Figure 4-7. Pro-ILC2 and ILC3 stimulatory cytokines are increased in *Stat1*^{-/-} mice during viral infection.

WT and *Stat1*^{-/-} mice were infected with RSV or mock-infected and lungs were harvested for cytokine measurements by ELISA or quantitative PCR. (A-C) Pro-ILC1 cytokines, (D-H) pro-ILC2 cytokines, and (I-K) pro-ILC3 cytokines. Measurements were collected from whole lung homogenates for all samples except (F) which was taken from the BAL. Data in (A-E) and (G-K) are representative of 2 similar experiments with 3 mice per group per time point and analyzed by two-way ANOVA. (F) Data analyzed by Student's t test. **p*<0.05, ***p*<0.01, and ****p*<0.001.

4.3.4. Disruption of IL-33 and IL-23 Signaling Inhibits ILC2 and ILC3 Activation in *Stat1*^{-/-} Mice

To determine the role of increased IL-33 expression during RSV infection in *Stat1*^{-/-} mice, we generated *Il-33*^{-/-} *Stat1*^{-/-} double knockout mice. We infected WT, *Stat1*^{-/-}, and *Il-33*^{-/-} *Stat1*^{-/-} mice with RSV or vehicle and measured the number of ILC2. RSV-infected *Stat1*^{-/-} mice had significantly increased numbers of IL-5⁺ and IL-13⁺ ILC2 compared to RSV-infected WT mice (Figure 4-8 A). However, compared to RSV-infected *Stat1*^{-/-} mice, *Il-33*^{-/-} *Stat1*^{-/-} mice had significantly decreased total numbers of IL-5⁺ and IL-13⁺ ILC2 (Figure 4-8 A). These data suggest that increased production of IL-33 contributes to the enhanced activity of IL-5⁺ and IL-13⁺ ILC2 in the *Stat1*^{-/-} mice compared to WT mice during viral infection.

Similarly, we sought to determine the role of differential IL-23 expression during RSV infection in *Stat1*^{-/-} mice. To assess this, we measured the number of IL-17A⁺ ILC3 in RSV-infected *Stat1*^{-/-} mice treated with an anti-IL-23p19 neutralizing antibody or an isotype control. RSV-infected *Stat1*^{-/-} mice had significantly increased numbers of IL-17A⁺ ILC3 compared to RSV-infected WT mice (Figure 4-8 B). However, compared to isotype-treated *Stat1*^{-/-} mice, *Stat1*^{-/-} mice treated with an anti-IL-23p19 neutralizing antibody had significantly decreased total numbers of IL-17A⁺ ILC3 (Figure 4-8 B). RSV-infected anti-IL-23p19-treated *Stat1*^{-/-} mice still had a significantly increased number of IL-17A⁺ ILC3 compared to WT RSV-infected mice, consistent with our bone marrow chimera experiments that suggested both cell-intrinsic and cell-extrinsic factors play a role in the dysregulation of IL-17A⁺ ILC3 during RSV infection (Figure 4-6 A, D and Figure 4-8 B). These data suggest that increases in IL-23 expression contribute to the enhanced activity of IL-17A⁺ ILC3 in *Stat1*^{-/-} compared to WT mice during viral infection.

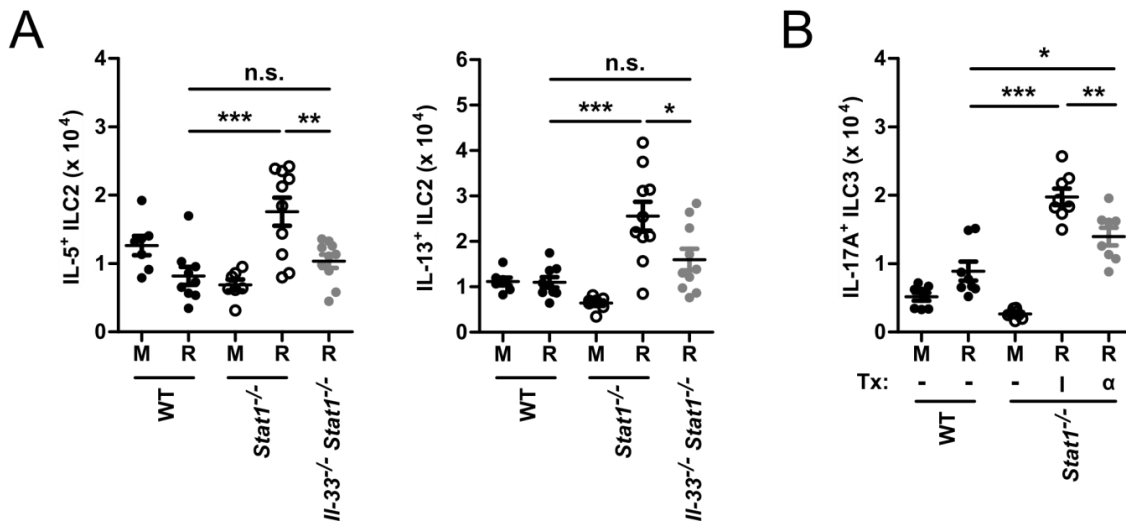


Figure 4-8. IL-33 and IL-23 are cell-extrinsic regulators of ILC that are dysregulated in *Stat1*^{-/-} mice and promote enhanced ILC2 and ILC3 responsiveness.

(A) WT, *Stat1*^{-/-}, and *Il-33*^{-/-} *Stat1*^{-/-} mice were infected with RSV or mock-infected and the total number of IL-5⁺ ILC2 and IL-13⁺ ILC2 were enumerated by flow cytometry at day 6 post-infection. (B) WT and *Stat1*^{-/-} mice were infected with RSV or mock-infected and treated with 250 μg of an anti-IL-23p19 neutralizing antibody (α) or isotype control (I) on day 0 and day 3 post-infection. The total number of IL-17A⁺ ILC3 was enumerated by flow cytometry at day 6 post-infection. Data are pooled from 2 independent experiments and evaluated by one-way ANOVA. *p<0.05, **p<0.01, and ***p<0.001. n.s. = not significant. M = mock-infected. R = RSV-infected.

4.3.5. IL-17A⁺ ILC3 Express Receptors for Type I and II Interferons and IL-27

ILC2 express interferon receptors and respond directly to interferons.^{69,80} We sought to determine whether IL-17A⁺ ILC3 also express interferon receptors. Initially, we evaluated for the expression of type I, II, and III IFNs in the first 5.5 days of RSV infection (Figure 4-9 A-D). We found that WT mice produced significantly more IFN- α , IFN- β , and IFN- λ during the first several days of RSV infection compared to *Stat1*^{-/-} mice. However, by day 5.5 post-infection, IFN- λ was detected in significantly higher levels in the lungs of *Stat1*^{-/-} mice compared to WT mice. No significant differences in IFN- γ expression were observed throughout the first 5.5 days of infection between WT and *Stat1*^{-/-} mice. We next assayed whether IL-17A⁺ ILC3 expressed receptors for these interferon species. Compared to isotype control staining, IL-17A⁺ ILC3 had detectable expression of IFN- α R, IFN- γ R1, and the IL-27R (Figure 4-9 E). IL-27, like interferons, signals through STAT1. Finally, we determined whether IFN treatment of IL-17A⁺ ILC3 *ex vivo* could induce phosphorylation of STAT1 (pSTAT1) to an activated state. Compared to vehicle treatment, culturing bulk lung cells *ex vivo* with IFN- β for 1 hour significantly induced pSTAT1 in IL-17A⁺ ILC3 (Figure 4-9 F). Similar phosphorylation was not observed with IFN- α treatment, and data were equivocal with high degrees of experiment to experiment variability for IFN- γ and IFN- λ 2 treatments (Figure 4-9 and data not shown).

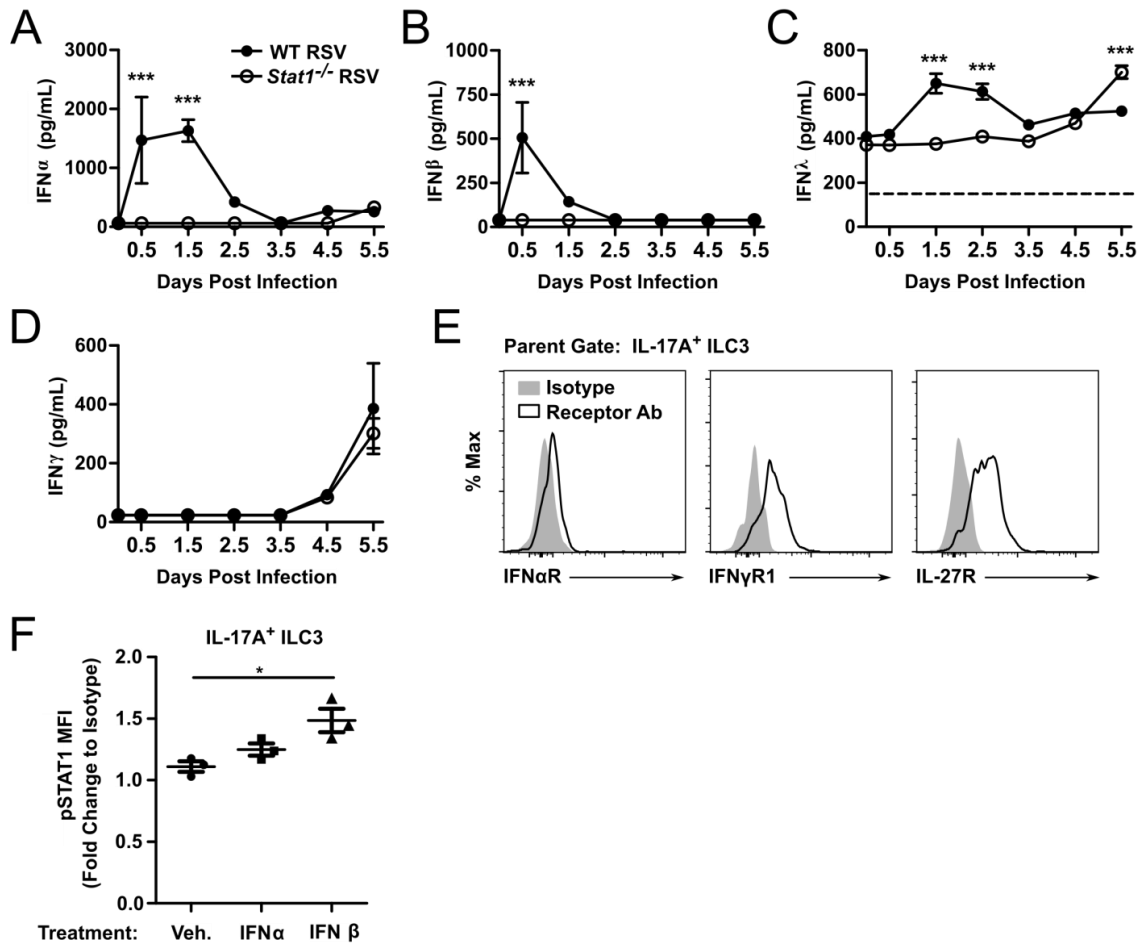


Figure 4-9. ILC3 express receptors for type I and type II IFNs and IL-27.

WT and *Stat1*^{-/-} mice were infected with RSV or mock-infected and lungs were harvested for cytokine measurements by ELISA. Shown are the concentrations of (A) IFN- α , (B) IFN- β , (C) IFN- γ , and (D) IFN- λ in the whole lung homogenate. (E) Expression of IFN- α R, IFN- γ R1, and IL-27R on IL-17A⁺ ILC3. (F) Phosphorylated STAT1 expression by flow cytometry in IL-17A⁺ ILC3 treated for 1 hour *ex vivo* with IFN- α or IFN- β . Data are representative to 2-3 independent experiments (A-E) or combined from 3 independent experiments (F) and evaluated by two-way ANOVA (A-D) or one-way ANOVA (F). * $p < 0.05$ and *** $p < 0.001$.

4.4. Discussion

The appropriate orchestration of immune cells is vital for promoting productive immune responses and restricting detrimental pathophysiology. Herein, we show that STAT1 is a broad regulator of cytokine-producing ILC responses in the context of viral infection, promoting anti-viral IFN- γ ⁺ ILC1 and restricting IL-5⁺ and IL-13⁺ ILC2 and IL-17A⁺ ILC3. To this end, STAT1 represses cytokine-producing ILC2 and ILC3 via both cell-intrinsic and cell-extrinsic mechanisms. Extrinsically, STAT1-deficiency led to a significant increase in the expression of IL-33 and IL-23 that correlated strongly with increases in IL-5⁺ and IL-13⁺ ILC2 and IL-17A⁺ ILC3 in these mice. Furthermore, the genetic deletion of IL-33 or the neutralization of IL-23p19 in the context of STAT1-deficiency partially attenuated the dysregulated activation of cytokine-producing ILC2 and ILC3, respectively. Collectively, these data demonstrate that cytokine-producing ILC responses are coordinated by STAT1-dependent cell-intrinsic and cell-extrinsic mechanisms in the context of viral infection.

Previous studies have started to elucidate the direct role of interferon signaling on ILC2 responses. Specifically, these studies have shown that type I and type II interferons directly repress ILC2 responses *in vitro* and *in vivo* in the context of viral infection or airway inflammation.^{69,80,252–254} Data from our bone marrow chimeric mouse experiments suggest cell-intrinsic factors, such as the previously described direct inhibition of ILC2 by interferons^{69,80,253}, play a role in regulating ILC frequencies during viral infection. Consistent with this literature, we identified that type I, II, and III IFNs are expressed in the lungs throughout RSV infection and that IL-17A⁺ ILC3 express receptors for type I and II IFNs as well as IL-27, another activator of STAT1. These data suggest that ILC3 may also be modulated directly by IFNs. Our chimeric

experiments further suggest that cell-extrinsic factors regulate ILC frequencies during viral infection via a previously undefined STAT1-dependent mechanism. These data were particularly strong for IL-17A⁺ ILC3, and consistent with these data we observed an increase in *Il23p19* during RSV infection in *Stat1*^{-/-} mice. While our bone marrow chimera experiments did not specifically identify a cell-extrinsic effect for STAT1-deficiency in regulating ILC2, we observed significantly enhanced production of IL-33 in *Stat1*^{-/-} compared to WT mice during RSV infection similar to *Il23p19*. Genetic deletion of *Il33* in STAT1-deficient mice significantly reduced the number of IL-5⁺ and IL-13⁺ ILC2 during RSV infection. It is not entirely clear why a cell-extrinsic effect for cytokine-producing ILC2 was not observed in our bone marrow chimeric mice despite a clear effect of IL-33 in our other experiments. It is possible that changes in the cell phenotype such as a downregulation of the IL-33 receptor post-transplant altered their capacity to respond, or that factors present in the WT recipient background in combination with donor *Stat1*^{-/-} ILC2 selectively potentiated these cells by a non-IL-33-dependent mechanism, masking our ability to detect a cell-extrinsic difference by this method. Regardless, our results using genetic deletion of *Il33* in the context of STAT1-deficiency strongly suggest an important role for STAT1 repression of IL-33 in regulating cytokine-producing ILC2 responses.

Some other unexpected results were observed in our bone marrow chimera experiments. Specifically, WT donor IL-5⁺ ILC2 were observed at a high level in mock-infected WT recipient mice. This may be due to an advantage compared to other ILC subsets in reseeding the tissue following transplant. Additionally, *Stat1*^{-/-} IL-5⁺ and IL-13⁺ ILC2 were more frequent in WT recipient mice compared to *Stat1*^{-/-} recipient mice during RSV infection, suggesting that additional environmental factors present in WT mice may add to STAT1-deficiency in promoting cytokine-producing ILC2. Finally, RSV-infection did not expand the number of WT

IL-13⁺ ILC2 as had been observed in our intact animals at day 6 post-infection shown in Figure 4-3. The comprehensive network of activators and inhibitors of ILC in these mixed bone marrow chimeric mice will need to be further defined to better understand all of these data. However, broadly, these data in conjunction with previously published studies extend our understanding of the role of STAT1 signaling on the ILC response during viral infection.

A role for STAT1 in regulating IL-33 had been suggested previously, but these experiments were performed using ectopic expression of IL-33 and IFN- γ in lung fibroblasts in the context of intact or disrupted STAT1 signaling.²⁵⁵ Using an *in vivo* model of RSV infection, we are the first to show that endogenous STAT1 signaling is sufficient to negatively repress IL-33 expression and regulate immune cell numbers. Moreover, we found that STAT1 negatively regulated IL-23, consistent with our previous work.²⁵⁰ Herein, we report for the first time that this repression of IL-23 by endogenous STAT1 attenuates the IL-17A⁺ ILC3 response to viral infection.

We identified an increase in the proliferation marker Ki67 in IL-13⁺ ILC2 and IL-17A⁺ ILC3, but not IL-5⁺ ILC2. It is possible that proliferative burst occurs earlier in the IL-5⁺ ILC2 compartment. Alternatively, cytokine-producing ILC2 and ILC3 may also arise from the activation of existing quiescent ILC in the tissue, differentiation of new ILC *in situ*, recruitment of ILC from other tissues, or the shifting of one ILC class to another. Additional investigative approaches will be necessary to better understand how these cytokine-producing ILC2 and ILC3 are accumulating in the lungs of *Stat1*^{-/-} mice during RSV infection.

ILC subsets have been shown to participate in a variety of physiologic and pathophysiologic processes. Accordingly, significant attention has been paid to the identification of activators and inhibitors of ILC subsets that could be exploited therapeutically. For ILC2, such

targets include lipid mediators PGI₂ (inhibitory), PGD₂ (activating), and LTD₄ (activating) as well as cytokines including IL-33 and TSLP.^{36,61,73,79,100,215} Retinoic acid has been shown to promote ILC3 in the gastrointestinal tract, and accordingly dietary modification of retinoic acid derivatives including vitamin A may present a viable therapeutic target.²⁵⁶ However, an effective and non-pathologic immune response often requires the coordinated activation and inhibition of multiple cell types. Targeting pathways that orchestrate this broader response may present a high-yield, efficacious approach to treating disease and promoting health. Our data suggest that STAT1 signaling represents such a pathway, promoting beneficial anti-viral ILC1 and repressing pathologic ILC2 and ILC3 responses by multiple mechanisms in the context of viral infection.

Endogenous mutations in STAT1 signaling alter disease susceptibility in humans. Chronic mucocutaneous candidiasis is a clinical syndrome characterized by recurrent infections of mucus membranes and skin with *Candida* species. A majority of these patients have been shown to have gain-of-function mutations in STAT1, which promote type 1 immune responses and repress type 17 responses, predisposing individuals to infection with fungal diseases.^{257–261} Additionally, loss-of-function mutations in STAT1 have also been identified that confer significant susceptibility to viral and mycobacterial infections.²⁶² Analysis of CD4⁺ T helper subsets in the context of either gain-of function STAT1 mutations show a strong concordance between the STAT1 signaling and CD4⁺ T helper activity, with increases in STAT1 signaling promoting Th1 cells and restricting Th17 cells.^{259,260} Our data suggest that ILC subsets are similarly regulated by STAT1 in mice, and it is intriguing to consider the role of ILC in human patients with mutations at the STAT1 locus, especially considering the prominence of ILC at mucosal sites.

Throughout, we focused our efforts on understanding the role of STAT1 signaling on cytokine-producing ILC, defining ILC1, ILC2, and ILC3 subsets stringently based on their capacity to produce canonical cytokines. While this allowed us to key in on the effects of STAT1 signaling on the major functional outputs of ILC, we were limited using this approach in our ability to understand the entirety of the ILC pool including both cytokine-producing and non-cytokine producing ILC. We chose to focus on cytokine production, as we found that during viral infection the expression of hallmark transcription factors, specifically GATA3, was not always present in IL-5 and IL-13 producing ILC. We reason that these cells may be ILC2 that have downregulated GATA3 as a negative feedback mechanism or possibly ex-ILC1/ILC3 that have shifted their cytokine production to a type 2 program but do not yet express detectable levels of GATA3 (data not shown). Similarly, it is unclear if the changes in cytokine-producing ILC are due to changing total numbers of ILC subsets, increases in the percentage of those subsets expressing cytokines, or other changes in the phenotypes of these cells. Such analyses are beyond the scope of this work, as our primary focus was on the production of type 1, 2, and 17 cytokines from ILC during viral infection.

Our data demonstrate that STAT1 is a chief regulator of cytokine-producing ILC1, ILC2, and ILC3 during viral infection. STAT1 promoted IFN- γ ⁺ ILC1 and acted to repress IL-5⁺ and IL-13⁺ ILC2 and IL-17A⁺ ILC3 via multiple mechanisms, both cell-intrinsic and cell-extrinsic. These data delineate a critical role of STAT1 in broadly orchestrating a productive cytokine-producing ILC response to viral infection.

CHAPTER 5

IL-33 PROMOTES THE EGRESS OF ILC2 FROM THE BONE MARROW

5.1. Introduction

While Chapters 3 and 4 focused on the responsiveness of ILC to viral infections within the lungs, we sought to better understand an earlier step ILC biology—the events that lead to bone marrow egress of ILC2. In order for the mucosal seeding of ILC2, which positions these cells to respond to stimuli such as allergens or viruses, they must first exit developmental niches. In this chapter, we aim to understand the role of IL-33 in egress of ILC2 from the bone marrow.

Innate lymphocytes (ILC) are mucosal effector cells that derive from the common lymphoid progenitor (CLP). They are embedded at environmental interfaces, where they can respond rapidly and directly in an antigen-independent manner to a wide array of insults. Subsets of ILC—group 1, 2, and 3—mirror the adaptive CD4⁺ T helper lymphocyte lineages Th1, Th2, and Th17 cells, respectively, in regard to their transcriptional governance and cytokine production. Group 2 ILC (ILC2) require GATA3 and produce abundant quantities of IL-5, IL-13, and/or IL-9, and under certain circumstances IL-4, similar to CD4⁺ Th2 cells. Known activators of ILC2 include IL-33, IL-25, thymic stromal lymphopoietin (TSLP), TNF-family member TL1A, and lipid mediators such as prostaglandin D₂ and leukotriene D₄. ILC2 have been implicated directly in the pathogenesis of inflammatory diseases including asthma, atopic dermatitis, chronic rhinosinusitis, viral infection, and helminth infection in both animal models and humans. Conversely, ILC2 have also been shown to be regulators of tissue homeostasis,

including in epithelial repair and healthy adipose tissue maintenance (reviewed in Morita et al., 2016).

Our understanding of ILC2 egress from the bone marrow and trafficking to peripheral tissues is highly limited. *Ccr9*^{-/-} mice have reduced numbers of ILC2 in the intestinal lamina propria and adoptively transferred ILC2 progenitors from *Ccr9*^{-/-} mice migrated more poorly than WT ILC2 progenitors to the gastrointestinal tract⁹⁸. Additionally, β_2 integrins and CRTH2 promote the migration of circulating ILC2 into the lungs during allergic airway inflammation and helminth infection, respectively^{100,101}. Critical signals that regulate ILC2 homing receptor profiles, bone marrow egress, and trafficking remain poorly defined.

Maintenance of ILC2 populations in mucosal tissues is thought to occur by multiple mechanisms. Intrinsically, ILC2 are long lived in the tissue⁵³. Under steady state conditions, data suggest ILC2 are replenished from ILC2 or ILC2 lineage progenitor cells that are *in situ* within these peripheral tissues⁹². However, in the context of protracted type 2 inflammation such as during *Nippostrongylus Brasiliensis* infection, ILC2 are in part reseeded hematogenously likely from sources such as the bone marrow⁹². Moreover, myeloablation and reconstitution with donor bone marrow leads to a significant accumulation of donor ILC2 in classically ILC2-rich sites including the colon and skin in humans²⁶⁴. Collectively, these data implicate both peripheral and central mechanisms in the maintenance of ILC2 frequencies in tissue, particularly in the context of disrupted homeostasis.

Development of ILC2 in the bone marrow has been the subject of intense interest. Thematically, our understanding of ILC2 development has focused largely on critical transcriptional regulators such as Bcl11b and ETS1 (Walker et al., 2015; Yu et al., 2015; Zook et al., 2016; and reviewed in Zook and Kee, 2016). However, the role of extracellular signals in

ILC2 development remains more poorly defined. Mice deficient in the *Il7r* or *Il2r* have markedly reduced numbers of ILC2, suggesting a critical role for these cytokines in ILC2 development and/or homeostasis^{37,38}. An *in vitro* system for the differentiation of CLP to ILC2 requires IL-7, Notch ligand, and IL-33^{38,42}. IL-33 is a hallmark activator of ILC2 in peripheral tissues and the most mature ILC2 lineage cell in the bone marrow, referred to as the ILC2 progenitor (ILC2P), expresses the IL-33 receptor ST2^{40,106}. However, a role for IL-33 *in vivo* in ILC2 lineage development or bone marrow egress remains unknown.

We sought to understand the role of IL-33, a quintessential peripheral activator of ILC2, in bone marrow ILC2 lineage development and egress. *Il33*^{-/-} and *St2*^{-/-} mice had significantly increased numbers of ILC2P in the bone marrow and reduced numbers of ILC2 in peripheral tissues compared to WT mice. ILC2P that developed in the absence of IL-33 signaling were comparable to WT ILC2P in their capacity to proliferate and produce IL-5 and IL-13. However, lack of IL-33 signaling precipitated critical changes in the chemokine receptor profile of ILC2P. Notably, ILC2P in *St2*^{-/-} mice expressed higher levels of *Cxcr4*, a receptor that promotes retention of B cells and granulocytes in the bone marrow, which stimulated the retention of ILC2P in the bone marrow. Finally, sub-lethal radiation exposure in parabiotic mice established a key role for hematogenous trafficking of ILC2 in the setting of disrupted tissue homeostasis. Collectively, these data implicate IL-33 as a key driver of bone marrow ILC2 lineage cell egress.

5.2. Methods

5.2.1. Mice

Female 8-12 week old *Il33*^{-/-}, *St2*^{-/-}, and *Tslpr*^{-/-} on a BALB/c genetic background were used throughout this manuscript, unless otherwise indicated, and were generated as previously described^{65,198,199,266}. Where indicated, WT C57BL/6 and *Il33*^{-/-} mice on a C57BL/6 background were used²⁶⁷. WT BALB/c, congenic CD45.1⁺ BALB/c (CByJ.SJL(B6)-Ptprc^a/J), and WT C57BL/6 mice were obtained from the Jackson Laboratory. Heterozygous CD45.1⁺ CD45.2⁺ BALB/c mice were generated from crossing BALB/c mice with CByJ.SJL(B6)-Ptprc^a/J mice. All animals were used in compliance with the revised 1996 “Guide for the care and use of laboratory animals” prepared by the Committee on Care and Use of Laboratory Animals of the Institute of Laboratory Animal Resources, National Research Council. All animal experiments were approved by the Vanderbilt Institutional Animal Care and Use Committee. Animals were housed under specific pathogen-free conditions. Animals were anesthetized with ketamine/xylazine and euthanized with pentobarbital overdose.

5.2.2. Flow cytometry

Bone marrow was isolated by flushing the tibia and femur with cold RPMI media. For mesenteric lymph nodes, tissue was grated through a 70 µm strainer into cold RPMI media. The external portions of the left and right ears were collected for evaluation of skin ILC2. For the disruption of the lungs and skin, tissue was mechanically minced and digested with 1 mg/mL collagenase (Cat. # C5138, Sigma-Aldrich) and 0.02 mg/mL DNase I (Cat. # D4527, Sigma-Aldrich) in RPMI with 5% FBS for 55 minutes at 37°C as previously described²²⁵. EDTA was

added to quench the enzymatic reaction and the tissue was filtered through a 70 μm strainer. RBC lysis was performed and all samples subsequently counted to assess total numbers of cells within each tissue. Three to five million cells were stained for flow cytometry in FACS buffer (PBS + 3% FBS). Cells were initially blocked with a 1:25 dilution of anti-CD16/CD32 blocking reagent (Cat. # 553142, BD Biosciences), and subsequently stained for combinations of the surface markers listed in Table 5-1. Viability dye (DAPI or PI) was added immediately prior to flow cytometric analysis. Samples were measured on a BD LSR II and analyzed with FlowJo Version X. Doublets were removed based on FSC/SSC properties and dead cells were excluded in all analyses as PI⁺ or DAPI⁺. ILC2 and ILC2P were defined as CD45⁺ Lin⁻ IL-25R⁺ CD25⁺ CD127⁺ where “Lin” represents a lineage cocktail containing antibodies against CD3, CD5, CD45R (B220), CD11b, Gr-1 (Ly-6G/C), 7-4, and Ter-119. ILC2 and ILC2P defined by this gating strategy co-expressed validated phenotypic markers found on ILC2 in a variety of tissues in wild type mice including CD90, ST2, and ICOS, though ST2 expression was not observed in the skin (Figure 5-1). In some experiments, cells were stained for donor source using anti-CD45.1 or anti-CD45.2 (Table 4-1). LMPP were defined as Lin⁻ CD25⁻ CD127⁻ Flt3⁺ c-Kit^{hi} Sca-1^{hi}. CLP were defined as Lin⁻ CD25⁻ CD127⁺ Flt3⁺ c-Kit^{lo} Sca-1^{lo}. CHILP were defined as Lin⁻ CD25⁻ CD127⁺ Flt3⁻ $\alpha\beta\gamma$ ^{hi}. ILCP were defined as Lin⁻ CD25⁻ CD127⁺ Flt3⁻ c-Kit⁺ $\alpha\beta\gamma$ ⁺ PD-1⁺.

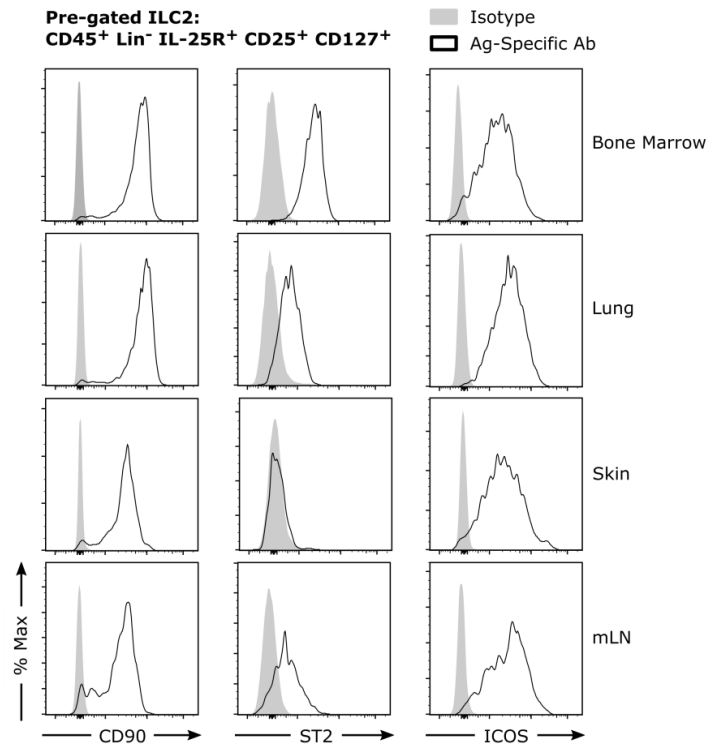


Figure 5-1. ILC2P surface phenotyping.

The expression of CD90, ST2, and ICOS on ILC2 in the bone marrow, lungs, skin, and mLN. Data are representative of 2-3 similar experiments.

Table 5-1. Flow Cytometry and FACS Antibodies.

Epitope	Clone	Manufacturer	Fluorophore	Dilution
Lineage Cocktail	130-092-613	Miltenyi	Biotin	1:25
CD3	17A2	eBioscience	Biotin	1:200
CD45	30-F11	Tonbo	rF710	1:400
CD45	30-F11	BD Biosciences	PerCP-Cy5.5	1:800
CD45.1	A20	BioLegend	BV510	1:100
CD45.2	104	BioLegend	BV421	1:100
CD25	PC61	BioLegend	APC	1:200
CD25	PC61	BioLegend	PE	1:200
CD25	PC61	BioLegend	BV421	1:200
CD25	PC61	eBioscience	AF488	1:200
CD127	SB/199	eBioscience	PE-Cy7	1:200
IL-25R	MUNC33	eBioscience	PE	1:200
IL-25R	MUNC33	eBioscience	eFluor660	1:50
CXCR4	2B11	eBioscience	PE	1:100
c-Kit	ACK2	eBioscience	AF700	1:100
PD-1	J43	eBioscience	FITC	1:100
Flt3	A2F10	eBioscience	PE-Cy5	1:400
$\alpha_4\beta_7$	DATK32	eBioscience	APC	1:100
Sca-1	D7	eBioscience	PE	1:200
CD90	30-H12	eBioscience	FITC	1:400
ST2	RMST2-2	eBioscience	PerCP-eF710	1:100
ICOS	C398.4A	eBioscience	APC	1:100

5.2.3. *In vitro* ILC2P culture

Bone marrow was prepared as described above. Following RBC lysis, samples were enriched for lineage negative cells by magnetic separation. Enriched cell fractions were prepared for FACS and ILC2P were sorted into RPMI media with 10% FBS, 2mM L-Glutamine, 1mM sodium pyruvate, 10 mM HEPES, and 100 units/mL of penicillin and streptomycin. In some assays, ILC2P were stained prior to culture with the dilution-based proliferation dye CellTrace Violet per the manufacturer instructions (Cat. # C34557, Life Technologies). ILC2P were plated at 2500 cells per well in 96-well round bottom plates. ILC2P were cultured with IL-2 (10 ng/mL, Cat. # 212-12, PeproTech) alone or in combination with IL-33 (0.1 ng/mL-10 ng/mL, Cat. # 210-33, PeproTech) for 1-5 days.

5.2.4. Protein Measurements

Cell culture supernatants from *in vitro* ILC2P cultures were collected for the measurement IL-5 and IL-13 by ELISA (Cat. # DY405 and DY413, R&D Systems) per manufacturer instructions.

5.2.5. BrdU Assay

Mice were treated *in vivo* with 1 mg of BrdU intraperitoneally for five consecutive days. Bone marrow was harvested 24 hours following the final treatment and cells were prepared for flow cytometric analysis per manufacturer instructions (Cat. # 552598, BD Biosciences). Briefly,

cells were stained with a fixable live/dead viability dye (Cat. #13-0868, Tonbo Biosciences) followed by anti-CD16/CD32 blockade and antibodies against ILC2P cell surface markers (Table S1). Cells were fixed and permeabilized, and the DNA was treated with DNase I for 1 hour at 37°C to expose BrdU epitopes. Cells were subsequently stained with an anti-BrdU antibody and measured by flow cytometry to assess the total number of BrdU⁺ ILC2P in the bone marrow.

5.2.6. Bone marrow chimeras

Six- to 10-week old heterozygous CD45.1⁺ CD45.2⁺ WT BALB/c recipients were lethally irradiated (9 Gy) and transplanted with a 1:1 mixture of whole bone marrow from age matched 6- to 10- week old WT congenic (CD45.1⁺) mice and *St2*^{-/-} mice (CD45.2⁺) via retro-orbital injection while anesthetized with ketamine/xylazine. Mice were provided with oral antibiotics for 2 weeks following transplant and maintained in sterile housing. Bone marrow grafts were allowed to reconstitute for 6 weeks. Mice were subsequently harvested for bone marrow, lungs, skin, and mLN to assess donor frequencies by flow cytometry. Residual cells remaining from the recipient mice (CD45.1⁺ CD45.2⁺) were excluded.

5.2.7. mRNA Quantification

ILC2P from WT and *St2*^{-/-} mice were enriched for lineage negative cells by magnetic separation and purified by FACS as described above. Cells were sorted into cold PBS and centrifuged at 10,000 x g for 5 minutes to remove the supernatant. mRNA was collected from the

pelleted ILC2P using the RNeasy Micro Kit (Cat. # 74004, QIAGEN) with on-column DNase treatment. cDNA was prepared using the SuperScript IV reverse transcriptase system (Cat. # 18091050, Invitrogen). Because of low cell input (fewer than 20,000 sorted ILC2P per sample), we performed a pre-amplification for our target genes as per manufacturer instructions (Cat. # 4384267, Applied Biosystems). A conventional quantitative PCR using FAM-MGB TaqMan primers listed in Table 5-2 was performed on an Applied Biosystems QuantStudio12k Flex Real-Time PCR machine and data were analyzed using Applied Biosystems QuantStudio 12k Flex Software v1.2.2. Six candidate housekeeping genes were evaluated for stable expression in ILC2P as previously described²⁶⁸, and target genes were normalized to the geometric mean Ct values of a pool of three of these stably expressed reference genes—Rpl13a, Ywhaz, and Hprt. Differential expression was assessed by using the $\Delta\Delta\text{Ct}$ protocol.

Table 5-2. Quantitative PCR Primers.

Gene Name	Assay ID	Manufacturer
<i>Ccr3</i>	Mm00515543_s1	Applied Biosystems
<i>Ccr4</i>	Mm01963217_u1	Applied Biosystems
<i>Ccr7</i>	Mm99999130_s1	Applied Biosystems
<i>Ccr8</i>	Mm99999115_s1	Applied Biosystems
<i>Ccr9</i>	Mm02528165_s1	Applied Biosystems
<i>Ccr10</i>	Mm01292449_m1	Applied Biosystems
<i>Cxcr4</i>	Mm01996749_s1	Applied Biosystems
<i>Cxcr6</i>	Mm02620517_s1	Applied Biosystems
<i>Cx3cr1</i>	Mm02620111_s1	Applied Biosystems
<i>Ccl1</i>	Mm00441236_m1	Applied Biosystems
<i>Ptgdr2 (Crth2)</i>	Mm00438315_s1	Applied Biosystems
<i>Slpr1</i>	Mm02619656_s1	Applied Biosystems
<i>Hprt</i>	Mm00446968_m1	Applied Biosystems
<i>Rpl13a</i>	Mm01612986_gH	Applied Biosystems
<i>Ywhaz</i>	Mm03950126_s1	Applied Biosystems

5.2.8. *In vivo* AMD3100 and IL-33 treatments

For CXCR4 blockade, mice were treated with intraperitoneal injections of 10 mg/kg AMD3100 (Cat. # A5602, Sigma-Aldrich) or vehicle PBS every six hours for a total of three consecutive doses. Mice were sacrificed four hours after the final dose of AMD3100. For IL-33 treatments, mice were anesthetized with ketamine/xylazine and treated with 1 µg of recombinant murine IL-33 (Cat. # 210-33, PeproTech) or vehicle (0.1% BSA in PBS) via retro-orbital injection. Mice were sacrificed 24 hours after IL-33 injection.

5.2.9. *In vivo* *Alternaria alternata* extract challenge

WT mice were anesthetized with ketamine/xylazine and challenged intranasally with either 5 µg of *Alternaria alternata* extract dissolved in 100 µl of PBS or 100 µl of PBS (vehicle) every 24 hours for four consecutive days. Mice were euthanized 24 hours after the final dose of *Alternaria* extract and serum, lungs, and bone marrow were collected for analysis.

5.2.10. Parabiosis

WT Congenic CD45.1⁺ BALB/c mice were sub-lethally irradiated (4 Gy) and parabiosed to WT CD45.2⁺ BALB/c mice. Mice were anesthetized with ketamine/xylazine and partially shaved to expose the surgical site. Surgical sites were sterilized with alcohol and betadine, and lateral incisions were made in the skin between the knee joint and the elbow joint. Sutures were placed connecting the knee and elbow joints of the two mice for anchoring. Skin was aligned

between the two mice and sutured from one mouse to the other to close the incision site.

Buprenorphine was administered for analgesia for the first 48 hours post-surgery. Wet food, dry food, and water was provided on the floor of the cage. As needed, mice were supplemented with physiologic saline to prevent dehydration.

5.2.11. Statistics

Statistical analyses were performed using GraphPad Prism version 5. Unpaired t-test or one-way ANOVA with Bonferroni post-test were used to determine statistical significance, as appropriate. When measured values were below the limit of detection, samples were assigned a value at half of the limit of detection to allow for statistical comparisons.

5.3. Results

5.3.1. Deficiency in IL-33 Signaling Promotes Accumulation of ILC2P in the Bone Marrow

IL-33 signaling via its receptor ST2 is a central pathway for the activation of ILC2 effector functions in peripheral tissues. Moreover, IL-33 has been used *in vitro* to stimulate the differentiation of ILC2 from CLP^{38,42}. We hypothesized that IL-33 promotes the development of ILC2 *in vivo*. Accordingly, we assayed for the number of ILC2P in the bone marrow of naïve BALB/c WT, *Il33*^{-/-}, and *St2*^{-/-} mice. ILC2P and peripheral ILC2 were defined as viable cells that were CD45⁺ Lin⁻ IL-25R⁺ CD25⁺ CD127⁺ (Figure 5-2 A). WT, *Il33*^{-/-}, and *St2*^{-/-} mice had similar numbers of bone marrow cells (Figure 5-2 B), but unexpectedly, we identified a significant

increase in the frequency and total number of ILC2P in *Il33*^{-/-} and *St2*^{-/-} mice compared to WT mice (Figure 5-2 C-D). A similar increase in the total number of bone marrow ILC2P was observed in *Il33*^{-/-} mice on a C57BL/6 background, indicating that this phenotype was independent of host genetic background (Figure 5-2 E). We next characterized the number of ILC2 in peripheral tissues. We focused on ILC2-rich tissues in disparate parts of the body, specifically the lung, skin, and mesenteric lymph nodes (mLN). Opposite our result in the bone marrow, we found a significant decrease in the frequency and total number of ILC2 in the lungs, skin, and mLN of *Il33*^{-/-} and *St2*^{-/-} mice compared to WT mice (Figure 5-3). These data suggested that IL-33 might affect ILC2P egress from the bone marrow.

In addition to IL-33, TSLP is a potent activator of ILC2. However, these two cytokines signal via distinct cellular pathways. IL-33 binds to ST2 to induce MyD88 activation and NF- κ B translocation to the nucleus, whereas TSLP binds to a heterodimer of the TSLPR and IL-7R α and activates STAT5. We assessed whether the effects on ILC2P/ILC2 frequency and bone marrow egress were unique to IL-33 signaling, or were part of a broader network of ILC2-activating cytokines that functioned redundantly. We measured the number of ILC2P in the bone marrow and ILC2 in the lungs of WT and *Tslpr*^{-/-} mice. In contrast to mice lacking IL-33 signaling, the loss of TSLPR signaling reduced the frequency and total number of ILC2P in the bone marrow (Figure 5-4 A-D) and ILC2 in the lungs (Figure 5-4 E-H) compared to WT mice. These data indicate that IL-33 acts distinctly from other ILC2-activating cytokines in regulating bone marrow ILC2P frequency and that TSLP may instead play an important role in ILC2 development.

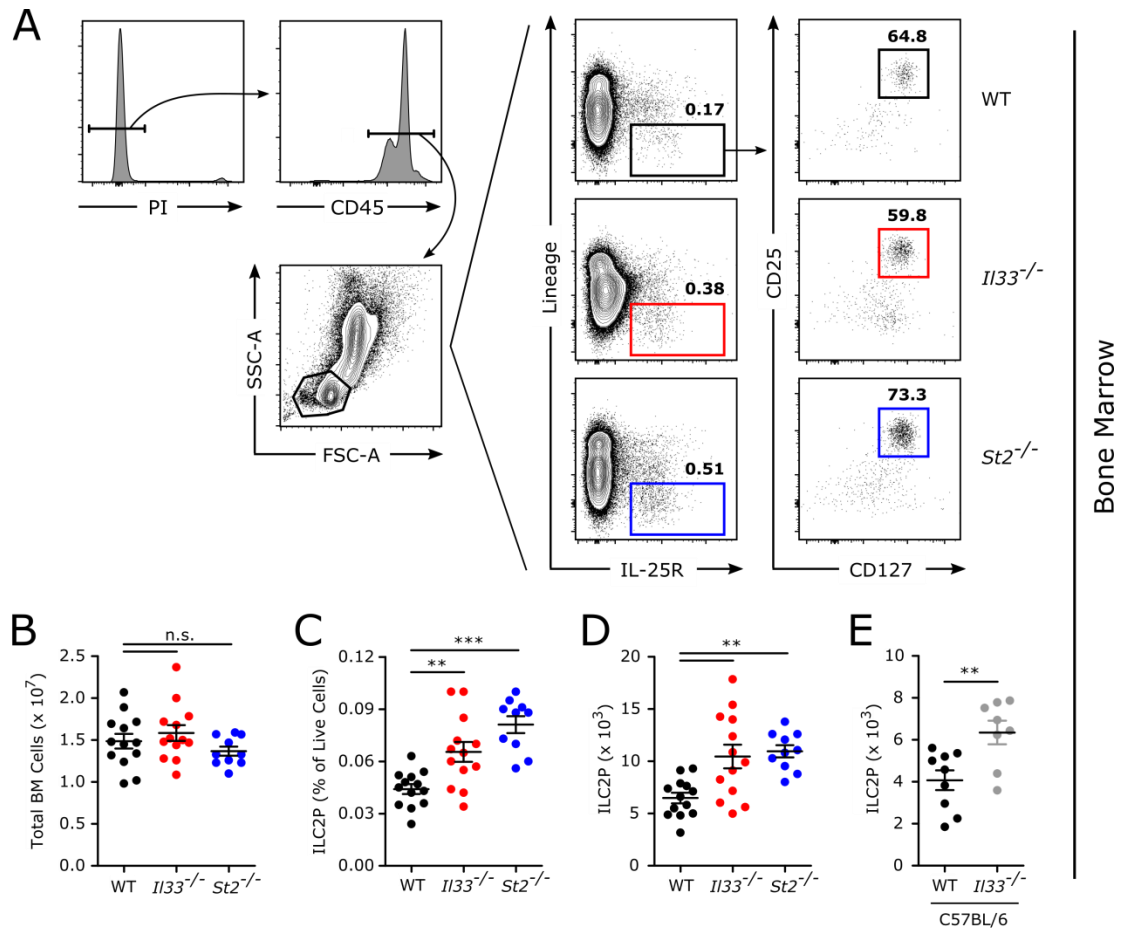


Figure 5-2. Deficiency in IL-33 signaling lead to an accumulation of ILC2P in the bone marrow.

Adult naïve WT BALB/c, *Il33*^{-/-}, and *St2*^{-/-} mice were sacrificed and bone marrow from one tibia and femur was prepared for flow cytometric analysis. (A) Gating strategy and representative gating of WT, *Il33*^{-/-}, and *St2*^{-/-} ILC2P. ILC2P were defined as viable CD45⁺ FSC-A^{lo} SSC-A^{lo} Lin⁻ IL-25R⁺ CD25⁺ CD127⁺ cells. (B) The total number of viable bone marrow cells, (C) ILC2P frequency among live bone marrow cells, and (D) the total number of ILC2P in the bone marrow. (E) The total number of ILC2P in the bone marrow of WT C57BL/6 and *Il33*^{-/-} mice on a C57BL/6 background. Data are combined from 2 (E) or 3 (A-D) independent experiments and displayed as the mean ± SEM. **p < 0.01 and ***p < 0.001 by one-way ANOVA with Bonferroni post-test (A-D) or unpaired t-test (E); n.s. = not significant.

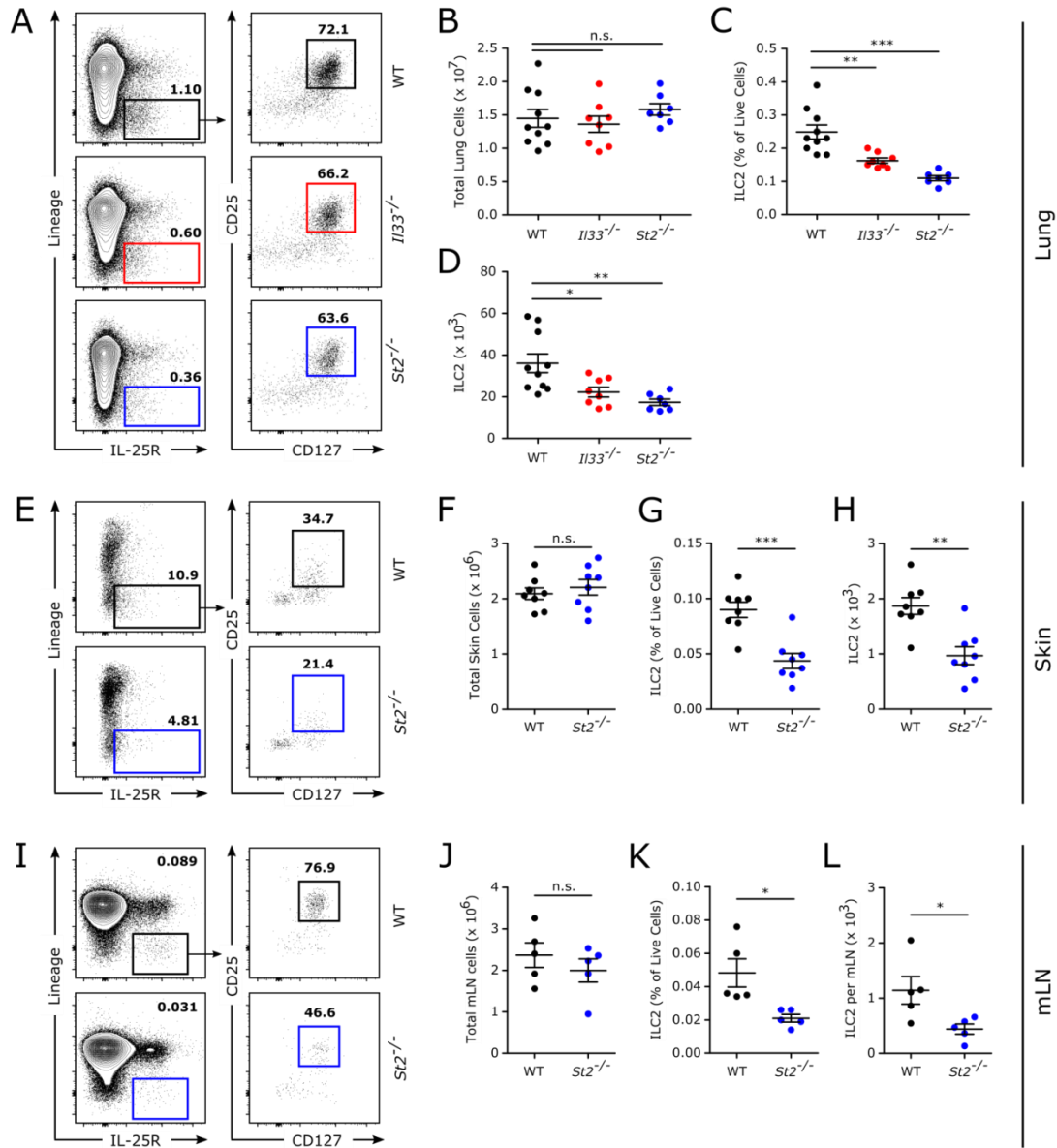


Figure 5-3. Deficiency in IL-33 signaling decreased the number of ILC2 in peripheral tissues.

Adult naïve WT, *Il33*^{-/-}, and/or *St2*^{-/-} mice were sacrificed and lungs, skin, and mesenteric lymph nodes were collected. (A) Representative gating of lung ILC2. (B) The total number of viable lung cells, (C) ILC2 frequency among live lung cells, and (D) the total number of ILC2 in the lungs. (E) Representative gating of skin ILC2. (F) The total number of viable skin cells, (G) ILC2 frequency among live skin cells, and (H) the total number of ILC2 in the skin. (I) Representative gating of mLN ILC2. (J) The total number of viable mLN cells, (K) ILC2 frequency among live mLN cells, and (L) the total number of ILC2 in the mLN normalized to the total number of mLN collected. Data are combined from 2 independent experiments and displayed as the mean \pm SEM. * $p < 0.05$, ** $p < 0.01$, and *** $p < 0.001$ by one-way ANOVA with Bonferroni post-test (B-D) or unpaired t-test (F-H, J-L); n.s. = not significant.

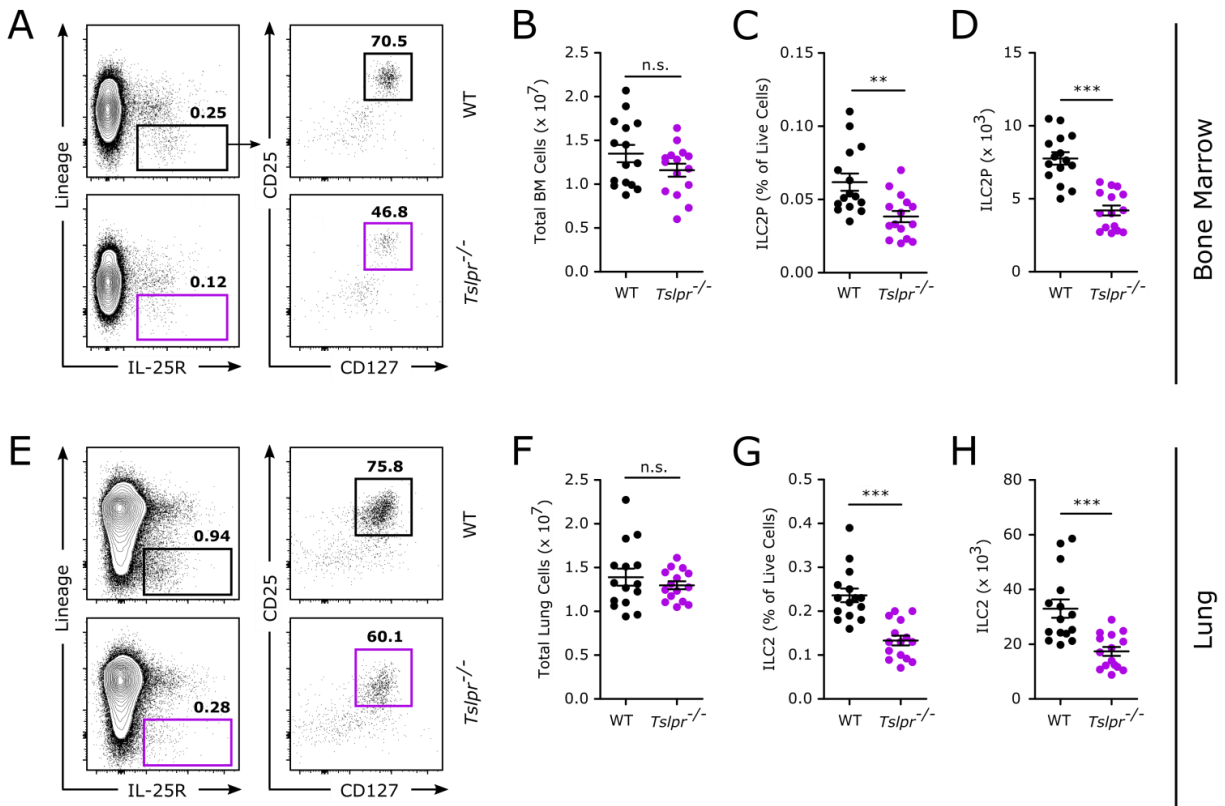


Figure 5-4. Deficiency in TSLP signaling reduced the number of ILC2P/ILC2 in the bone marrow and peripheral tissues.

Adult naïve WT and *Tslpr*^{-/-} mice were sacrificed and the lungs and bone marrow were prepared for flow cytometric analysis. (A) Representative ILC2P gating in the bone marrow, (B) The total number of viable bone marrow cells, (C) ILC2P frequency among live bone marrow cells, and (D) the total number of ILC2P in the bone marrow. (E) Representative gating of lung ILC2. (F) The total number of viable lung cells, (G) ILC2 frequency among live lung cells, and (H) the total number of ILC2 in the lungs. Data are combined from 3 independent experiments and displayed as the mean ± SEM. ***p* < 0.01 and ****p* < 0.001 by unpaired t-test.

5.3.2. IL-33 Deficiency Does Not Appreciably Alter the Hallmark Functional Capacities of ILC2

We considered whether the increase in ILC2P frequency might be a compensatory effect for reduced proliferative potential or cytokine producing capacity of these cells in the *Il33*^{-/-} and *St2*^{-/-} mice. Accordingly, we compared these functional capacities in ILC2P from mice with or without intact IL-33 signaling. ILC2P from the bone marrow of WT and *Il33*^{-/-} mice were enriched by magnetic selection for lineage negative cells and purified by FACS. Sorted ILC2P were cultured in supplemented RPMI with IL-2 alone or IL-2 in combination with IL-33. IL-2 alone sustains ILC2P cultures but does not induce proliferation or cytokine production. Conversely, IL-33 is a potent stimulus for ILC2P, rapidly induce proliferation and production of IL-5 and IL-13⁷⁹. ILC2P from *Il33*^{-/-} mice have developed in the absence of IL-33, but readily express ST2 and are poised to respond to IL-33. Thus, we were able to consider the developmental role of IL-33 on the proliferative capacity and cytokine expression of ILC2P.

Prior to culture, we stained ILC2P with CellTrace Violet to measure proliferation. Following 5 days of *in vitro* culture, we harvested ILC2P for flow cytometric analysis of CellTrace Violet dye dilution (Figure 5-5 A). For both WT and *Il33*^{-/-} ILC2P, IL-2 alone did not induce proliferation. IL-2 and IL-33 in combination induced robust proliferation as measured by serial dye dilution in both WT and *Il33*^{-/-} ILC2P. Importantly, no difference was observed in the proliferation between WT and *Il33*^{-/-} ILC2P in response to IL-33. Similarly, the proliferation index measuring the average number of divisions a starting cell undergoes based on CellTrace Violet dye dilution was identical between WT and *Il33*^{-/-} ILC2P (Figure 5-5 B). Finally, we counted the number of cells in each well following 5 days of culture (Figure 5-5 C). IL-33 in

combination with IL-2 induced a significant increase in the total number of WT and *Il33*^{-/-} ILC2P compared to IL-2 alone. However, no difference was observed in the number of ILC2P between IL-33-stimulated WT and *Il33*^{-/-} cultures.

We also collected supernatants from these ILC2P cultures to assess the cytokine expressing capacity of WT and *Il33*^{-/-} ILC2P. IL-2 alone did not induce IL-5 or IL-13 production from either WT or *Il33*^{-/-} ILC2P. Stimulation with IL-2 and IL-33 in combination significantly induced IL-5 and IL-13 expression in both strains of ILC2P. A very slight (<10%) but reproducible difference in IL-5 expression was detected, with WT ILC2P producing marginally higher quantities of IL-5 than *Il33*^{-/-} ILC2P (Figure 5-5 D). No significant difference was observed in the expression of IL-13 between WT and *Il33*^{-/-} ILC2P (Figure 5-5 E). Collectively, these data specify that ILC2P that develop in the absence of IL-33 signaling are functionally similar to WT ILC2P in their capacity to proliferate and express IL-5 and IL-13.

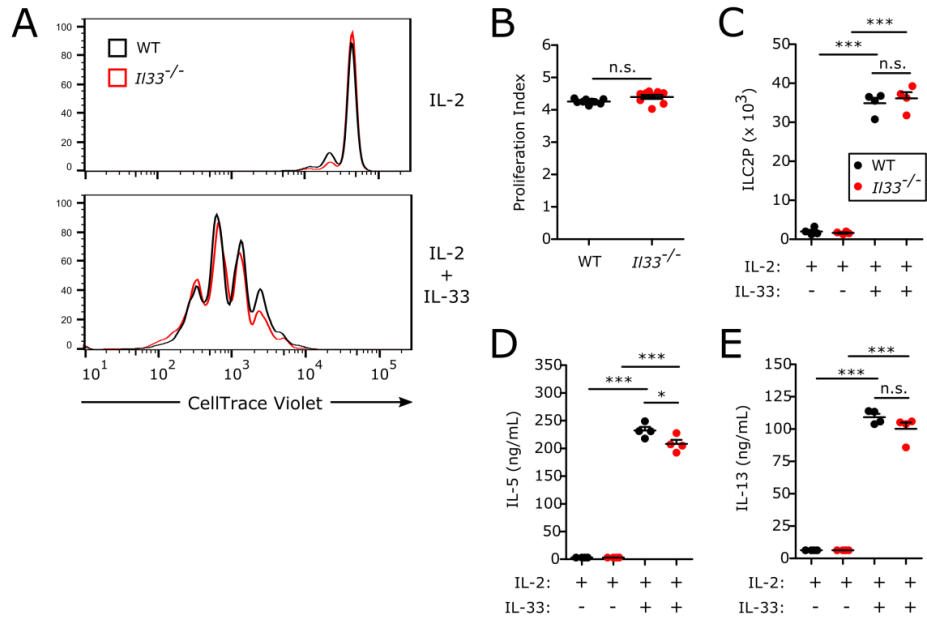


Figure 5-5. IL-33-deficient ILC2P were comparably functional to WT ILC2P.

ILC2P from the bone marrow of WT and *Il33^{-/-}* mice were enriched by magnetic separation and purified by FACS. Sorted ILC2P were stained with the dilution-based proliferation dye CellTrace Violet and cultured in supplemented RPMI media in the presence of IL-2 (10 ng/mL) ± IL-33 (0.1-10 ng/mL) for 5 days. (A) Representative CellTrace Violet dilution peaks. (B) Proliferation index quantifying the average number of proliferations events undergone by each ILC2P derived from CellTrace Violet staining. (C) Cell counts of ILC2P post-stimulation. (D) IL-5 and (E) IL-13 concentrations in the supernatants as measured by ELISA. Data are representative of 3 similar experiments and displayed as the mean ± SEM. * $p < 0.05$ and *** $p < 0.001$ by one-way ANOVA with Bonferroni post-test (C-E) or unpaired t-test (B); n.s. = not significant.

5.3.3. Lack of IL-33 Signaling Does Not Alter the Rate of *De Novo* ILC2P Generation in the Bone Marrow

We also considered whether the difference in ILC2P numbers in the bone marrow of mice competent for or lacking IL-33 signaling could be explained by a different rate of generation of these cells from precursors. First, we looked at the abundance of upstream progenitor cells, specifically lymphoid-primed multipotent progenitors (LMPP), common lymphoid progenitors (CLP), common helper innate lymphoid progenitors (CHILP), and innate lymphoid cell progenitors (ILCP), in the bone marrow of WT and *St2*^{-/-} mice (gating strategy shown in Figure 5-6). LMPP and CLP can differentiate into T, B, NK, and all ILC with varying efficiencies²⁶⁹, and CHILP and ILCP are restricted to ILC1, ILC2, and ILC3 as well as lymphoid tissue inducer (LTi) cells or ILC1, ILC2, and ILC3 only, respectively^{41,44}. We did not observe any significant differences in the total number of LMPP, CLP, CHILP, or ILCP populations between WT and *St2*^{-/-} mice (Figure 5-7 A-D). Therefore, the first divergence in cell frequency in the ILC2 developmental lineage that we observed occurred at the mature ILC2P stage.

To directly assess the rate of ILC2P lymphopoiesis, we injected WT and *St2*^{-/-} mice daily with BrdU for 5 days and harvested their bone marrow 24 hours following the final injection to evaluate for BrdU incorporation in ILC2P (Figure 5-7 E). BrdU incorporation is a property of lymphopoiesis and marks *de novo* generated cells in the bone marrow allowing us to assess the rate of ILC2P development. A small fraction of BrdU⁺ ILC2P was measured in both WT and *St2*^{-/-} mice. However, no significant difference in the number of BrdU⁺ ILC2P was observed (Figure 5-7 E). These data collectively suggest that ILC2P are being generated from precursors at a similar rate in the presence or absence of IL-33 signaling, indicating that variation in the rate of

ILC2P development was an unlikely explanation for the difference in ILC2P numbers in WT, *Il33*^{-/-}, and *St2*^{-/-} mice.

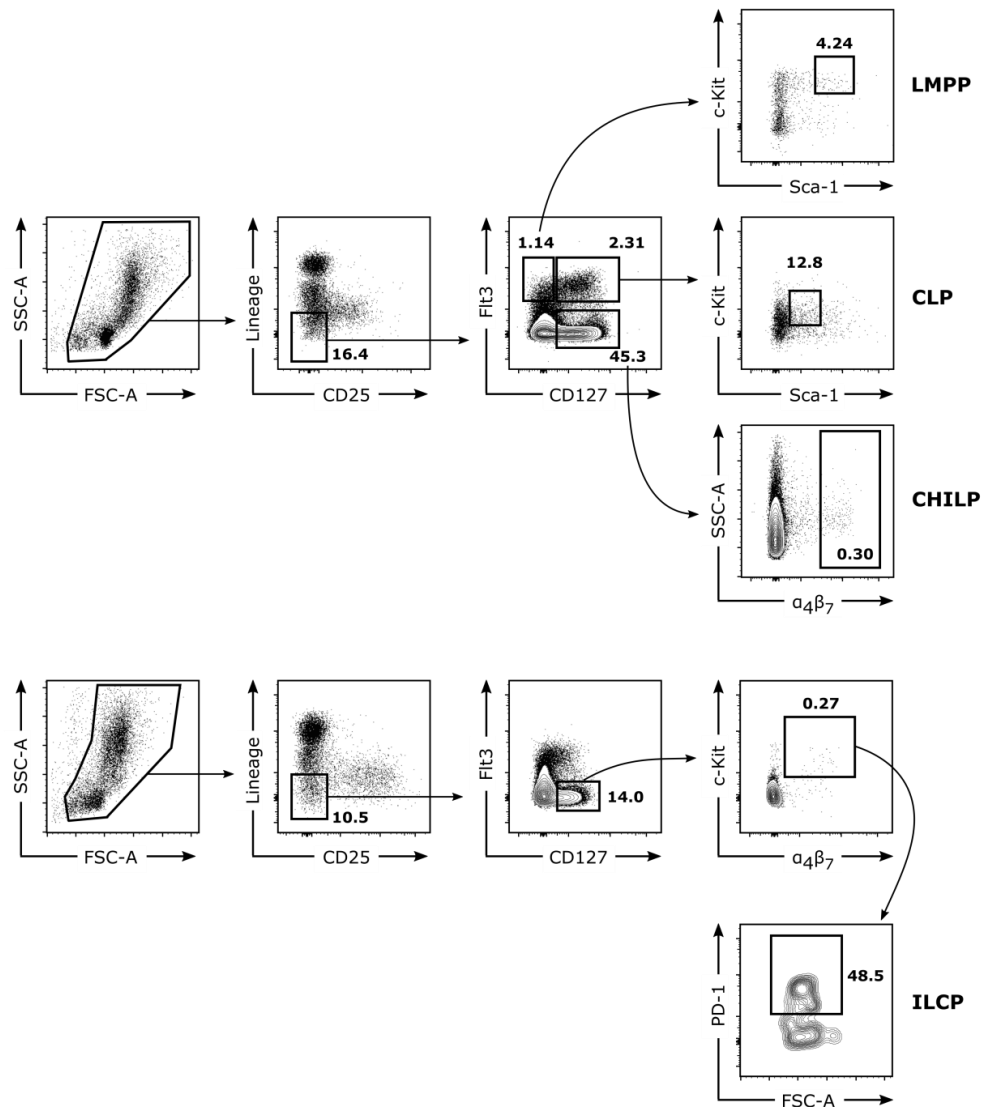


Figure 5-6. Gating strategy for LMPP, CLP, CHILP, and ILCP in the bone marrow.

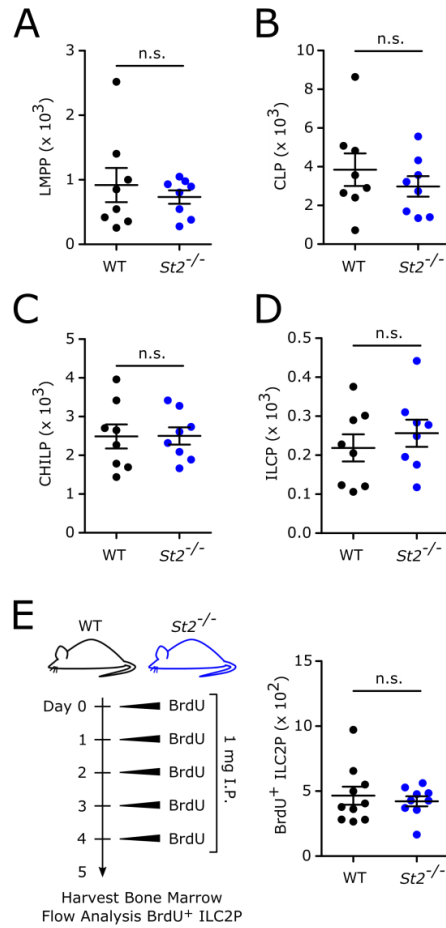


Figure 5-7. Lymphopoiesis of ILC2P *in vivo* did not require IL-33.

Adult naïve WT and *St2*^{-/-} mice were sacrificed and bone marrow from one tibia and femur was prepared for flow cytometric analysis. The total number of progenitors in the ILC2 lineage were quantified: (A) LMPP defined as Lin⁻ CD25⁻ CD127⁻ Flt3⁺ c-Kit^{hi} Sca-1^{hi}, (B) CLP defined as Lin⁻ CD25⁻ CD127⁺ Flt3⁺ c-Kit^{lo} Sca-1^{lo}, (C) CHILP defined as Lin⁻ CD25⁻ CD127⁺ Flt3⁻ α4β7^{hi}, and (D) ILCP defined as Lin⁻ CD25⁻ CD127⁺ Flt3⁻ c-Kit⁺ α4β7⁺ PD-1⁺. WT and *St2*^{-/-} mice were treated daily with 1 mg of BrdU intraperitoneally and harvested 24 hours after the final dose. (E) The experimental design and total number of BrdU⁺ ILC2P in the bone marrow. Data are combined from 2 independent experiments and displayed as the mean ± SEM; n.s. = not significant by unpaired t-test.

5.3.4. ILC2P/ILC2 Frequencies in *St2*^{-/-} mice are Established by an ILC2P/ILC2 Cell-Intrinsic Mechanism

Given that ILC2P in *Il33*^{-/-} mice were functionally similar to WT ILC2P and that a lack of IL-33 signal did not alter *de novo* generation of ILC2P, we hypothesized that ILC2P accumulated in the bone marrow of mice lacking IL-33 signaling due to an impedance in ILC2P bone marrow egress. To explore this hypothesis, we first determined if the frequencies of ILC2P/ILC2 were established by an ILC2P/ILC2 cell-intrinsic or cell-extrinsic mechanism. To test this, we used a mixed bone marrow chimera model (Figure 5-7 A). Whole bone marrow from congenic WT (CD45.1⁺) and *St2*^{-/-} (CD45.2⁺) mice was mixed in a 1:1 ratio. Ten million total cells from this mixture were transplanted into lethally irradiated WT (CD45.1⁺ CD45.2⁺) mice and allowed to reconstitute for 6 weeks. In the bone marrow, *St2*^{-/-} (CD45.2⁺) ILC2P were observed at a significantly higher frequency than WT (CD45.1⁺) ILC2P, consistent with our observation in germline knockout mice (Figure 5-7 B). In the lungs, skin, and mLN, WT (CD45.1⁺) ILC2 were observed at a higher frequency than *St2*^{-/-} (CD45.2⁺) ILC2, also consistent with our observation in germline knockout mice (Figure 5-7 C-E). Accordingly, these data indicate that the frequencies of ILC2P and ILC2 are established by an ST2-dependent cell-intrinsic mechanism.

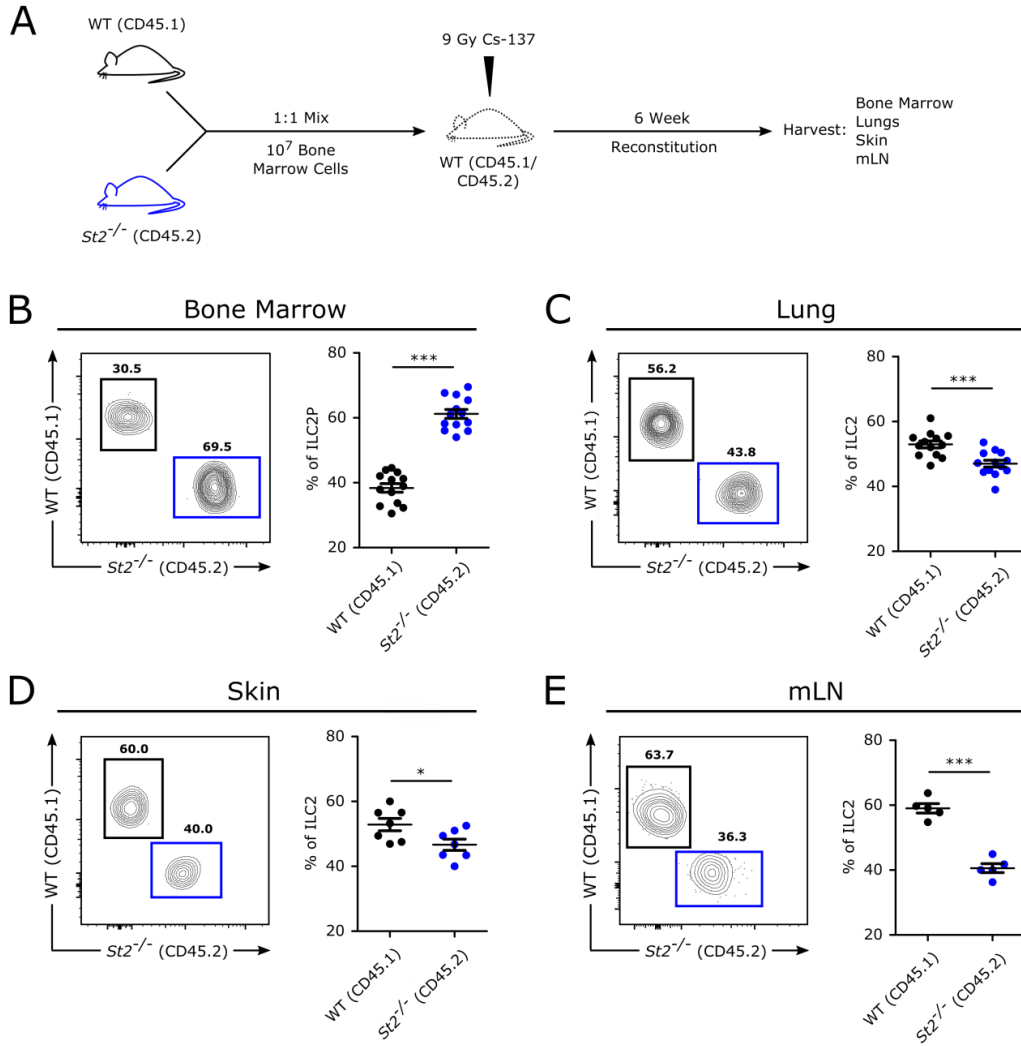


Figure 5-8. Tissue frequencies of ILC2/ILC2P were established by a cell-intrinsic, ST2-dependent mechanism.

Six-week old heterozygous CD45.1⁺ CD45.2⁺ WT mice were lethally irradiated and reconstituted with 10 million cells of a 1:1 mixture of CD45.1⁺ WT and CD45.2⁺ $St2^{-/-}$ total bone marrow cells. (A) Experimental design. (B) ILC2P representative gating and pooled analyses of WT and $St2^{-/-}$ -derived ILC2P displayed as frequencies of donor-derived ILC2P. ILC2 representative gating and pooled analyses of WT and $St2^{-/-}$ -derived ILC2 displayed as frequencies of donor-derived ILC2 in the (C) lungs, (D) skin, and (E) and mLN. Data are combined from 2 (D-E) or 3 (B-C) independent experiments and displayed as the mean \pm SEM. * $p < 0.05$ and *** $p < 0.001$ by unpaired t-test; n.s. = not significant.

5.3.5. *St2*^{-/-} ILC2P Differentially Express Multiple Chemokine Receptors

Given that our data indicated an ILC2P cell-intrinsic mechanism for altered ILC2P frequency in mice lacking IL-33 signaling, and that the ability of ILC2P to egress from the bone marrow in mice lacking IL-33 may be compromised, we considered whether IL-33 modified the chemokine receptor profile on ILC2P. To assess this, lineage negative cells were enriched from the bone marrow of WT and *St2*^{-/-} mice by magnetic separation and ILC2P were purified by FACS. Chemokine receptor expression was assessed in these sorted ILC2P by qPCR. We interrogated the expression levels of chemokine receptors and chemokine-associated proteins known to be expressed by ILC2 or CD4⁺ Th2 cells. Compared to WT ILC2P, *St2*^{-/-} ILC2P had significantly increased expression of *Cx3cr1*, *Ccr7*, *Ccr9*, *Cxcr4*, and *Ptgdr2* and significantly decreased expression of *Ccl1* (Figure 5-9 A). Collectively, these data implicate IL-33 signaling during ILC2P development in the bone marrow as a critical regulator of the chemokine receptor profile on these cells.

5.3.6. IL-33 is a Direct Negative Regulator of CXCR4 on ILC2P *In Vitro*

Among the chemokine receptors that were differentially regulated, we focused on CXCR4. CXCR4 signaling via its ligand SDF-1 (CXCL12) promotes retention of developing B cells, granulocytes, and leukocyte progenitor cells in the bone marrow²⁷⁰. Loss of CXCR4 signaling, either by downregulation of the receptor or reduction in ligand, allows for efficient egress of B cells, granulocytes, and leukocyte progenitor cells from the bone marrow. Given that we observed increased expression of *Cxcr4* in *St2*^{-/-} ILC2P, we hypothesized that augmented

CXCR4 signaling was contributing to poor egress and retention of ILC2P in *St2^{-/-}* mice compared to WT mice. In evaluating this hypothesis, we first sought to understand whether IL-33 could directly regulate the expression of CXCR4 on ILC2P. We isolated ILC2P by magnetic enrichment for lineage negative cells and FACS purification. We cultured these ILC2P for 24 hours in IL-2 alone or with IL-33 at 0.1, 1, or 10 ng/mL. After 24 hours, we assessed the expression of CXCR4 by flow cytometry. CXCR4 expression was readily detectable on these cells compared to isotype staining (Figure 5-9 B). Compared to IL-2 alone, IL-2 in combination with IL-33 downregulated the expression of CXCR4 in an IL-33 dose-dependent manner as measured by MFI (Figure 5-9 B-C). These data are consistent with our chemokine receptor analysis, and demonstrate that IL-33 can directly and negatively regulate the expression of CXCR4.

5.3.7. Blockade of CXCR4 Reduces Bone Marrow ILC2P Frequency in *St2^{-/-}* mice

Given the known role of CXCR4 in bone marrow retention of other leukocyte lineages and the ability of IL-33 to negatively regulate the expression of CXCR4, we sought to determine whether increased CXCR4 signaling was required for the disproportionate retention of ILC2P in the bone marrow of mice lacking IL-33 signaling. To test this, we treated WT and *St2^{-/-}* mice with consecutive doses of AMD3100, a potent, selective CXCR4 antagonist that blocks the function of CXCR4. Following our final AMD3100 treatment, we assessed the number of ILC2P in the bone marrow (Figure 5-9 D). Compared to WT mice, vehicle treated *St2^{-/-}* mice had significantly increased numbers of ILC2P consistent with our initial observation. AMD3100 treatment in *St2^{-/-}* mice, however, significantly reduced the total number of ILC2P as compared

to vehicle treated *St2*^{-/-} mice (Figure 5-9 D). These data strongly suggest that the augmented expression of *Cxcr4* in *St2*^{-/-} mice above WT levels was involved in retention of ILC2P in the bone marrow, and that blockade of this chemokine receptor allowed for egress of ILC2P.

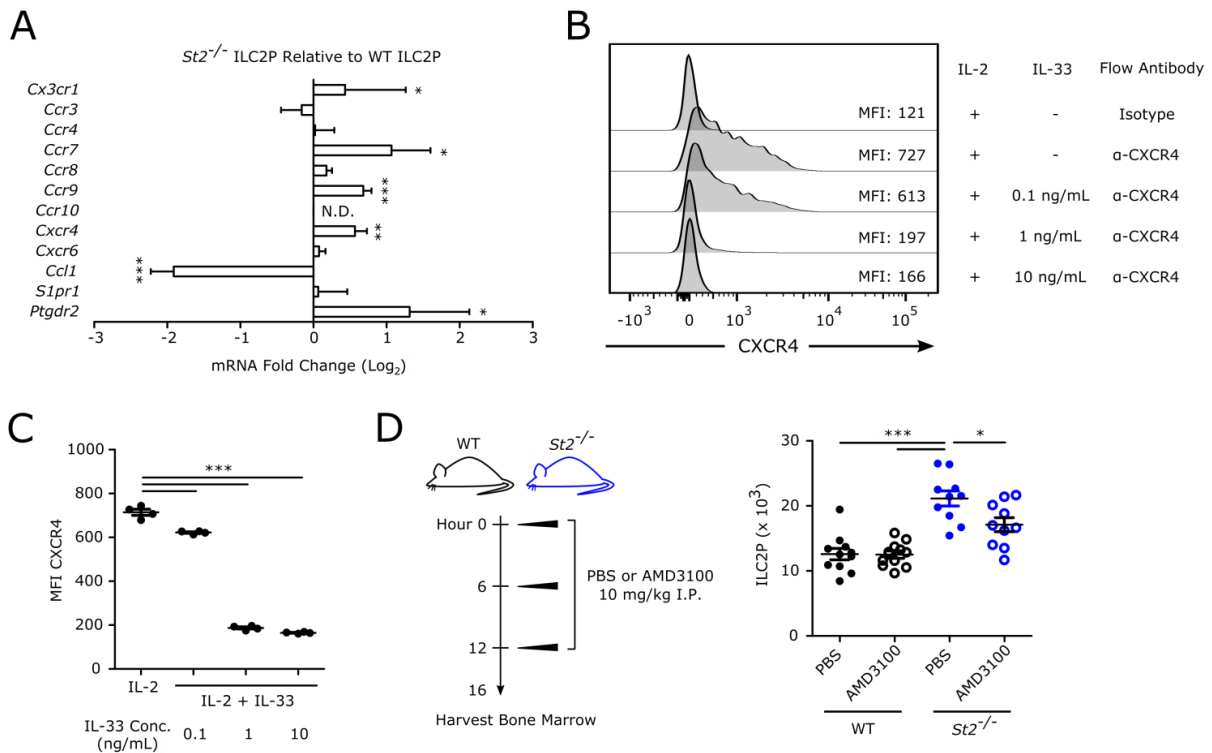


Figure 5-9. CXCR4 on ILC2P promoted their bone marrow retention and was negatively regulated by IL-33 signaling.

(A) ILC2P were magnetically enriched and FACS purified from WT and *St2*^{-/-} mice for quantitative RT-PCR of chemokine receptors and signals. Data were normalized to a pooled set of three housekeeping genes and differential expression was assessed by the $\Delta\Delta C_t$ method. Data are shown as the expression level in *St2*^{-/-} ILC2P compared to WT ILC2P and displayed as a log₂ fold change. (B) Magnetically enriched and FACS purified ILC2P from WT mice were treated for 24 hours *in vitro* with IL-2 in combination with varying doses of IL-33 and assessed for CXCR4 expression. (C) Quantification of B. (D) WT and *St2*^{-/-} mice were treated with three doses of AMD3100 (10 mg/kg) or PBS vehicle given every 6 hours and bone marrow was collected for flow cytometric analysis 4 hours after the final AMD3100 dose. Data are combined from 3 independent experiments (A, D) or are representative of 3 similar experiments (B-C) and displayed as the mean \pm SEM. **p* < 0.05, ***p* < 0.01, and ****p* < 0.001 by one-way ANOVA with Bonferroni post-test (C and D) or unpaired t-test (A); n.s. = not significant and N.D. = not detected.

5.3.8. Intravenously-Delivered IL-33 Drives the Egress of ILC2P from the Bone Marrow

Numerous human diseases including asthma and atopic dermatitis have been associated with increased IL-33 in the plasma as well as increases in circulating ILC2²⁷¹. We hypothesized that serum IL-33 may precipitate egress of ILC2 from the bone marrow, providing disease relevance to this mechanism. To assess the direct effect of IL-33 on bone marrow ILC2P egress, we intravenously injected recombinant murine IL-33 (rIL-33) or vehicle into mice and assessed the number of ILC2P in the bone marrow 24 hours later. Compared to vehicle treatment, intravenous delivery of IL-33 significantly and robustly reduced the frequency and total number of ILC2P in the bone marrow (Figure 5-10 A, C, and D). There was also a modest decrease in the total number of bone marrow cells, suggesting that exogenous IL-33 may be promoting egress of other cells types (Figure 5-10 B). These data indicate that IL-33 is a potent inducer of ILC2P egress from the bone marrow.

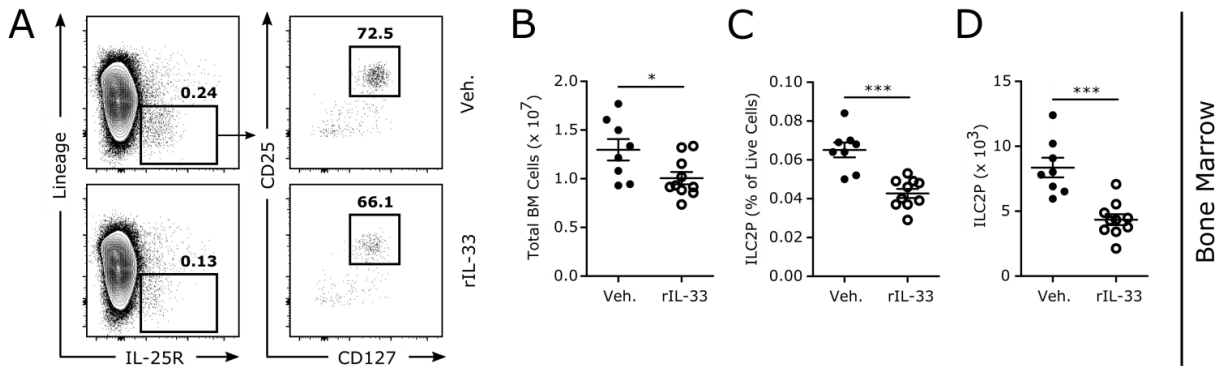


Figure 5-10. Direct intravenous administration of IL-33 promoted ILC2P egress from the bone marrow.

Adult naïve WT mice were treated intravenously with recombinant murine IL-33 (rIL-33) or vehicle (0.1% BSA in PBS) and harvested 24 hours later for flow cytometric analysis. (A) Representative gating for bone marrow ILC2P, (B) the total number of viable bone marrow cells, (C) ILC2P frequency among live bone marrow cells, and (D) the total number of ILC2P in the bone marrow. Data are combined from 2 independent experiments and displayed as the mean \pm SEM. * $p < 0.05$ and *** $p < 0.001$ by unpaired t-test.

5.3.9. Allergic Airway Inflammation Drives the Egress of ILC2P from the Bone Marrow

We next determined the extent of ILC2P bone marrow egress in the context of disease. *Alternaria alternata* is a fungal species that is associated with significant asthma morbidity in humans and drives allergic airway inflammation in mice^{74,79,102,272}. We challenged mice intranasally with *Alternaria* extract or vehicle for four consecutive days and harvested the mice 24 hours later (Figure 5-11 A). We identified a significant accumulation of ILC2 and their associated cytokine products IL-5 and IL-13 in the lungs of *Alternaria* extract-challenged mice compared to vehicle-challenge mice (Figure 5-12), consistent with prior reports^{74,79,102}. Intranasal challenge with *Alternaria* extract significantly altered the cellular composition of the bone marrow, with a strong trend for a decrease in total bone marrow cell number driven largely by a statistically significant decrease in the number of total lymphocytes (Figure 5-11 B-D). Among these lymphocytes, there was a statistically significant decline in the frequency and total number of ILC2P in the bone marrow of mice challenged with *Alternaria* extract compared to vehicle (Figure 5-11 B, E, and F). Concurrently, intranasal *Alternaria* extract challenge stimulated an increase in serum IL-33 concentrations compared to vehicle (Figure 5-11 G). Collectively, these data demonstrated that allergic airway inflammation promotes egress of ILC2P from the bone marrow and that this may be driven by increase serum concentrations of IL-33.

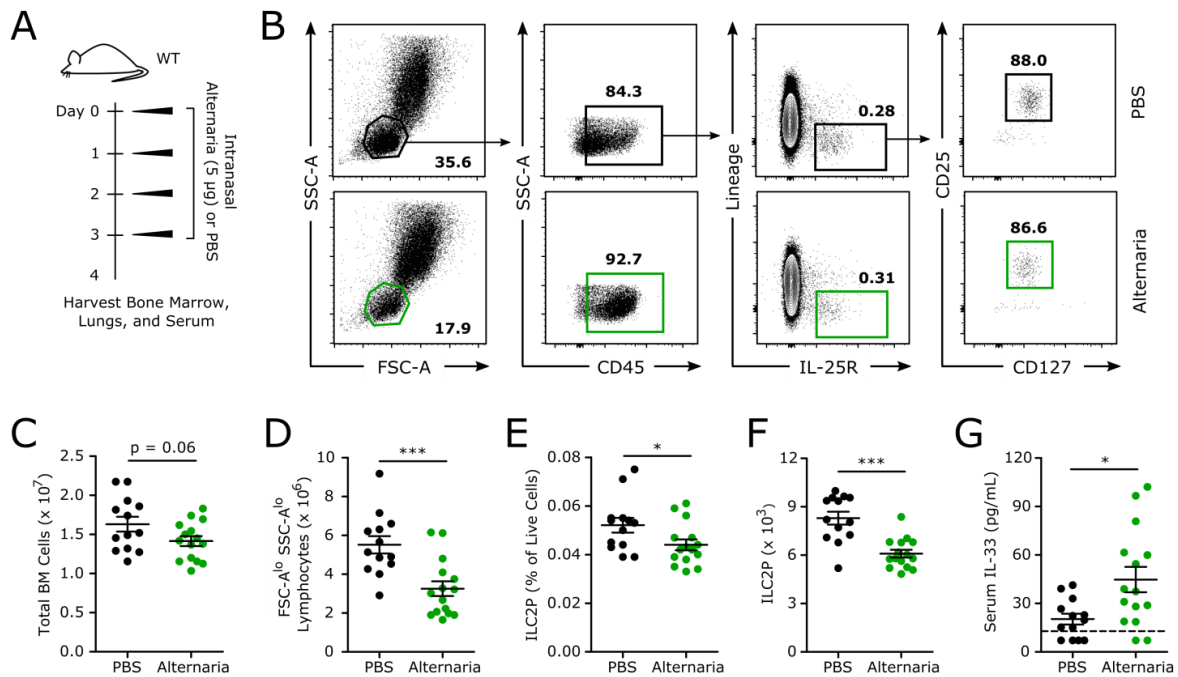


Figure 5-11. Allergic airway inflammation induced by the fungal aeroallergen *Alternaria alternata* promoted increased serum IL-33 and ILC2P egress from the bone marrow. (A) Adult naïve WT mice were treated for four consecutive days with intranasal injections of *Alternaria alternata* extract or PBS vehicle and harvested 24 hours after the final treatment. (B) Representative gating for ILC2P in the bone marrow. (C) The total number of viable bone marrow cells and (D) the total number of bone marrow lymphocytes. (E) ILC2P frequency among live bone marrow cells and (F) the total number of ILC2P in the bone marrow. (G) The concentration of IL-33 in the serum as measured by ELISA. Data are combined from 3 independent experiments (C-G) or representative of 3 independent experiments (B) and displayed as the mean \pm SEM. * $p < 0.05$ and *** $p < 0.001$ by unpaired t-test. Dashed line indicates the limit of detection of the assay.

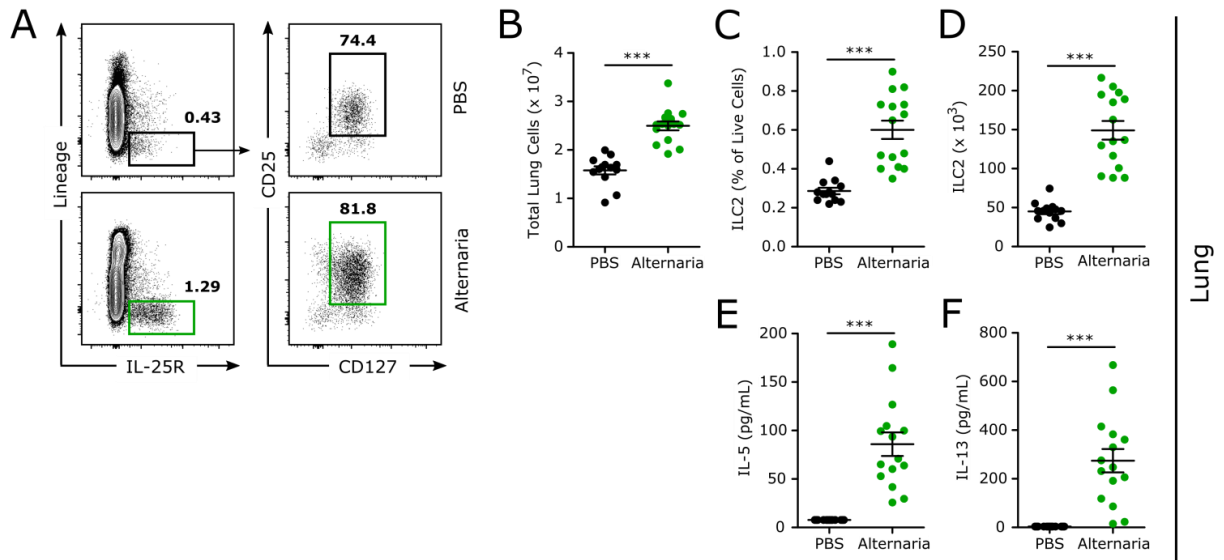


Figure 5-12. Allergic airway inflammation induced by the fungal aeroallergen *Alternaria alternata*.

Adult naïve WT mice were treated for four consecutive days with intranasal injections of *Alternaria alternata* extract or PBS vehicle and harvested 24 hours after the final treatment. (A) Representative gating for ILC2 in the lungs. (B) The total number of viable lung cells, (C) ILC2 frequency among live lung cells, and (D) the total number of ILC2 in the lungs. Whole lung homogenate concentrations of (E) IL-5 and (F) IL-13. Data are combined from 3 independent experiments (B-F) or representative of 3 independent experiments (A) and displayed as the mean \pm SEM. *** $p < 0.001$ by unpaired t-test.

5.3.10. Hematogenous Reseeding of Peripheral Tissues by ILC2 Occurs in the Context of Disrupted Tissue Homeostasis

ILC2 are primarily maintained in naïve, adult mice by local *in situ* mechanisms. Parabiosis experiments in adult, naïve mice spanning 1 month or 4 months have shown that in several peripheral tissues, infiltrating ILC2 represent fewer than 5% of the total ILC2 population⁹². However, data in both humans and mice hint that disrupted homeostasis may induce some degree of hematogenous reseeding by ILC2^{92,101,264}. We sought to determine whether disruption of tissue homeostasis could induce migration and hematogenous reseeding of tissues by ILC2. We reasoned that mobilization of ILC2 by signals such as IL-33 may increase the pool of hematogenously available ILC2 for reseeding. To evaluate tissue reseeding, we employed a parabiosis system in which a congenic WT CD45.1⁺ mouse (recipient) received a sub-lethal dose of gamma radiation to disrupt homeostasis (Figure 5-13 A). This radiation-conditioned mouse was surgically connected to a naïve WT CD45.2⁺ mouse (donor) and allowed to reconstitute for 4 weeks. After 4 weeks, we evaluated the frequency of donor ILC2 in the lungs, skin, and mLN of the irradiated recipient mouse. We readily detected donor ILC2 cells within the lungs, skin, and mLN of the radiation-conditioned recipient mice, with average donor frequencies of 27%, 22%, and 35%, respectively (Figure 5-13 B-E). These frequencies were well above those observed in prior reports of parabiosis experiments in naïve mice, where fewer than 5% of the cells were from the opposing mouse⁹². These data suggest that hematogenous reseeding of tissues by ILC2 can be a participatory mechanism under circumstances when tissue homeostasis has been disrupted.

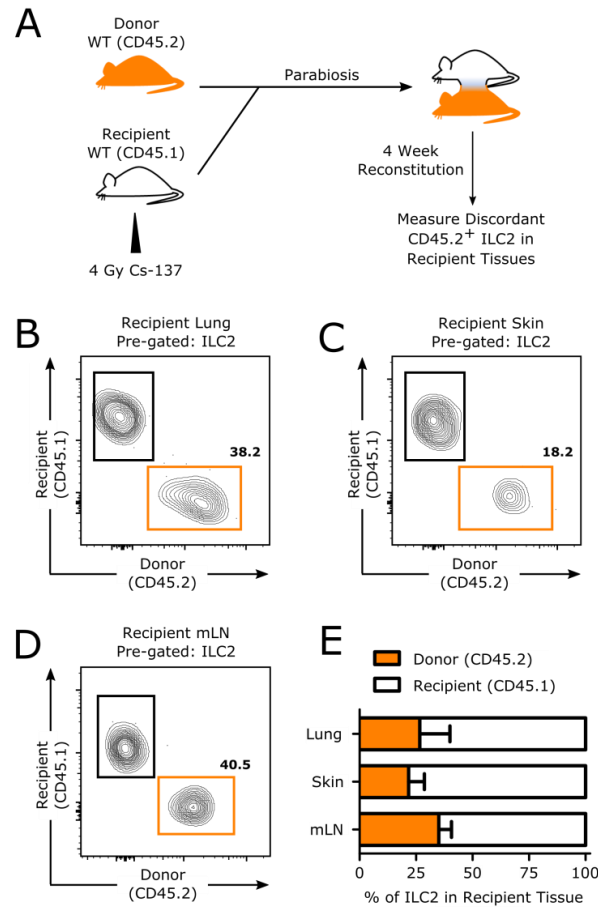


Figure 5-13. ILC2 reseeded peripheral tissues by hematogenous spread in the context of disrupted homeostasis.

Congenic CD45.1⁺ WT mice (recipient) were sublethally irradiated and parabiosed to CD45.2⁺ WT mice (donor) and allowed to equilibrate for 4 weeks. (A) Experimental design. The frequency of donor CD45.2⁺ ILC2 was measured in the (B) lungs, (C) skin, and (D) mLN of recipient mice. (E) Average ILC2 donor frequencies from 3-4 parabiosis pairs per tissue. Data are representative of 2 independent experiments (B-D) or combined from 2 independent experiments (E) and displayed as the mean ± SEM.

5.4. Discussion

In this study, we evaluated the effect of IL-33 on development and egress of ILC2P from the bone marrow. Compared to WT controls, mice lacking IL-33 signaling had a significant accumulation of ILC2P in the bone marrow. Our data suggest this effect on ILC2P is primarily due to defective egress rather than aberrant development. Using bone marrow chimeric mice, we identified that IL-33 signaling intrinsic to the ILC2P was required to establish bone marrow frequencies. We found that *St2^{-/-}* ILC2P displayed altered expression of multiple chemokine receptors, including the bone marrow retentive receptor *Cxcr4*, which was upregulated compared to WT ILC2P. IL-33 negatively regulated the expression of ILC2P CXCR4 *in vitro* and disruption of CXCR4 signaling reduced the number of ILC2P in the bone marrow of *St2^{-/-}* mice. Furthermore, increasing serum IL-33 concentrations via direct intravenous injection robustly mobilized ILC2P to egress from the bone marrow. Parabiosis in the context of radiation-induced disruption of homeostasis demonstrated the potential relevance of circulating ILC2. Collectively, these data establish a key role for IL-33 in promoting the egress of ILC2P from the bone marrow.

Several prior reports have identified modest reductions in the number of ILC2 in peripheral tissues of naïve or vehicle treated mice in the absence of IL-33 signaling^{65,87,102,273}. We had initially hypothesized that this may be due to a developmental impediment, as IL-33 promotes ILC2 differentiation from CLP *in vitro*^{38,42}. Surprisingly, IL-33 appeared dispensable for the development of ILC2 that are able to proliferate and produce IL-5 and IL-13. It is possible that ILC2 functions beyond proliferative potential and IL-5/IL-13 producing capacity may be affected by development in an IL-33-deficient environment, but further characterization of developing ILC2 will be necessary to assess this.

Rather than affecting development, our data point to a vital role for IL-33 in promoting efficient egress of ILC2P from the bone marrow. We identified that ILC2P-expressed CXCR4 is mechanistically involved in retaining ILC2P in the bone marrow in the absence of IL-33 signaling. Blockade of CXCR4 reduced the number of *St2^{-/-}* ILC2P in the bone marrow, though not entirely back to WT levels. Additional IL-33-dependent pathways likely collaborate with CXCR4 to promote retention or egress of ILC2P. In neutrophils and hematopoietic stem cells, CXCR4 works in conjunction with integrin VLA-4 to mediate retention in the bone marrow^{274,275}. It is intriguing to consider VLA-4/VCAM-1 as a potential collaborator, but further work will be needed to establish a role for integrins in ILC2 bone marrow retention. WHIM syndrome is a rare autosomal dominant disorder in which mutations in CXCR4 lead to hyperactive or prolonged signaling through this receptor²⁷⁶. Patients with WHIM syndrome present with recurrent infections, hypogammaglobulinemia, and retention of neutrophils in the bone marrow. WHIM syndrome may represent a clinical scenario in which we can better understand the role of CXCR4 signaling in human ILC2 biology.

Increased plasma concentrations of IL-33 have been observed in numerous human diseases including asthma²⁷⁷⁻²⁷⁹, atopic dermatitis²⁸⁰, allergic rhinitis²⁸¹, inflammatory bowel disease^{282,283}, rheumatoid arthritis^{284,285}, and psoriasis²⁸⁶, among others. In many of these diseases, ILC2 are thought to participate in driving inflammation. Our data in mice demonstrate the intravenous delivery of IL-33 mobilizes ILC2 to egress from the bone marrow. It is interesting to consider whether a similar effect exists in humans, and whether anti-IL-33 therapeutics currently in development may reduce inflammation by not only blocking local tissue effects but also reducing the recruitment of new ILC2. Beyond disease, IL-33 is a central perinatal signal that leads to the initial seeding and accumulation of ILC2 in peripheral

tissues^{87,88}. Within the first few weeks of life, IL-33 expression peaks within the tissue and this correlates with an enrichment of tissue-embedded ILC2. It remains unclear whether this initial burst of IL-33 expression after birth extends to the serum or bone marrow, and if so, whether a similar IL-33-dependent ILC2 egress mechanism augments this perinatal tissue seeding.

IL-33 regulated the expression of multiple chemokine receptors in ILC2P. Specifically, IL-33 decreased the expression of *Cx3cr1*, *Ccr7*, *Ccr9*, *Cxcr4*, and *Ptgdr2* and increased the expression of *Ccl1*. Notably, CCR9 is a gut-trophic signaling pathway²⁷⁰, and IL-33 may be skewing ILC2 migration towards sites outside of the gastrointestinal tract. Within the gastrointestinal tract, tuft cell-derived IL-25 is thought to be a key regulator of ILC2-responsiveness^{71,72}. Tuft cells are not major sources of IL-33, and any trafficking bias induced by IL-33 may function to guide cells to areas of higher IL-33 content. Further work will be needed to understand whether IL-33 affects the preferential accumulation of ILC2 within one tissue over another. Additionally, *Ccl1* and its receptor *Ccr8* were previously identified to be expressed at high levels by small intestinal ILC2, suggesting a possible autocrine feed-forward loop¹⁵². We identified that IL-33 signaling increased the expression of *Ccl1*, though no differences in expression were observed in *Ccr8* expression between WT and *St2*^{-/-} mice. The CCL1/CCR8 axis promotes the migration of CD4⁺ Th2 cells towards sites of allergic inflammation²⁷⁰. Our data may fit a hypothetical model whereby IL-33 promotes mobilization of ILC2 to egress from the bone marrow and simultaneously upregulates the CCL1/CCR8 chemotactic system that guides newly egressed ILC2 towards sites of type 2 inflammation. Additional investigation will be required to assess the functional significance of IL-33 regulation of *Ccl1* in bone marrow ILC2P.

Given the effect of IL-33 on regulating chemokine receptor expression in bone marrow ILC2P, it is plausible the IL-33 may also shape the chemokine receptor profiles of peripheral

ILC2. Beyond retention of cells in the bone marrow, CXCR4 is involved in a number of biological processes including the trafficking of lymphocytes into secondary lymphoid organs²⁷⁰. ILC2 readily cycle between tissues and adjacent lymph nodes⁹⁹ and also interface with the adaptive immune system^{37,54,115,117,118,121,287,288}. Whether peripherally expressed IL-33 affects ILC2 trafficking between tissues and secondary lymphoid organs in a CXCR4-dependent manner remains unknown. IL-33 may also work in combination with other signals to exert tissue-specific effects on ILC2 chemokine receptor expression, and additional characterization will be needed on a tissue-by-tissue basis.

Herein, our data provide evidence that IL-33 promotes the egress of ILC2P from the bone marrow. Mice lacking IL-33 signaling had a significant accumulation of ILC2P in the bone marrow, mechanistically driven in part by an overexpression of *Cxcr4*. Intravenously-delivered IL-33 rapidly and significantly mobilized ILC2P to egress from the bone marrow, providing potential human disease relevance. These data broadly expand our understanding of IL-33 biology and ILC2 migration.

CHAPTER 6

SUMMARY AND CONCLUSION

6.1. Synopsis of Findings

ILC2 are potent effector cells of the innate immune response that rapidly respond to allergic and allergic-type stimuli and mediate pathophysiologic changes in tissues such as the lung. Our data in Chapter 3 support a significant role for ILC2 and TSLP in mediating early mucus production and airway hyperactivity in a mouse model of severe RSV infection. ILC2 responses precede T cells in this model, demonstrating a critical role for innate cells in inducing classical T-cell-associated pathologies during RSV infection. The cytokine TSLP was necessary for this induction of ILC2, differentiating the activation of ILC2 in this model of RSV compared to models of rhinovirus and influenza infection, which depend on IL-33 and/or IL-25.

In Chapter 4, we demonstrate that the ILC response to RSV infection as a whole is broadly regulated by a major anti-viral pathway—interferon signaling to activate STAT1. STAT1 signaling attenuated ILC2 and ILC3 responses and supported the activation of classical NK cells. This balance of ILC was broadly consistent with minimizing pathophysiologic changes in the airways and maximizing viral clearance, though the relative contribution of ILC was not assessed. This STAT1-mediated restriction of ILC2 and ILC3 was mediated by both cell-intrinsic and cell-extrinsic pathways. Specifically in regard to cell-extrinsic pathways, we found that STAT1 repressed the production of IL-33 and IL-23, potent activators of ILC2 and ILC3, respectively.

Finally, in Chapter 5 we demonstrate that ILC2 exit the bone marrow for putative hematogenous trafficking to sites of allergic inflammation via IL-33 signaling. IL-33 is dispensable for ILC2 development but instead promotes the efficient egress of ILC2 from the bone marrow by downregulating CXCR4 on ILC2. Similar results were obtained in the context of allergic airway inflammation, where we observed a significant increase in the serum concentration of IL-33 that correlated with a loss of ILC2 from the bone marrow. Parabiosis studies extend our current understanding of ILC2 trafficking, demonstrating significant potential for the hematogenous spread of ILC2 in the context of disrupted tissue homeostasis. These findings are summarized in Figure 6-1.

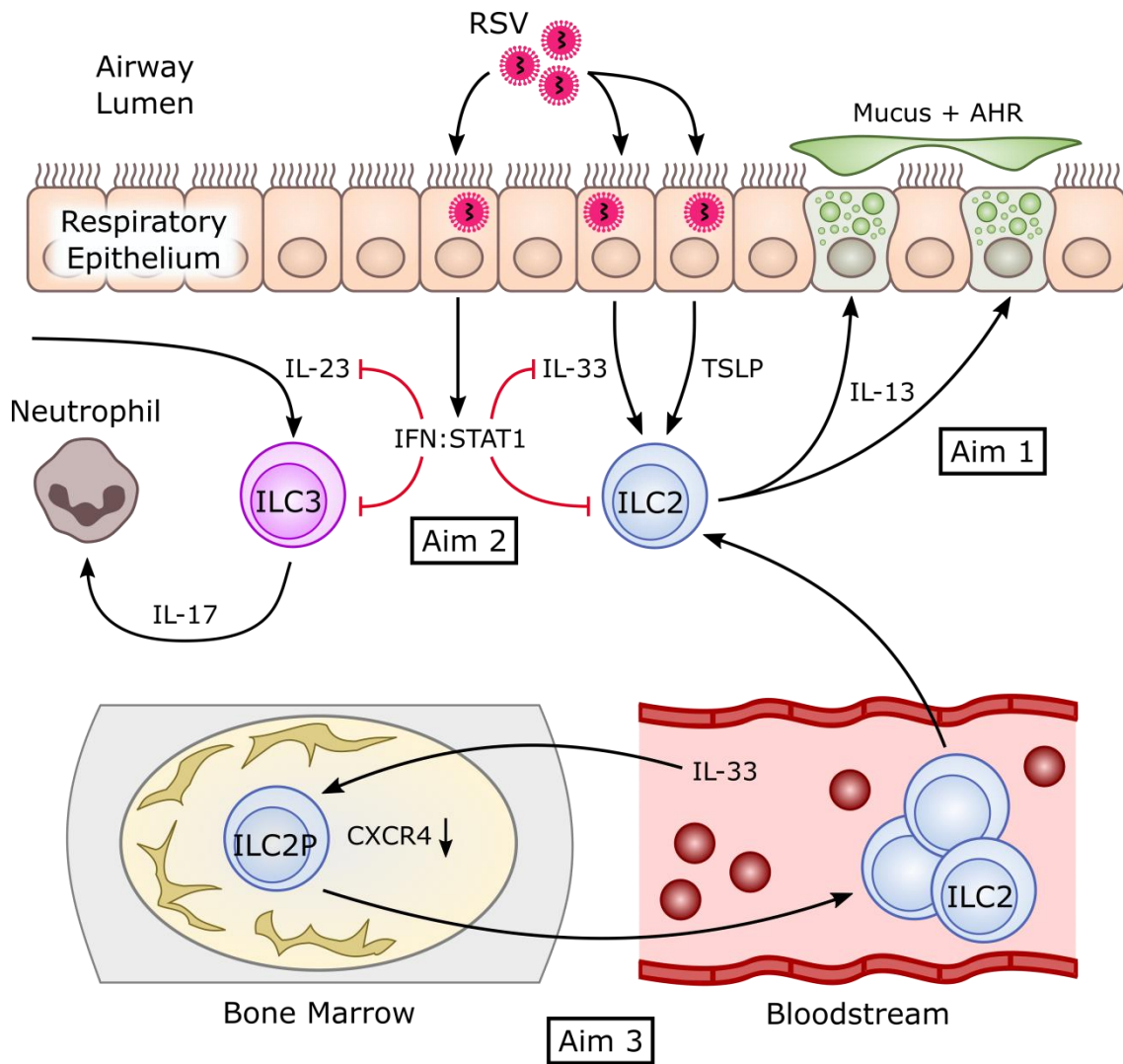


Figure 6-1. Graphical Summary of Dissertation Results

In Aim 1, we found that RSV infection induce the release of IL-33 and TSLP. In particular, TSLP activated ILC2 to express IL-13, which led to airway mucus accumulation and airway hyperreactivity (AHR). In Aim 2, we found that interferon:STAT1 signaling restrained ILC2 and ILC3 responses to RSV by repressing IL-23 and IL-33 as well as acting via a direct ILC cell-intrinsic effect. Finally, in Aim 3 we found that IL-33 promotes the efficient egress of ILC2 progenitor cells from the bone marrow for hematogenous spread by downregulating CXCR4 on ILC2 progenitors in the bone marrow.

6.2. Limitations in the Investigation of ILC

6.2.1. Identification and Visualization of ILC

Challenges remain in defining ILC and visualizing them in tissue. Specifically, identification strategies for ILC2 remain varied with only moderate consistency. Among consensus markers, ILC2 are lineage negative defined as negative for T, B, NK cell, granulocyte, macrophage, mast cell, basophil, and erythroid markers. ILC2 are also unanimously considered positive for CD90 and CD127, though not all investigators gate ILC2 using both markers (including our research group, where to date we have only used CD90 sparingly). ILC2 are governed by the transcription factor GATA3, and so GATA3 staining has been used to selectively mark ILC2 but requires either reporter mice or fixation and intracellular staining. Several surface markers have been employed by different investigators to mark ILC2 including ST2, IL-25R, ICOS, and KLRG1. However, reports suggest these markers may be variably expressed in different ILC2 fractions (natural ILC2 versus inflammatory ILC2), across different tissues, under inflammatory conditions, and in ILC2 from males versus females.^{289,290} Indeed, we demonstrate heterogeneity in the expression level of ST2 across tissues in Chapter 5, and have also found (in experiments not shown in this dissertation) variations in KLRG1 expression in lung ILC2 as defined by GATA3, IL-5, or IL-13 expression. CD25 has also been used to mark ILC including ILC2, but its expression levels are significantly lower in ILC2 in certain tissues in quiescent ILC2 compared to activated ILC2.

Given the heterogeneity in strategies used to identify ILC2, the ability to extrapolate results from one system to another is limited. More rigorous characterization of ILC2 in

different tissues, as well as the developmental relationship between ILC2 in disparate parts of the body, may help clarify identification strategies for ILC2 that can be applied more broadly and with higher sensitivity and specificity for ILC2. Initial studies to this effect have been performed focusing on ILC1 and ILC3 subsets¹⁵², and future “-omics” investigations will likely help to clarify this issue.

Similarly, very limited *in situ* analysis of ILC2 has been performed because the identification strategies for ILC2 largely exceed the capacity to image them with traditional microscopy. In naïve mice, IL-5 production has been shown to be restricted to ILC2 in certain tissues and some investigations have used IL-5-positivity to identify ILC2 at baseline.²⁵³ However, such analyses may be significantly confounded in inflammatory situations. Others have focused on CD3 negative cells that expresses an ILC-specific marker such as GATA3 or ST2, but these markers are not necessarily unique to ILC2.¹²³ Most interestingly, one group stained for a panel of lineage markers similar to flow cytometry and computationally subtracted this staining to reveal lineage negative cells that they further characterized by CD127 and GATA3 staining.¹⁴⁶ While robust, this approach required significant computational expertise.

Major advances in our understanding of other cell types have come from visualizing them within the tissue. While modern flow cytometry (and more recently, mass cytometry) allows us to analyze the phenotype of cells in great detail, it provides no evidence about the spatial arrangement of these cells in tissue. For instance, in our studies, do ILC2P cluster in the bone marrow around niches rich in CXCL12, the ligand for CXCR4? Or, do ILC2 in the lungs expand in specific regions that might reveal new mechanistic insight into ILC2 activation? Further work will be required to enhance our *in situ* characterization of ILC2 to complement the evidence gained from flow cytometric evaluations like those performed in this dissertation.

6.2.2. Modeling the Role of ILC2 in Allergic Disease

Beyond identification of ILC2, the models used to mimic human allergic disease and to assess the necessity and sufficiency of ILC2 in these contexts have limitations. For instance, models of airway inflammation used to induce ILC2 generally involve the instillation of a high dose of allergen straight into the airways over the period of a few days to skew towards innate cell activation. Alternatively, classical allergen challenge models using adjuvants such as alum in combination with an antigen such as ovalbumin induce strong CD4⁺ Th2 cell responses without many of the characteristic innate cell activation features. Both models require significant doses and relatively short exposure times. However, individuals with allergic airway disease are often exposed to environmental antigens in lower doses but across a substantially longer time period. The employment of more chronic allergen models may help to elucidate what the balance of innate and adaptive immune contributions are in a more human-like allergen challenge system.

Limitations also exist in the mouse model of RSV infection. The use of neonatal mice may serve as a better mimic for human disease, as infants are the most likely to suffer from severe infection.²⁹¹ However, it is important to note that mouse and human development *in utero* and *ex utero* differs substantially, and establishing comparable ages between mice and humans is not without challenges. Moreover, the composition of the T cell compartment of adult mice housed in specific pathogen free cages is strikingly similar to human infants.²⁹² Therefore, while age may be an important consideration, further work will be necessary to characterize the ideal age for RSV infection in mice to mimic human infections in infants. An approach we have taken

over the last several years to improve upon the mouse RSV infection model is to employ the use of clinical isolates of RSV, including in Chapter 3 and 4 of this work. These are clinical isolates that have known human pathogenicity, and generally mimic the immune response observed during severe RSV infection in humans better than classical laboratory strains such as A2 or Long. The development of mouse-adapted RSV similar to mouse adapted influenza (PR8) may also offer advantages.

Finally, several approaches have been employed to evaluate the role of ILC2 in disease. $Rag^{-/-}$ mice lack T cells and $Rag^{-/-}\gamma c^{-/-}$ mice lack both T cells and ILC2, allowing for the use of adoptive transfer and depletion studies to assess for the ILC2-specific contribution to disease. However, more recent evidence highlighting critical crosstalk between ILC2 and adaptive cells suggest this model may have limitations.⁵⁴ ILC2 depend upon the transcription factor $ROR\alpha$, and mice with a spontaneous mutation “stagger” ($Rora^{sg/sg}$) have a profound loss of ILC2 but not other ILC.⁹⁰ These mice do not live into adulthood, however, because of neurologic abnormalities requiring adoptive transfers or conditional deletions of $ROR\alpha$ to be used.⁵⁴ While specific to ILC2 within the ILC lineage, $ROR\alpha$ is expressed by $CD4^+$ Th17 cells and $ROR\alpha$ -deficiency reduces Th17 cell differentiation and IL-17 production.²⁹³ Finally, ILC2 are depleted in ICOS-T mice that express a transgenic loxP-flanked diphtheria toxin receptor (DTR) in the endogenous ICOS locus and a CD4-Cre recombinase, allowing for the selective removal the DTR from $CD4^+$ T cells. The remaining ICOS⁺ cells, notably ILC2, express the DTR and diphtheria toxin exposure depletes ILC2 by approximately 90%.⁵⁴ The ICOS-T mouse represents quality model for depletion, but not total elimination, of ILC2 though is limited by its conditional nature and may not represent an ideal model for studying ILC2 development across a longer arc of time or *in utero*. Similar to above, the identification of unique markers of ILC2 that

differentiate them from T cells will position the field to better develop models that selectively deplete ILC2 without substantial alterations in other cell types, allowing for better analysis of ILC2 function in an otherwise intact immune system.

6.3. Implications and Future Directions

6.3.1. Targeting ILC2 in Allergic Disease

The development of new therapeutics to better treat allergic diseases including asthma is of paramount importance. Current asthma therapies include inhaled corticosteroids, anti-IgE and anti-IL-5 monoclonal antibodies, leukotriene inhibitors, and β 2-agonists, among others. While these approaches have significantly decreased the burden of allergic disease, there remain concerns about adverse events, cost, and effectiveness in all patients. Approximately 5-8% of individuals have severe refractory asthma that fails to respond to current therapies.²⁹⁴ Given the volume of evidence in recent years supporting a role for IL-25, IL-33, and TSLP in augmenting type 2 immune responses, these cytokines have emerged as high-priority targets for pharmacologic intervention. To date, the most advanced investigational new drug (IND) is AMG-157, an anti-TSLP neutralizing antibody. In a phase II trial, patients were randomized to placebo or AMG-157 and receive doses on days 1, 29, and 57 of the study. Experimental allergen challenges were completed on days 41-43 and 83-85 of the protocol, and demonstrated that patients receiving AMG-157 had a smaller reduction in FEV1 compared to placebo treatment during the early and late phase allergen response.⁸⁶ Several IND are in the pipeline or in preclinical development targeting IL-33 binding to ST2. One IND, AMG-282, is an anti-ST2

antibody and is currently in phase I clinical trials for mild allergic asthma and CRS (NCT01928368 and NCT02170337). A second IND, ANB020, is being evaluated in phase II trials for the treatment of peanut allergy (NCT02920021).

As IL-25, IL-33, and TSLP therapeutics proceed through development, it is worth noting several considerations for their use that can be gleaned from preclinical data. First, there appear to be distinct requirements for IL-25, IL-33, or TSLP in activating ILC2 with different respiratory viruses in mice. Rhinovirus-induced activation of ILC2 requires either IL-25 or IL-33, whereas ILC2 are primarily activated by IL-33 in the context of influenza.^{124–127,194} In Chapter 3, we demonstrate that RSV activates ILC2 via TSLP. A report published around the same time as our work demonstrated that IL-33 may also play a role in RSV-induced ILC2 activation.¹⁰⁵ We found that IL-33-deficiency did not decrease the number of ILC2, though reduced IL-13 protein was found in the lungs suggesting IL-33 may toggle cytokine production rather than ILC2 number. The heterogeneity in cytokine-stimuli identified in these studies for different viruses suggest that, while all of the cytokines have ILC2-enhancing capacity, the most effective therapeutic intervention may vary by virus species. Our work provides critical insights into expanding the potential targets in the context of viral infection, being the first evidence for a TSLP-signaling requirement in ILC2 activation during viral infection. Given the potential clinical delays in viral identification in patients presenting to the hospital, an alternative approach may be combinatorial targeting of IL-25, IL-33, and TSLP. In mice, disruption of all three cytokines during the initiation and maintenance of house dust mite-induced asthma reduced airway eosinophilia, IL-4, IL-5, and IL-13 cytokine production, and luminal mucus staining to a greater degree than disruption of any individual cytokine alone.²⁹⁵

Interestingly, the cytokine-expressing spectrum of ILC2 may depend upon whether they are stimulated with IL-25, IL-33, or TSLP. In our RSV model (Chapter 3), activation of ILC2 with TSLP induced IL-13⁺ ILC2 but not IL-5⁺ ILC2. This is in contrast to treatment of mice with *Alternaria alternata*, which produced higher levels of IL-5⁺ ILC2 compared to IL-13⁺ ILC2 and is highly dependent upon IL-33 signaling.^{79,102} This skewing towards IL-5 or IL-13 may be related to IL-33 or TSLP-dependent signaling, respectively. *In vitro* evidence with human ILC2 suggest that stimulation with various combinations of IL-25, IL-33, and TSLP alter the surface expression of CD127, CRTH2, IL-25R, TSLPR, and ST2 as well as the expression of IL-13 and GM-CSF depending upon which combination of IL-25, IL-33, and TSLP are present in the media.¹⁰⁷ These data provide further evidence that matching the appropriate therapeutic to a given disease will be critical in maximizing effectiveness.

6.3.2. Coordination of ILC Responses

While substantial and important effort has been invested in understanding individual activators and inhibitors of specific ILC subsets, an appropriate immune response to a given insult is likely to require the simultaneous activation and inhibition of different ILC subsets. In Chapter 4, we identified STAT1 signaling as a convergent pathway that regulates the balance of ILC1, ILC2, and ILC3 in a manner consistent with anti-viral immunity. This is particularly relevant as asthma is a heterogeneous disease, often with significant type 2 inflammation but also with features of type 1 and type 17 immunity.^{296,297} The capacity to appropriately regulate all three classes of ILC concurrently represents an ideal pharmacologic goal. To date, such targets remain elusive. We provide evidence that STAT1 may represent such a target, at least in the

context of viral infection. Evidence suggests that toggling STAT1 to a more activated state, as might be the case with a pharmacologic intervention, may improve anti-viral immunity. In mice, a constitutively hyper-responsive version of STAT1 improved antiviral function.²⁹⁸ The identification of additional pathways in different disease states that regulate the appropriate balance of ILC may prove particularly useful therapeutically.

6.3.3. Establishment and Maintenance of the Type 2 Immunologic Niche

The events that orchestrate initial seeding of tissues with ILC2 and their subsequent maintenance throughout life are incompletely understood. Several recent reports have implicated an early burst of IL-33 expression in the lungs of post-natal mice with the accumulation of ILC2 by 1-2 weeks after birth.⁸⁷⁻⁸⁹ Mice lacking IL-33 or ST2 have reduced accumulation of ILC2 by postnatal days 7, 10, and 14 compared to wild type mice. This ILC2 infiltration recruits eosinophils and M2 macrophages. Moreover, the number of ILC2 in a two week old mouse is comparable to adult mice, demonstrating that initial seeding of tissues with ILC2 is largely completed very early in life.^{87,88}

Questions remain about the source of ILC2 and the factors that guide ILC2 to various tissues. While ILC progenitors including ILC2P are readily found within the bone marrow, it remains to be proven that this is the only source or the primary source. Though the bone marrow is a likely contributor, ILC progenitors can also be found in the fetal gut and neonatal spleen, suggesting sources of ILC may be varied.^{59,269} Little is known about the chemotaxis of ILC2 under any circumstances. CCR9 promotes the accumulation of ILC2 in the small intestine at baseline.^{40,98} However, the majority of evidence for ILC2 trafficking comes from studies in

inflammatory models. In models of helminth infection or allergic inflammation, PGD₂ and β₂ integrins guide ILC2 to the lungs.^{100,101} PGD₂ has been shown to induce chemotaxis of human ILC2 *in vitro* as well.⁷³ Our data in Chapter 5 focus primarily on the events of bone marrow ILC2 egress induced by IL-33, with presumed implications for hematogenous trafficking. Given the enhanced IL-33 signaling tension in the postnatal period, it is possible that an IL-33-mediated egress mechanism is involved in the early ILC2 seeding events. IL-33 has been found to be weakly chemotactic itself and may recruit ILC2 to the lungs where IL-33 is highly expressed in the postnatal period, though other pathways such as CCR9 and those yet to be described likely play a role in the guidance of ILC2 to tissues.^{64,73}

The tissue maintenance of ILC2 populations in adult mice, during homeostatic and inflammatory conditions, is an area of active investigation. Specifically, conflicting data exist about whether ILC2 are exclusively tissue-derived or can be reconstituted from hematogenous sources.^{69,92,100,101} Our data in Chapter 5 provide evidence to support a role for hematogenous trafficking in the context of disrupted tissue homeostasis. Parabiosis studies have been the predominant approach to studying trafficking of ILC. In adult, naïve mice, ILC including ILC2 did not migrate to the opposing parabiont in any appreciable capacity across 1 or 4 months of parabiosis.⁹² Similar results were obtained in parabiosis pairs with a diphtheria toxin-induced depletion of Foxp3⁺ regulator T cells (Tregs), which results in systemic lymphoproliferation and fatal autoimmunity.⁹² However, in a model of *Nippostrongylus brasiliensis* (*N.b.*) infection, which induces a strong, smoldering type 2 immune response in the lungs and intestine, moderate infiltration of hematogenously derived ILC2 was observed at day 15 post-infection with approximately 10% of the ILC2 from the donor mouse suggesting a total infiltrating fraction of 20%. Importantly, *N.b.* infection activates a substantial ILC2 response but not ILC1 or ILC3,

and neither ILC1 nor ILC3 were found to traffic to the lungs or intestine in the context of *N.b.* infection.⁹² In a separate parabiosis study, mice were given IL-33 intranasally on day 34 and 36 post-parabiosis, and the number of host and donor ILC2 were assessed on day 39 post-parabiosis. In this model, fewer than 5% of the ILC2 were donor-derived.⁶⁹

Several important differences may explain the divergent results from these studies. The length of the inflammatory stimulus appears to play a critical role in whether ILC migrate. During *N.b.* infection, migration was observed at day 15 post-infection but not day 7 post-infection. The studies evaluating ILC migration during Treg depletion and IL-33 intranasal exposure were harvested 9 and 5 days post-exposure, respectively, and may not be capturing this delayed, substantial migration observed during *N.b.* infection. Additionally, the quality of the inflammation may play a role. *N.b.* infection induces a strong type 2 immune response, and it is only ILC2 but ILC1 and ILC3 that traffic in this context. Though IL-33 intranasally is also a type 2 polarizing stimulus, only two doses were given, which may not have been substantial or protracted enough of an inflammatory insult to induce tissue reseeded of new ILC2. Similarly, the inflammation associated with Treg depletion is broad and not type 2-specific, which may have attenuated the effect on ILC2 recruitment.

The Kaede transgenic mouse model has provided further evidence for ILC trafficking in adult mice by allowing investigators to selectively photoconvert a fluorescent protein in one area of the mouse and monitor for their trafficking to other tissues. Specifically, ILC2 and ILC3 were shown to migrate from the intestinal tissue to surrounding lymph nodes in significant quantities.⁹⁹ Multiple studies in humans support a role for ILC trafficking in the context of disrupted tissue homeostasis. In patients with severe combined immunodeficiency (SCID) who received hematopoietic stem cell transplants, tissue reconstitution of ILC with donor cells only

occurred in the context of pre-transplant myeloablation.²⁶⁴ In addition, in patients with aspirin-exacerbated respiratory disease (AERD), ILC2 rapidly accumulated in the inflamed nasal mucosa after COX-1 inhibitor exposure and this correlated with a decrease in circulating ILC2 in the blood.¹⁴⁷ These data in humans support a role for hematogenous trafficking of ILC2 to sites of tissue disruption, either by radiation exposure or hypersensitivity reaction. In this dissertation, we demonstrate that substantial ILC2 recruitment through the blood occurs in the context of low-dose exposure to gamma radiation in multiple peripheral tissues. Our data support a role for ILC2 trafficking through the blood in replenishing peripheral ILC2 populations in adult mice, specifically in the context of disrupted tissue homeostasis.

A generally type 2 immune skewed environment exists in the lungs in the postnatal period, though the overall goals of this are not entirely understood. As described above, ILC2 may in part precipitate this with the recruitment of eosinophils and the polarization of macrophages towards an M2 phenotype. IL-33 coordinates with ILC2-derived IL-13 to activate dendritic cells, restrain dendritic cell IL-12 production, and increase the expression of dendritic cell OX40L, positioning these cells to skew CD4⁺ T cell differentiation towards Th2 cells.⁸⁷ It is hypothesized that type 1 immune responses are suppressed in the lungs of infants to restrict damaging inflammation, and that enhanced type 2 responses may be a natural consequence. However, the pathways described here are driven by a well-regulated bolus of IL-33 production in neonates, suggesting a more actively intentional skewing towards type 2 immunity. This may be primarily in support of tissue development, as pro-growth signals such as amphiregulin are a staple of type 2 immune cells including ILC2.^{68,299,300} IL-33-activated ILC2 appear to be a major initiator in neonates that coordinates the establishment of a type 2 niche within mucosal tissues that may persist throughout life and predispose to asthma.

6.3.4. Functional Significance of ILC

ILC share numerous functional similarities with adaptive CD4⁺ T cells, provoking the question—what is the functional significance of ILC, or are they simply redundant to CD4⁺ T cells? Insights in the global transcriptional control were recently published comparing ILC subsets with their CD4⁺ T helper counterparts.³⁰¹ Broadly, the chromatin landscape of quiescent ILC is in an open arrangement at key cytokine producing loci and regulatory regions. This is broadly consistent with the rapid responsiveness of ILC. Moreover, this chromatin signature most closely aligns with differentiated T helper rather than naïve T helper cells. Hence, quiescent ILC appear to look like differentiated T cells, though it seems underwhelming to consider the only functional difference between ILC and T cells to be their capacity to respond quickly (though in theory that may be true). Some differences, however, were observed in transcriptomic analyses between ILC and T cells in categories such as cell surface markers, metabolic enzymes, chemokine receptors, and secreted factors, though further analysis will be required to understand the functional significance of these differences.³⁰²

A provocative report analyzing human patients following hematopoietic stem cell (HSC) transplant suggest that ILC may be entirely redundant.²⁶⁴ Patients who received HSC transplant without prior myeloablation reconstituted their T and B cell compartments but not ILC. Over the arc of years to decades, these patients showed no major susceptibility to warts, human papilloma virus, ENT infection, diarrhea, or respiratory disease compared to patients who received HSC transplant following myeloablation and whose ILC compartments were partially restored. These data suggest ILC may be dispensable in adults, at best redundant and at worst unimportant

entirely. The bulk of literature outlined in the introduction would suggest it is unlikely that ILC are unimportant, but whether their functions can be compensated for in adults remains unresolved. This study represents an elegant approach to unraveling this mystery, though some limitations exist. This study focused primarily on children and adults, though ILC as discussed above may be most important in infancy. Moreover, ILC have been implicated in adipose tissue homeostasis, but extensive metabolic parameters were not considered as part of this analysis.^{206,273} In summary, the overwhelming evidence in animal models and the correlative data in humans suggest that ILC likely have a functional role, though further work will be necessary to understand whether which functions are unique and which are redundant.

6.4. Closing

The work outlined in this dissertation lends credence to the importance of ILC2 during respiratory viral infection, and the pathways including TSLP and STAT1 that regulate those responses. Furthermore, this dissertation provides evidence that IL-33 promotes bone marrow egress of ILC2 lineage cells that may perpetuate ILC2-driven inflammation in the periphery. Overall, these data provide important advancements in our understanding of ILC biology and suggest potential meaningful strategies for therapeutic intervention in allergic disease.

REFERENCES

1. Ebert, C. S. & Pillsbury, H. C. Epidemiology of Allergy. *Otolaryngol. Clin. North Am.* **44**, 537–548 (2011).
2. Salo, P. M. *et al.* Prevalence of allergic sensitization in the United States: Results from the National Health and Nutrition Examination Survey (NHANES) 2005-2006. *J. Allergy Clin. Immunol.* **134**, 350–359 (2014).
3. Sicherer, S. H. & Sampson, H. A. Food allergy. *J. Allergy Clin. Immunol.* **125**, S116–S125 (2010).
4. Jarvis, D. & Burney, P. ABC of allergies. The epidemiology of allergic disease. *BMJ* **316**, 607–10 (1998).
5. Smits, H. H. *et al.* Microbes and asthma: Opportunities for intervention. *J. Allergy Clin. Immunol.* **137**, 690–697 (2016).
6. Wu, P. & Hartert, T. V. Evidence for a causal relationship between respiratory syncytial virus infection and asthma. *Expert Rev. Anti. Infect. Ther.* **9**, 731–45 (2011).
7. Gern, J. E. *et al.* Patterns of immune development in urban preschoolers with recurrent wheeze and/or atopy. *J. Allergy Clin. Immunol.* (2017). doi:10.1016/j.jaci.2016.10.052
8. Masoli, M., Fabian, D., Holt, S., Beasley, R. & Global Initiative for Asthma (GINA) Program. The global burden of asthma: executive summary of the GINA Dissemination Committee Report. *Allergy* **59**, 469–478 (2004).
9. Fanta, C. H. Asthma. *N. Engl. J. Med.* **360**, 1002–1014 (2009).
10. Akinbami, L. J., Simon, A. E. & Rossen, L. M. Changing Trends in Asthma Prevalence Among Children. *Pediatrics* **137**, e20152354 (2016).
11. Winer, R. A., Qin, X., Harrington, T., Moorman, J. & Zahran, H. Asthma Incidence among Children and Adults: Findings from the Behavioral Risk Factor Surveillance System Asthma Call-back Survey—United States, 2006–2008. *J. Asthma* **49**, 16–22 (2012).
12. Sullivan, P. W. *et al.* The relationship between asthma, asthma control and economic outcomes in the United States. *J. Asthma* **51**, 769–778 (2014).
13. Weiss, K. B., Gergen, P. J. & Hodgson, T. A. An Economic Evaluation of Asthma in the United States. *N. Engl. J. Med.* **326**, 862–866 (1992).
14. Subbarao, P., Mandhane, P. J. & Sears, M. R. Asthma: epidemiology, etiology and risk factors. *CMAJ* **181**, E181-90 (2009).
15. Tatum, A. J. & Shapiro, G. G. The effects of outdoor air pollution and tobacco smoke on asthma. *Immunol. Allergy Clin. North Am.* **25**, 15–30 (2005).
16. Riedl, M. & Diaz-Sanchez, D. Biology of diesel exhaust effects on respiratory function. *J. Allergy Clin. Immunol.* **115**, 221–228 (2005).
17. Johnston, S. L. Overview of Virus-induced Airway Disease. *Proc. Am. Thorac. Soc.* **2**, 150–156 (2005).

18. Nicholson, K. G., Kent, J. & Ireland, D. C. Respiratory viruses and exacerbations of asthma in adults. *BMJ* **307**, 982–6 (1993).
19. Johnston, S. L. *et al.* Community study of role of viral infections in exacerbations of asthma in 9-11 year old children. *BMJ* **310**, 1225–9 (1995).
20. Heymann, P. W. *et al.* Viral infections in relation to age, atopy, and season of admission among children hospitalized for wheezing. *J. Allergy Clin. Immunol.* **114**, 239–247 (2004).
21. Glezen, W. P., Taber, L. H., Frank, A. L. & Kasel, J. A. Risk of primary infection and reinfection with respiratory syncytial virus. *Am. J. Dis. Child.* **140**, 543–6 (1986).
22. Carroll, K. N. *et al.* The severity-dependent relationship of infant bronchiolitis on the risk and morbidity of early childhood asthma. *J. Allergy Clin. Immunol.* **123**, 1055–1061.e1 (2009).
23. Escobar, G. J. *et al.* Recurrent Wheezing in the Third Year of Life Among Children Born at 32 Weeks' Gestation or Later. *Arch. Pediatr. Adolesc. Med.* **164**, 915–22 (2010).
24. Wu, P. *et al.* Evidence of a Causal Role of Winter Virus Infection during Infancy in Early Childhood Asthma. *Am. J. Respir. Crit. Care Med.* **178**, 1123–1129 (2008).
25. Blanken, M. O. *et al.* Respiratory syncytial virus and recurrent wheeze in healthy preterm infants. *N. Engl. J. Med.* **368**, 1791–9 (2013).
26. Morgan, W. J. *et al.* Outcome of Asthma and Wheezing in the First 6 Years of Life. *Am. J. Respir. Crit. Care Med.* **172**, 1253–1258 (2005).
27. Yoshihara, S. *et al.* Effect of Palivizumab Prophylaxis on Subsequent Recurrent Wheezing in Preterm Infants. *Pediatrics* (2013). doi:10.1542/peds.2013-0982
28. Croft, M., So, T., Duan, W. & Soroosh, P. The significance of OX40 and OX40L to T-cell biology and immune disease. *Immunol. Rev.* **229**, 173–91 (2009).
29. Blanchard, C. *et al.* Eotaxin-3 and a uniquely conserved gene-expression profile in eosinophilic esophagitis. *J. Clin. Invest.* **116**, 536–47 (2006).
30. Garcia-Zepeda, E. A. *et al.* Human eotaxin is a specific chemoattractant for eosinophil cells and provides a new mechanism to explain tissue eosinophilia. *Nat. Med.* **2**, 449–456 (1996).
31. Menzies-Gow, A. *et al.* Eotaxin (CCL11) and eotaxin-2 (CCL24) induce recruitment of eosinophils, basophils, neutrophils, and macrophages as well as features of early- and late-phase allergic reactions following cutaneous injection in human atopic and nonatopic volunteers. *J. Immunol.* **169**, 2712–8 (2002).
32. Kurowska-Stolarska, M. *et al.* IL-33 Amplifies the Polarization of Alternatively Activated Macrophages That Contribute to Airway Inflammation. *J. Immunol.* **183**, 6469–6477 (2009).
33. Spits, H. *et al.* Innate lymphoid cells--a proposal for uniform nomenclature. *Nat. Rev. Immunol.* **13**, 145–9 (2013).
34. Klose, C. S. N. & Artis, D. Innate lymphoid cells as regulators of immunity, inflammation and tissue homeostasis. *Nat. Immunol.* **17**, 765–774 (2016).

35. Price, A. E. *et al.* Systemically dispersed innate IL-13-expressing cells in type 2 immunity. *Proc. Natl. Acad. Sci. U. S. A.* **107**, 11489–94 (2010).
36. Neill, D. R. *et al.* Nuocytes represent a new innate effector leukocyte that mediates type-2 immunity. *Nature* **464**, 1367–70 (2010).
37. Moro, K. *et al.* Innate production of T(H)2 cytokines by adipose tissue-associated c-Kit(+)/Sca-1(+) lymphoid cells. *Nature* **463**, 540–4 (2010).
38. Wong, S. H. *et al.* Transcription factor ROR α is critical for nuocyte development. *Nat. Immunol.* **13**, 229–36 (2012).
39. Satoh-Takayama, N. *et al.* IL-7 and IL-15 independently program the differentiation of intestinal CD3⁺ NKp46⁺ cell subsets from Id2-dependent precursors. *J. Exp. Med.* **207**, 273–280 (2010).
40. Hoyler, T. *et al.* The transcription factor GATA-3 controls cell fate and maintenance of type 2 innate lymphoid cells. *Immunity* **37**, 634–48 (2012).
41. Klose, C. S. N. *et al.* Differentiation of Type 1 ILCs from a Common Progenitor to All Helper-like Innate Lymphoid Cell Lineages. *Cell* **157**, 340–356 (2014).
42. Xu, W. *et al.* NFIL3 Orchestrates the Emergence of Common Helper Innate Lymphoid Cell Precursors. *Cell Rep.* **10**, 2043–2054 (2015).
43. Zook, E. C. *et al.* The ETS1 transcription factor is required for the development and cytokine-induced expansion of ILC2. *J. Exp. Med.* **213**, 687–696 (2016).
44. Constantinides, M. G., McDonald, B. D., Verhoef, P. A. & Bendelac, A. A committed precursor to innate lymphoid cells. *Nature* (2014). doi:10.1038/nature13047
45. Yu, Y. *et al.* Single-cell RNA-seq identifies a PD-1hi ILC progenitor and defines its development pathway. *Nature* **539**, 102–106 (2016).
46. Walker, J. A. *et al.* Bcl11b is essential for group 2 innate lymphoid cell development. *J. Exp. Med.* **212**, 875–882 (2015).
47. Yu, Y. *et al.* The transcription factor Bcl11b is specifically expressed in group 2 innate lymphoid cells and is essential for their development. *J. Exp. Med.* **212**, 865–874 (2015).
48. Califano, D. *et al.* Transcription Factor Bcl11b Controls Identity and Function of Mature Type 2 Innate Lymphoid Cells. *Immunity* **43**, 354–368 (2015).
49. Yagi, R. *et al.* The transcription factor GATA3 is critical for the development of all IL-7R α -expressing innate lymphoid cells. *Immunity* **40**, 378–88 (2014).
50. Mjösberg, J. *et al.* The transcription factor GATA3 is essential for the function of human type 2 innate lymphoid cells. *Immunity* **37**, 649–59 (2012).
51. Furusawa, J. *et al.* Critical Role of p38 and GATA3 in Natural Helper Cell Function. *J. Immunol.* **191**, 1818–1826 (2013).
52. Klein Wolterink, R. G. J. *et al.* Essential, dose-dependent role for the transcription factor Gata3 in the development of IL-5+ and IL-13+ type 2 innate lymphoid cells. *Proc. Natl. Acad. Sci. U. S. A.* **110**, 10240–5 (2013).
53. Nussbaum, J. C. *et al.* Type 2 innate lymphoid cells control eosinophil homeostasis.

- Nature* **502**, 245–8 (2013).
54. Oliphant, C. J. *et al.* MHCII-mediated dialog between group 2 innate lymphoid cells and CD4(+) T cells potentiates type 2 immunity and promotes parasitic helminth expulsion. *Immunity* **41**, 283–95 (2014).
 55. Possot, C. *et al.* Notch signaling is necessary for adult, but not fetal, development of ROR γ t⁺ innate lymphoid cells. *Nat. Immunol.* **12**, 949–958 (2011).
 56. Lee, J. S. *et al.* AHR drives the development of gut ILC22 cells and postnatal lymphoid tissues via pathways dependent on and independent of Notch. *Nat. Immunol.* **13**, 144–151 (2011).
 57. Cherrier, M., Sawa, S. & Eberl, G. Notch, Id2, and ROR γ t sequentially orchestrate the fetal development of lymphoid tissue inducer cells. *J. Exp. Med.* **209**, (2012).
 58. Yang, Q. *et al.* T cell factor 1 is required for group 2 innate lymphoid cell generation. *Immunity* **38**, 694–704 (2013).
 59. Bando, J. K., Liang, H.-E. & Locksley, R. M. Identification and distribution of developing innate lymphoid cells in the fetal mouse intestine. *Nat. Immunol.* **16**, 153–60 (2015).
 60. Lim, A. I. *et al.* Systemic Human ILC Precursors Provide a Substrate for Tissue ILC Differentiation. *Cell* **168**, 1086–1100.e10 (2017).
 61. Halim, T. Y. F., Krauss, R. H., Sun, A. C. & Takei, F. Lung natural helper cells are a critical source of Th2 cell-type cytokines in protease allergen-induced airway inflammation. *Immunity* **36**, 451–63 (2012).
 62. Kim, B. S. *et al.* TSLP elicits IL-33-independent innate lymphoid cell responses to promote skin inflammation. *Sci. Transl. Med.* **5**, 170ra16 (2013).
 63. Barlow, J. L. *et al.* IL-33 is more potent than IL-25 in provoking IL-13-producing nuocytes (type 2 innate lymphoid cells) and airway contraction. *J. Allergy Clin. Immunol.* **132**, 933–41 (2013).
 64. Salimi, M. *et al.* A role for IL-25 and IL-33-driven type-2 innate lymphoid cells in atopic dermatitis. *J. Exp. Med.* **210**, 2939–50 (2013).
 65. Hardman, C. S., Panova, V. & McKenzie, A. N. J. IL-33 citrine reporter mice reveal the temporal and spatial expression of IL-33 during allergic lung inflammation. *Eur. J. Immunol.* **43**, 488–98 (2013).
 66. Moussion, C., Ortega, N. & Girard, J.-P. The IL-1-Like Cytokine IL-33 Is Constitutively Expressed in the Nucleus of Endothelial Cells and Epithelial Cells In Vivo: A Novel ‘Alarmin’? *PLoS One* **3**, e3331 (2008).
 67. Carriere, V. *et al.* IL-33, the IL-1-like cytokine ligand for ST2 receptor, is a chromatin-associated nuclear factor in vivo. *Proc. Natl. Acad. Sci. U. S. A.* **104**, 282–7 (2007).
 68. Monticelli, L. A. *et al.* Innate lymphoid cells promote lung-tissue homeostasis after infection with influenza virus. *Nat. Immunol.* **12**, 1045–54 (2011).
 69. Moro, K. *et al.* Interferon and IL-27 antagonize the function of group 2 innate lymphoid cells and type 2 innate immune responses. *Nat. Immunol.* **17**, 76–86 (2016).

70. von Moltke, J. *et al.* Leukotrienes provide an NFAT-dependent signal that synergizes with IL-33 to activate ILC2s. *J. Exp. Med.* **214**, 27–37 (2017).
71. Howitt, M. R. *et al.* Tuft cells, taste-chemosensory cells, orchestrate parasite type 2 immunity in the gut. *Science* (80-.). **351**, 1329–1333 (2016).
72. von Moltke, J., Ji, M., Liang, H.-E. & Locksley, R. M. Tuft-cell-derived IL-25 regulates an intestinal ILC2–epithelial response circuit. *Nature* **529**, 221–225 (2015).
73. Xue, L. *et al.* Prostaglandin D2 activates group 2 innate lymphoid cells through chemoattractant receptor-homologous molecule expressed on TH2 cells. *J. Allergy Clin. Immunol.* **133**, 1184–1194.e7 (2014).
74. Doherty, T. A. *et al.* Lung type 2 innate lymphoid cells express cysteinyl leukotriene receptor 1, which regulates TH2 cytokine production. *J. Allergy Clin. Immunol.* **132**, 205–13 (2013).
75. Yu, X. *et al.* TNF superfamily member TL1A elicits type 2 innate lymphoid cells at mucosal barriers. *Mucosal Immunol.* **7**, 730–40 (2014).
76. Ohne, Y. *et al.* IL-1 is a critical regulator of group 2 innate lymphoid cell function and plasticity. *Nat. Immunol.* **17**, 646–655 (2016).
77. Taylor, S. *et al.* PD-1 regulates KLRG1⁺ group 2 innate lymphoid cells. *J. Exp. Med.* **214**, 1663–1678 (2017).
78. Suzuki, M., Morita, R., Hirata, Y., Shichita, T. & Yoshimura, A. Spred1, a Suppressor of the Ras-ERK Pathway, Negatively Regulates Expansion and Function of Group 2 Innate Lymphoid Cells. *J. Immunol.* **195**, 1273–81 (2015).
79. Zhou, W. *et al.* Prostaglandin I2 Signaling and Inhibition of Group 2 Innate Lymphoid Cell Responses. *Am. J. Respir. Crit. Care Med.* **193**, 31–42 (2016).
80. Duerr, C. U. *et al.* Type I interferon restricts type 2 immunopathology through the regulation of group 2 innate lymphoid cells. *Nat. Immunol.* **17**, 65–75 (2016).
81. Maazi, H. *et al.* Activated Plasmacytoid Dendritic Cells regulate Type 2 Innate Lymphoid Cells-mediated Airway Hyperreactivity. *J. Allergy Clin. Immunol.* (2017). doi:10.1016/j.jaci.2017.04.043
82. Galle-Treger, L. *et al.* Nicotinic acetylcholine receptor agonist attenuates ILC2-dependent airway hyperreactivity. *Nat. Commun.* **7**, 13202 (2016).
83. Krishnamoorthy, N. *et al.* Cutting Edge: Maresin-1 Engages Regulatory T Cells To Limit Type 2 Innate Lymphoid Cell Activation and Promote Resolution of Lung Inflammation. *J. Immunol.* **194**, 863–867 (2015).
84. Rigas, D. *et al.* Type 2 innate lymphoid cell suppression by regulatory T cells attenuates airway hyperreactivity and requires inducible T-cell costimulator–inducible T-cell costimulator ligand interaction. *J. Allergy Clin. Immunol.* **139**, 1468–1477.e2 (2017).
85. Noval Rivas, M., Burton, O. T., Oettgen, H. C. & Chatila, T. IL-4 production by group 2 innate lymphoid cells promotes food allergy by blocking regulatory T-cell function. *J. Allergy Clin. Immunol.* **138**, 801–811.e9 (2016).
86. Gauvreau, G. M. *et al.* Effects of an anti-TSLP antibody on allergen-induced asthmatic

- responses. *N. Engl. J. Med.* **370**, 2102–10 (2014).
87. de Kleer, I. M. *et al.* Perinatal Activation of the Interleukin-33 Pathway Promotes Type 2 Immunity in the Developing Lung. *Immunity* **45**, 1285–1298 (2016).
 88. Saluzzo, S. *et al.* First-Breath-Induced Type 2 Pathways Shape the Lung Immune Environment. *Cell Rep.* **18**, 1893–1905 (2017).
 89. Steer, C. A. *et al.* Group 2 innate lymphoid cell activation in the neonatal lung drives type 2 immunity and allergen sensitization. *J. Allergy Clin. Immunol.* (2017). doi:10.1016/j.jaci.2016.12.984
 90. Halim, T. Y. F. *et al.* Retinoic-acid-receptor-related orphan nuclear receptor alpha is required for natural helper cell development and allergic inflammation. *Immunity* **37**, 463–74 (2012).
 91. O’Sullivan, T. E. *et al.* Adipose-Resident Group 1 Innate Lymphoid Cells Promote Obesity-Associated Insulin Resistance. *Immunity* **45**, 428–441 (2016).
 92. Gasteiger, G., Fan, X., Dikiy, S., Lee, S. Y. & Rudensky, A. Y. Tissue residency of innate lymphoid cells in lymphoid and nonlymphoid organs. *Science* **350**, 981–5 (2015).
 93. Roediger, B. *et al.* Cutaneous immunosurveillance and regulation of inflammation by group 2 innate lymphoid cells. *Nat. Immunol.* **14**, 564–73 (2013).
 94. Paclik, D., Stehle, C., Lahmann, A., Hutloff, A. & Romagnani, C. ICOS regulates the pool of group 2 innate lymphoid cells under homeostatic and inflammatory conditions in mice. *Eur. J. Immunol.* **45**, 2766–2772 (2015).
 95. Maazi, H. *et al.* ICOS:ICOS-Ligand Interaction Is Required for Type 2 Innate Lymphoid Cell Function, Homeostasis, and Induction of Airway Hyperreactivity. *Immunity* **42**, 538–551 (2015).
 96. Monticelli, L. A. *et al.* Arginase 1 is an innate lymphoid-cell-intrinsic metabolic checkpoint controlling type 2 inflammation. *Nat. Immunol.* **17**, 656–65 (2016).
 97. Wilhelm, C. *et al.* Critical role of fatty acid metabolism in ILC2-mediated barrier protection during malnutrition and helminth infection. *J. Exp. Med.* **213**, 1409–1418 (2016).
 98. Kim, M. H., Taparowsky, E. J. & Kim, C. H. Retinoic Acid Differentially Regulates the Migration of Innate Lymphoid Cell Subsets to the Gut. *Immunity* **43**, 107–119 (2015).
 99. Mackley, E. C. *et al.* CCR7-dependent trafficking of ROR γ ⁺ ILCs creates a unique microenvironment within mucosal draining lymph nodes. *Nat. Commun.* **6**, 5862 (2015).
 100. Wojno, E. D. T. *et al.* The prostaglandin D₂ receptor CRTH2 regulates accumulation of group 2 innate lymphoid cells in the inflamed lung. *Mucosal Immunol.* **8**, 1313–23 (2015).
 101. Karta, M. R. *et al.* β 2 Integrins Rather than β 1 Integrins Mediate Alternaria -induced ILC2 Trafficking to the Lung. *J. Allergy Clin. Immunol.* (2017). doi:10.1016/j.jaci.2017.03.010
 102. Bartemes, K. R. *et al.* IL-33-responsive lineage- CD25⁺ CD44(hi) lymphoid cells mediate innate type 2 immunity and allergic inflammation in the lungs. *J. Immunol.* **188**, 1503–13

- (2012).
103. Klein Wolterink, R. G. J. *et al.* Pulmonary innate lymphoid cells are major producers of IL-5 and IL-13 in murine models of allergic asthma. *Eur. J. Immunol.* **42**, 1106–16 (2012).
 104. Imai, Y. *et al.* Skin-specific expression of IL-33 activates group 2 innate lymphoid cells and elicits atopic dermatitis-like inflammation in mice. *Proc. Natl. Acad. Sci. U. S. A.* **110**, 13921–6 (2013).
 105. Saravia, J. *et al.* Respiratory Syncytial Virus Disease Is Mediated by Age-Variable IL-33. *PLoS Pathog.* **11**, e1005217 (2015).
 106. Spooner, C. J. *et al.* Specification of type 2 innate lymphocytes by the transcriptional determinant Gfi1. *Nat. Immunol.* **14**, 1229–36 (2013).
 107. Camelo, A. *et al.* IL-33, IL-25, and TSLP induce a distinct phenotypic and activation profile in human type 2 innate lymphoid cells. *Blood Adv.* **1**, (2017).
 108. Liu, S. *et al.* Steroid resistance of airway type 2 innate lymphoid cells from patients with severe asthma: The role of thymic stromal lymphopoietin. *J. Allergy Clin. Immunol.* (2017). doi:10.1016/j.jaci.2017.03.032
 109. Kabata, H. *et al.* Thymic stromal lymphopoietin induces corticosteroid resistance in natural helper cells during airway inflammation. *Nat. Commun.* **4**, 2675 (2013).
 110. Castanhinha, S. *et al.* Pediatric severe asthma with fungal sensitization is mediated by steroid-resistant IL-33. *J. Allergy Clin. Immunol.* **136**, 312–322.e7 (2015).
 111. Morikawa, T. *et al.* Activation of group 2 innate lymphoid cells exacerbates and confers corticosteroid-resistance to mouse nasal type 2 inflammation. *Int. Immunol.* (2017). doi:10.1093/intimm/dxx030
 112. KleinJan, A. *et al.* Enforced expression of Gata3 in T cells and group 2 innate lymphoid cells increases susceptibility to allergic airway inflammation in mice. *J. Immunol.* **192**, 1385–94 (2014).
 113. Verhoef, P. A. *et al.* Intrinsic functional defects of type 2 innate lymphoid cells impair innate allergic inflammation in promyelocytic leukemia zinc finger (PLZF)?deficient mice. *J. Allergy Clin. Immunol.* **137**, 591–600.e1 (2016).
 114. Johansson, K., Malmhäll, C., Ramos-Ramírez, P. & Rådinger, M. MicroRNA-155 is a critical regulator of type 2 innate lymphoid cells and IL-33 signaling in experimental models of allergic airway inflammation. *J. Allergy Clin. Immunol.* **139**, 1007–1016.e9 (2017).
 115. Halim, T. Y. F. *et al.* Group 2 Innate Lymphoid Cells Are Critical for the Initiation of Adaptive T Helper 2 Cell-Mediated Allergic Lung Inflammation. *Immunity* **40**, 425–435 (2014).
 116. Halim, T. Y. F. *et al.* Group 2 Innate Lymphoid Cells Are Critical for the Initiation of Adaptive T Helper 2 Cell-Mediated Allergic Lung Inflammation. *Immunity* **40**, 425–35 (2014).
 117. Halim, T. Y. F. *et al.* Group 2 innate lymphoid cells license dendritic cells to potentiate memory TH2 cell responses. *Nat. Immunol.* **17**, 57–64 (2015).

118. Drake, L. Y., Iijima, K. & Kita, H. Group 2 innate lymphoid cells and CD4⁺ T cells cooperate to mediate type 2 immune response in mice. *Allergy* **69**, 1300–1307 (2014).
119. Lee, J.-B. *et al.* IL-25 and CD4⁺ T H 2 cells enhance type 2 innate lymphoid cell–derived IL-13 production, which promotes IgE-mediated experimental food allergy. *J. Allergy Clin. Immunol.* **137**, 1216–1225.e5 (2016).
120. Feldman, S. *et al.* Chronic airway inflammation provides a unique environment for B cell activation and antibody production. *Clin. Exp. Allergy* **47**, 457–466 (2017).
121. Drake, L. Y., Iijima, K., Bartemes, K. & Kita, H. Group 2 Innate Lymphoid Cells Promote an Early Antibody Response to a Respiratory Antigen in Mice. *J. Immunol.* **197**, 1335–1342 (2016).
122. Maggi, L. *et al.* Human circulating group 2 innate lymphoid cells can express CD154 and promote IgE production. *J. Allergy Clin. Immunol.* **139**, 964–976.e4 (2017).
123. Kim, B. S. *et al.* Basophils Promote Innate Lymphoid Cell Responses in Inflamed Skin. *J. Immunol.* **193**, 3717–3725 (2014).
124. Chang, Y.-J. *et al.* Innate lymphoid cells mediate influenza-induced airway hyper-reactivity independently of adaptive immunity. *Nat. Immunol.* **12**, 631–8 (2011).
125. Gorski, S. A., Hahn, Y. S. & Braciale, T. J. Group 2 innate lymphoid cell production of IL-5 is regulated by NKT cells during influenza virus infection. *PLoS Pathog.* **9**, e1003615 (2013).
126. Hong, J. Y. *et al.* Neonatal rhinovirus induces mucous metaplasia and airways hyperresponsiveness through IL-25 and type 2 innate lymphoid cells. *J. Allergy Clin. Immunol.* (2014). doi:10.1016/j.jaci.2014.04.020
127. Beale, J. *et al.* Rhinovirus-induced IL-25 in asthma exacerbation drives type 2 immunity and allergic pulmonary inflammation. *Sci. Transl. Med.* **6**, 256ra134 (2014).
128. Bartemes, K. R., Kephart, G. M., Fox, S. J. & Kita, H. Enhanced innate type 2 immune response in peripheral blood from patients with asthma. *J. Allergy Clin. Immunol.* **134**, 671–678.e4 (2014).
129. Liu, T. *et al.* Type 2 innate lymphoid cells: A novel biomarker of eosinophilic airway inflammation in patients with mild to moderate asthma. *Respir. Med.* **109**, 1391–1396 (2015).
130. Smith, S. G. *et al.* Increased numbers of activated group 2 innate lymphoid cells in the airways of patients with severe asthma and persistent airway eosinophilia. *J. Allergy Clin. Immunol.* **137**, 75–86.e8 (2016).
131. Christianson, C. A. *et al.* Persistence of asthma requires multiple feedback circuits involving type 2 innate lymphoid cells and IL-33. *J. Allergy Clin. Immunol.* **136**, 59–68.e14 (2015).
132. Nagakumar, P. *et al.* Type 2 innate lymphoid cells in induced sputum from children with severe asthma. *J. Allergy Clin. Immunol.* **137**, 624–626.e6 (2016).
133. Chen, R. *et al.* Allergen-induced Increases in Sputum Levels of Group 2 Innate Lymphoid Cells in Asthmatic Subjects. *Am. J. Respir. Crit. Care Med.* rccm.201612-2427OC (2017).

doi:10.1164/rccm.201612-2427OC

134. Jia, Y. *et al.* IL-13⁺ Type 2 Innate Lymphoid Cells Correlate with Asthma Control Status and Treatment Response. *Am. J. Respir. Cell Mol. Biol.* **55**, 675–683 (2016).
135. Doherty, T. A. *et al.* Allergen challenge in allergic rhinitis rapidly induces increased peripheral blood type 2 innate lymphoid cells that express CD84. *J. Allergy Clin. Immunol.* **133**, 1203–1205.e7 (2014).
136. Dhariwal, J. *et al.* Mucosal Type 2 Innate Lymphoid Cells are a Key Component of the Allergic Response to Aeroallergen. *Am. J. Respir. Crit. Care Med.* rccm.201609-1846OC (2017). doi:10.1164/rccm.201609-1846OC
137. Fan, D. *et al.* Allergen-Dependent Differences in ILC2s Frequencies in Patients With Allergic Rhinitis. *Allergy. Asthma Immunol. Res.* **8**, 216 (2016).
138. Lao-Araya, M., Steveling, E., Scadding, G. W., Durham, S. R. & Shamji, M. H. Seasonal increases in peripheral innate lymphoid type 2 cells are inhibited by subcutaneous grass pollen immunotherapy. *J. Allergy Clin. Immunol.* **134**, 1193–1195.e4 (2014).
139. Mjösberg, J. M. *et al.* Human IL-25- and IL-33-responsive type 2 innate lymphoid cells are defined by expression of CRTH2 and CD161. *Nat. Immunol.* **12**, 1055–62 (2011).
140. Bal, S. M. *et al.* IL-1 β , IL-4 and IL-12 control the fate of group 2 innate lymphoid cells in human airway inflammation in the lungs. *Nat. Immunol.* **17**, 636–645 (2016).
141. Miljkovic, D. *et al.* Association between Group 2 Innate Lymphoid Cells enrichment, nasal polyps and allergy in Chronic Rhinosinusitis. *Allergy* **69**, 1154–1161 (2014).
142. Ho, J. *et al.* Group 2 innate lymphoid cells (ILC2s) are increased in chronic rhinosinusitis with nasal polyps or eosinophilia. *Clin. Exp. Allergy* **45**, 394–403 (2015).
143. Poposki, J. A. *et al.* Group 2 innate lymphoid cells are elevated and activated in chronic rhinosinusitis with nasal polyps. *Immunity, Inflamm. Dis.* (2017). doi:10.1002/iid3.161
144. Shaw, J. L. *et al.* IL-33-Responsive Innate Lymphoid Cells Are an Important Source of IL-13 in Chronic Rhinosinusitis with Nasal Polyps. *Am. J. Respir. Crit. Care Med.* **188**, 432–439 (2013).
145. Walford, H. H. *et al.* Increased ILC2s in the eosinophilic nasal polyp endotype are associated with corticosteroid responsiveness. *Clin. Immunol.* **155**, 126–135 (2014).
146. Brügger, M.-C. *et al.* In Situ Mapping of Innate Lymphoid Cells in Human Skin: Evidence for Remarkable Differences between Normal and Inflamed Skin. *J. Invest. Dermatol.* **136**, 2396–2405 (2016).
147. Eastman, J. J. *et al.* Group 2 innate lymphoid cells are recruited to the nasal mucosa in patients with aspirin-exacerbated respiratory disease. *J. Allergy Clin. Immunol.* (2017). doi:10.1016/j.jaci.2016.11.023
148. Doherty, T. A. *et al.* Group 2 innate lymphocytes (ILC2) are enriched in active eosinophilic esophagitis. *J. Allergy Clin. Immunol.* **136**, 792–794.e3 (2015).
149. Kwon, B.-I. *et al.* Innate Type 2 Immunity Is Associated with Eosinophilic Pleural Effusion in Primary Spontaneous Pneumothorax. *Am. J. Respir. Crit. Care Med.* **188**, 577–585 (2013).

150. Constantinides, M. G. *et al.* PLZF expression maps the early stages of ILC1 lineage development. *Proc. Natl. Acad. Sci.* **112**, 5123–5128 (2015).
151. Fuchs, A. *et al.* Intraepithelial Type 1 Innate Lymphoid Cells Are a Unique Subset of IL-12- and IL-15-Responsive IFN- γ -Producing Cells. *Immunity* **38**, 769–781 (2013).
152. Robinette, M. L. *et al.* Transcriptional programs define molecular characteristics of innate lymphoid cell classes and subsets. *Nat. Immunol.* **16**, 306–17 (2015).
153. Yang, Z., Tang, T., Wei, X., Yang, S. & Tian, Z. Type 1 innate lymphoid cells contribute to the pathogenesis of chronic hepatitis B. *Innate Immun.* **21**, 665–673 (2015).
154. Kramer, B. *et al.* Compartment-specific distribution of human intestinal innate lymphoid cells is altered in HIV patients under effective therapy. *PLOS Pathog.* **13**, e1006373 (2017).
155. Bernink, J. H. *et al.* Human type 1 innate lymphoid cells accumulate in inflamed mucosal tissues. *Nat. Immunol.* **14**, 221–229 (2013).
156. Di Liberto, D. *et al.* Predominance of Type 1 Innate Lymphoid Cells in the Rectal Mucosa of Patients With Non-Celiac Wheat Sensitivity: Reversal After a Wheat-Free Diet. *Clin. Transl. Gastroenterol.* **7**, e178 (2016).
157. Graves, C. L. *et al.* Intestinal Epithelial Cell Regulation of Adaptive Immune Dysfunction in Human Type 1 Diabetes. *Front. Immunol.* **7**, 679 (2017).
158. Rodríguez-Carrio, J. *et al.* Brief Report: Altered Innate Lymphoid Cell Subsets in Human Lymph Node Biopsy Specimens Obtained During the At-Risk and Earliest Phases of Rheumatoid Arthritis. *Arthritis Rheumatol.* **69**, 70–76 (2017).
159. Vacca, P. *et al.* Identification of diverse innate lymphoid cells in human decidua. *Mucosal Immunol.* **8**, 254–264 (2015).
160. Silver, J. S. *et al.* Inflammatory triggers associated with exacerbations of COPD orchestrate plasticity of group 2 innate lymphoid cells in the lungs. *Nat. Immunol.* **17**, 626–635 (2016).
161. Abt, M. C. *et al.* Innate Immune Defenses Mediated by Two ILC Subsets Are Critical for Protection against Acute *Clostridium difficile* Infection. *Cell Host Microbe* **18**, 27–37 (2015).
162. Ebihara, T. *et al.* Runx3 specifies lineage commitment of innate lymphoid cells. *Nat. Immunol.* **16**, 1124–1133 (2015).
163. Satoh-Takayama, N. *et al.* Microbial Flora Drives Interleukin 22 Production in Intestinal NKp46+ Cells that Provide Innate Mucosal Immune Defense. *Immunity* **29**, 958–970 (2008).
164. Buonocore, S. *et al.* Innate lymphoid cells drive interleukin-23-dependent innate intestinal pathology. *Nature* **464**, 1371–1375 (2010).
165. Round, J. L. & Mazmanian, S. K. The gut microbiota shapes intestinal immune responses during health and disease. *Nat. Rev. Immunol.* **9**, 313–23 (2009).
166. Mortha, A. *et al.* Microbiota-dependent crosstalk between macrophages and ILC3 promotes intestinal homeostasis. *Science* **343**, 1249288 (2014).

167. Hepworth, M. R. *et al.* Innate lymphoid cells regulate CD4⁺ T-cell responses to intestinal commensal bacteria. *Nature* **498**, 113–117 (2013).
168. Hepworth, M. R. *et al.* Group 3 innate lymphoid cells mediate intestinal selection of commensal bacteria-specific CD4⁺ T cells. *Science* (80-.). **348**, 1031–1035 (2015).
169. von Burg, N. *et al.* Activated group 3 innate lymphoid cells promote T-cell-mediated immune responses. *Proc. Natl. Acad. Sci.* **111**, 12835–12840 (2014).
170. Dudakov, J. A., Hanash, A. M. & van den Brink, M. R. M. Interleukin-22: Immunobiology and Pathology. *Annu. Rev. Immunol.* **33**, 747–785 (2015).
171. Sonnenberg, G. F., Fouser, L. A. & Artis, D. Border patrol: regulation of immunity, inflammation and tissue homeostasis at barrier surfaces by IL-22. *Nat. Immunol.* **12**, 383–390 (2011).
172. Giacomini, P. R. *et al.* Epithelial-intrinsic IKK α expression regulates group 3 innate lymphoid cell responses and antibacterial immunity. *J. Exp. Med.* **212**, 1513–28 (2015).
173. Sanos, S. L. *et al.* ROR γ t and commensal microflora are required for the differentiation of mucosal interleukin 22–producing NKp46⁺ cells. *Nat. Immunol.* **10**, 83–91 (2009).
174. Zheng, Y. *et al.* Interleukin-22 mediates early host defense against attaching and effacing bacterial pathogens. *Nat. Med.* **14**, 282–9 (2008).
175. Aparicio-Domingo, P. *et al.* Type 3 innate lymphoid cells maintain intestinal epithelial stem cells after tissue damage. *J. Exp. Med.* **212**, 1783–91 (2015).
176. Li, Z. *et al.* Epidermal Notch1 recruits ROR γ ⁺ group 3 innate lymphoid cells to orchestrate normal skin repair. *Nat. Commun.* **7**, 11394 (2016).
177. Kim, H. Y. *et al.* Interleukin-17–producing innate lymphoid cells and the NLRP3 inflammasome facilitate obesity-associated airway hyperreactivity. *Nat. Med.* **20**, 54–61 (2013).
178. Geremia, A. *et al.* IL-23-responsive innate lymphoid cells are increased in inflammatory bowel disease. *J. Exp. Med.* **208**, 1127–33 (2011).
179. Bernink, J. H. *et al.* Interleukin-12 and -23 Control Plasticity of CD127⁺ Group 1 and Group 3 Innate Lymphoid Cells in the Intestinal Lamina Propria. *Immunity* **43**, 146–160 (2015).
180. Leader, S. & Kohlhasse, K. Respiratory syncytial virus-coded pediatric hospitalizations, 1997 to 1999. *Pediatr. Infect. Dis. J.* **21**, 629–32 (2002).
181. Reassessment of the indications for ribavirin therapy in respiratory syncytial virus infections. American Academy of Pediatrics Committee on Infectious Diseases. *Pediatrics* **97**, 137–40 (1996).
182. Klassen, T. P. *et al.* Dexamethasone in salbutamol-treated inpatients with acute bronchiolitis: a randomized, controlled trial. *J. Pediatr.* **130**, 191–6 (1997).
183. Plint, A. C. *et al.* Epinephrine and dexamethasone in children with bronchiolitis. *N. Engl. J. Med.* **360**, 2079–89 (2009).
184. Corneli, H. M. *et al.* A multicenter, randomized, controlled trial of dexamethasone for

- bronchiolitis. *N. Engl. J. Med.* **357**, 331–9 (2007).
185. The IMPact-RSV Study Group. Palivizumab, a humanized respiratory syncytial virus monoclonal antibody, reduces hospitalization from respiratory syncytial virus infection in high-risk infants. *Pediatrics* **102**, 531–7 (1998).
 186. Feltes, T. F. *et al.* Palivizumab prophylaxis reduces hospitalization due to respiratory syncytial virus in young children with hemodynamically significant congenital heart disease. *J. Pediatr.* **143**, 532–40 (2003).
 187. Committee on Infectious Diseases and Bronchiolitis Guidelines Committee. Updated guidance for palivizumab prophylaxis among infants and young children at increased risk of hospitalization for respiratory syncytial virus infection. *Pediatrics* **134**, e620-38 (2014).
 188. Johnson, J. E., Gonzales, R. A., Olson, S. J., Wright, P. F. & Graham, B. S. *The histopathology of fatal untreated human respiratory syncytial virus infection. Modern pathology an official journal of the United States and Canadian Academy of Pathology Inc* **20**, 108–119 (2007).
 189. Cohn, L., Homer, R. J., Marinov, A., Rankin, J. & Bottomly, K. Induction of airway mucus production By T helper 2 (Th2) cells: a critical role for interleukin 4 in cell recruitment but not mucus production. *J. Exp. Med.* **186**, 1737–47 (1997).
 190. Zhu, Z. *et al.* Pulmonary expression of interleukin-13 causes inflammation, mucus hypersecretion, subepithelial fibrosis, physiologic abnormalities, and eotaxin production. *J. Clin. Invest.* **103**, 779–788 (1999).
 191. Turner, J.-E. *et al.* IL-9-mediated survival of type 2 innate lymphoid cells promotes damage control in helminth-induced lung inflammation. *J. Exp. Med.* (2013). doi:10.1084/jem.20130071
 192. Barlow, J. L. *et al.* Innate IL-13-producing nuocytes arise during allergic lung inflammation and contribute to airways hyperreactivity. *J. Allergy Clin. Immunol.* **129**, 191-8–4 (2012).
 193. Doherty, T. A. *et al.* STAT6 regulates natural helper cell proliferation during lung inflammation initiated by *Alternaria*. *Am. J. Physiol. Lung Cell. Mol. Physiol.* **303**, L577-88 (2012).
 194. Jackson, D. J. *et al.* IL-33-Dependent Type 2 Inflammation during Rhinovirus-induced Asthma Exacerbations In Vivo. *Am. J. Respir. Crit. Care Med.* **190**, 1373–82 (2014).
 195. Stokes, K. L. *et al.* Differential pathogenesis of respiratory syncytial virus clinical isolates in BALB/c mice. *J. Virol.* **85**, 5782–93 (2011).
 196. Larkin, E. K. *et al.* Objectives, design and enrollment results from the Infant Susceptibility to Pulmonary Infections and Asthma Following RSV Exposure Study (INSPIRE). *BMC Pulm. Med.* **15**, 45 (2015).
 197. Graham, B. S., Perkins, M. D., Wright, P. F. & Karzon, D. T. Primary respiratory syncytial virus infection in mice. *J. Med. Virol.* **26**, 153–62 (1988).
 198. Zhou, B. *et al.* Thymic stromal lymphopoietin as a key initiator of allergic airway inflammation in mice. *Nat. Immunol.* **6**, 1047–53 (2005).

199. Carpino, N. *et al.* Absence of an essential role for thymic stromal lymphopoietin receptor in murine B-cell development. *Mol. Cell. Biol.* **24**, 2584–92 (2004).
200. Sokol, C. L., Barton, G. M., Farr, A. G. & Medzhitov, R. A mechanism for the initiation of allergen-induced T helper type 2 responses. *Nat. Immunol.* **9**, 310–8 (2008).
201. Mosconi, I. *et al.* Intestinal bacteria induce TSLP to promote mutualistic T-cell responses. *Mucosal Immunol.* **6**, 1157–67 (2013).
202. Cahenzli, J., Köller, Y., Wyss, M., Geuking, M. B. & McCoy, K. D. Intestinal microbial diversity during early-life colonization shapes long-term IgE levels. *Cell Host Microbe* **14**, 559–70 (2013).
203. Peebles, R. S., Sheller, J. R., Johnson, J. E., Mitchell, D. B. & Graham, B. S. Respiratory syncytial virus infection prolongs methacholine-induced airway hyperresponsiveness in ovalbumin-sensitized mice. *J. Med. Virol.* **57**, 186–92 (1999).
204. Peebles, R. S. *et al.* Respiratory syncytial virus infection does not increase allergen-induced type 2 cytokine production, yet increases airway hyperresponsiveness in mice. *J. Med. Virol.* **63**, 178–88 (2001).
205. Tripp, R. A., Moore, D. & Anderson, L. J. TH(1)- and TH(2)-TYPE cytokine expression by activated T lymphocytes from the lung and spleen during the inflammatory response to respiratory syncytial virus. *Cytokine* **12**, 801–7 (2000).
206. Molofsky, A. B. *et al.* Innate lymphoid type 2 cells sustain visceral adipose tissue eosinophils and alternatively activated macrophages. *J. Exp. Med.* **210**, 535–49 (2013).
207. Lee, H.-C. *et al.* Thymic stromal lymphopoietin is induced by respiratory syncytial virus-infected airway epithelial cells and promotes a type 2 response to infection. *J. Allergy Clin. Immunol.* **130**, 1187–1196.e5 (2012).
208. Han, J. *et al.* Responsiveness to respiratory syncytial virus in neonates is mediated through thymic stromal lymphopoietin and OX40 ligand. *J. Allergy Clin. Immunol.* **130**, 1175–1186.e9 (2012).
209. Petersen, B. C., Dolgachev, V., Rasky, A. & Lukacs, N. W. IL-17E (IL-25) and IL-17RB promote respiratory syncytial virus-induced pulmonary disease. *J. Leukoc. Biol.* **95**, 809–815 (2014).
210. Soumelis, V. *et al.* Human epithelial cells trigger dendritic cell mediated allergic inflammation by producing TSLP. *Nat. Immunol.* **3**, 673–80 (2002).
211. Liu, Y.-J. *et al.* TSLP: an epithelial cell cytokine that regulates T cell differentiation by conditioning dendritic cell maturation. *Annu. Rev. Immunol.* **25**, 193–219 (2007).
212. Mohapatra, A. *et al.* Group 2 innate lymphoid cells utilize the IRF4-IL-9 module to coordinate epithelial cell maintenance of lung homeostasis. *Mucosal Immunol.* (2015). doi:10.1038/mi.2015.59
213. Kim, H. Y. *et al.* Innate lymphoid cells responding to IL-33 mediate airway hyperreactivity independently of adaptive immunity. *J. Allergy Clin. Immunol.* **129**, 216–27–6 (2012).
214. Shiraki, Y., Ishibashi, Y., Hiruma, M., Nishikawa, A. & Ikeda, S. Cytokine secretion

- profiles of human keratinocytes during *Trichophyton tonsurans* and *Arthroderma benhamiae* infections. *J. Med. Microbiol.* **55**, 1175–85 (2006).
215. Doherty, T. A. *et al.* Lung type 2 innate lymphoid cells express cysteinyl leukotriene receptor 1, which regulates TH2 cytokine production. *J. Allergy Clin. Immunol.* **132**, 205–13 (2013).
 216. Collins, P. L. & Graham, B. S. Viral and host factors in human respiratory syncytial virus pathogenesis. *J. Virol.* **82**, 2040–55 (2008).
 217. Carroll, K. N. & Hartert, T. V. The impact of respiratory viral infection on wheezing illnesses and asthma exacerbations. *Immunol. Allergy Clin. North Am.* **28**, 539–61, viii (2008).
 218. Wierenga, E. A. *et al.* Evidence for compartmentalization of functional subsets of CD2+ T lymphocytes in atopic patients. *J. Immunol.* **144**, 4651–6 (1990).
 219. Robinson, D. S. *et al.* Predominant TH2-like bronchoalveolar T-lymphocyte population in atopic asthma. *N. Engl. J. Med.* **326**, 298–304 (1992).
 220. Walker, C. *et al.* Allergic and nonallergic asthmatics have distinct patterns of T-cell activation and cytokine production in peripheral blood and bronchoalveolar lavage. *Am. Rev. Respir. Dis.* **146**, 109–15 (1992).
 221. Kato, A., Favoreto, S., Avila, P. C. & Schleimer, R. P. TLR3- and Th2 cytokine-dependent production of thymic stromal lymphopoietin in human airway epithelial cells. *J. Immunol.* **179**, 1080–7 (2007).
 222. Kouzaki, H., O’Grady, S. M., Lawrence, C. B. & Kita, H. Proteases induce production of thymic stromal lymphopoietin by airway epithelial cells through protease-activated receptor-2. *J. Immunol.* **183**, 1427–34 (2009).
 223. Sonnenberg, G. F. & Artis, D. Innate lymphoid cells in the initiation, regulation and resolution of inflammation. *Nat. Med.* **21**, 698–708 (2015).
 224. Chen, J., Waddell, A., Lin, Y.-D. & Cantorna, M. T. Dysbiosis caused by vitamin D receptor deficiency confers colonization resistance to *Citrobacter rodentium* through modulation of innate lymphoid cells. *Mucosal Immunol.* **8**, 618–26 (2015).
 225. Stier, M. T. *et al.* Respiratory syncytial virus infection activates IL-13-producing group 2 innate lymphoid cells through thymic stromal lymphopoietin. *J. Allergy Clin. Immunol.* **138**, 814–824.e11 (2016).
 226. Alwan, W. H., Kozłowska, W. J. & Openshaw, P. J. Distinct types of lung disease caused by functional subsets of antiviral T cells. *J. Exp. Med.* **179**, 81–9 (1994).
 227. Graham, M. B., Braciale, V. L. & Braciale, T. J. Influenza virus-specific CD4+ T helper type 2 T lymphocytes do not promote recovery from experimental virus infection. *J. Exp. Med.* **180**, 1273–82 (1994).
 228. Maloy, K. J. *et al.* CD4(+) T cell subsets during virus infection. Protective capacity depends on effector cytokine secretion and on migratory capability. *J. Exp. Med.* **191**, 2159–70 (2000).
 229. Lu, X. *et al.* Galectin-9 ameliorates respiratory syncytial virus-induced pulmonary

- immunopathology through regulating the balance between Th17 and regulatory T cells. *Virus Res.* **195**, 162–71 (2015).
230. Kulcsar, K. A., Baxter, V. K., Greene, I. P. & Griffin, D. E. Interleukin 10 modulation of pathogenic Th17 cells during fatal alphavirus encephalomyelitis. *Proc. Natl. Acad. Sci. U. S. A.* **111**, 16053–8 (2014).
231. Gil-Cruz, C. *et al.* Fibroblastic reticular cells regulate intestinal inflammation via IL-15-mediated control of group 1 ILCs. *Nat. Immunol.* **17**, 1388–1396 (2016).
232. Biron, C. A., Nguyen, K. B., Pien, G. C., Cousens, L. P. & Salazar-Mather, T. P. NATURAL KILLER CELLS IN ANTIVIRAL DEFENSE: Function and Regulation by Innate Cytokines. *Annu. Rev. Immunol.* **17**, 189–220 (1999).
233. de Weerd, N. A. & Nguyen, T. The interferons and their receptors--distribution and regulation. *Immunol. Cell Biol.* **90**, 483–91 (2012).
234. Parronchi, P. *et al.* IL-4 and IFN (alpha and gamma) exert opposite regulatory effects on the development of cytolytic potential by Th1 or Th2 human T cell clones. *J. Immunol.* **149**, 2977–83 (1992).
235. Brinkmann, V., Geiger, T., Alkan, S. & Heusser, C. H. Interferon alpha increases the frequency of interferon gamma-producing human CD4+ T cells. *J. Exp. Med.* **178**, 1655–63 (1993).
236. Rogge, L. *et al.* Selective expression of an interleukin-12 receptor component by human T helper 1 cells. *J. Exp. Med.* **185**, 825–31 (1997).
237. Smeltz, R. B., Chen, J., Ehrhardt, R. & Shevach, E. M. Role of IFN-gamma in Th1 differentiation: IFN-gamma regulates IL-18R alpha expression by preventing the negative effects of IL-4 and by inducing/maintaining IL-12 receptor beta 2 expression. *J. Immunol.* **168**, 6165–72 (2002).
238. Scott, P. IFN-gamma modulates the early development of Th1 and Th2 responses in a murine model of cutaneous leishmaniasis. *J. Immunol.* **147**, 3149–55 (1991).
239. Koltsida, O. *et al.* IL-28A (IFN- λ 2) modulates lung DC function to promote Th1 immune skewing and suppress allergic airway disease. *EMBO Mol. Med.* **3**, 348–61 (2011).
240. Harrington, L. E. *et al.* Interleukin 17-producing CD4+ effector T cells develop via a lineage distinct from the T helper type 1 and 2 lineages. *Nat. Immunol.* **6**, 1123–32 (2005).
241. Durbin, J. E. *et al.* The role of IFN in respiratory syncytial virus pathogenesis. *J. Immunol.* **168**, 2944–52 (2002).
242. Durbin, J. E., Hackenmiller, R., Simon, M. C. & Levy, D. E. Targeted disruption of the mouse Stat1 gene results in compromised innate immunity to viral disease. *Cell* **84**, 443–50 (1996).
243. Miller, A. L., Bowlin, T. L. & Lukacs, N. W. Respiratory syncytial virus-induced chemokine production: linking viral replication to chemokine production in vitro and in vivo. *J. Infect. Dis.* **189**, 1419–30 (2004).
244. Durbin, J. E. *et al.* The role of IFN in respiratory syncytial virus pathogenesis. *J. Immunol.* **168**, 2944–52 (2002).

245. Moore, M. L. *et al.* STAT1 negatively regulates lung basophil IL-4 expression induced by respiratory syncytial virus infection. *J. Immunol.* **183**, 2016–26 (2009).
246. Peebles, R. S. *et al.* Immune interaction between respiratory syncytial virus infection and allergen sensitization critically depends on timing of challenges. *J. Infect. Dis.* **184**, 1374–9 (2001).
247. Newcomb, D. C. *et al.* IL-17A induces signal transducers and activators of transcription-6-independent airway mucous cell metaplasia. *Am. J. Respir. Cell Mol. Biol.* **48**, 711–6 (2013).
248. Newcomb, D. C. *et al.* IL-13 regulates Th17 secretion of IL-17A in an IL-10-dependent manner. *J. Immunol.* **188**, 1027–35 (2012).
249. Moore, M. L., Chi, M. H., Goleniewska, K., Durbin, J. E. & Peebles, R. S. Differential regulation of GM1 and asialo-GM1 expression by T cells and natural killer (NK) cells in respiratory syncytial virus infection. *Viral Immunol.* **21**, 327–39 (2008).
250. Hashimoto, K. *et al.* Respiratory syncytial virus infection in the absence of STAT 1 results in airway dysfunction, airway mucus, and augmented IL-17 levels. *J. Allergy Clin. Immunol.* **116**, 550–7 (2005).
251. Johnson, T. R. *et al.* Role for innate IFNs in determining respiratory syncytial virus immunopathology. *J. Immunol.* **174**, 7234–41 (2005).
252. Han, M. *et al.* IFN- γ Blocks Development of an Asthma Phenotype in Rhinovirus-infected Baby Mice by Inhibiting ILC2s. *Am. J. Respir. Cell Mol. Biol.* (2016). doi:10.1165/rcmb.2016-0056OC
253. Molofsky, A. B. *et al.* Interleukin-33 and Interferon- γ Counter-Regulate Group 2 Innate Lymphoid Cell Activation during Immune Perturbation. *Immunity* **43**, 161–74 (2015).
254. Bi, J. *et al.* NK Cells Alleviate Lung Inflammation by Negatively Regulating Group 2 Innate Lymphoid Cells. *J. Immunol.* 1601830 (2017). doi:10.4049/jimmunol.1601830
255. Kopach, P. *et al.* IFN- Directly Controls IL-33 Protein Level through a STAT1- and LMP2-dependent Mechanism. *J. Biol. Chem.* **289**, 11829–11843 (2014).
256. Goverse, G. *et al.* Vitamin A Controls the Presence of ROR γ + Innate Lymphoid Cells and Lymphoid Tissue in the Small Intestine. *J. Immunol.* **196**, 5148–55 (2016).
257. Depner, M. *et al.* The Extended Clinical Phenotype of 26 Patients with Chronic Mucocutaneous Candidiasis due to Gain-of-Function Mutations in STAT1. *J. Clin. Immunol.* **36**, 73–84 (2016).
258. Sampaio, E. P. *et al.* Signal transducer and activator of transcription 1 (STAT1) gain-of-function mutations and disseminated coccidioidomycosis and histoplasmosis. *J. Allergy Clin. Immunol.* **131**, 1624–34 (2013).
259. Uzel, G. *et al.* Dominant gain-of-function STAT1 mutations in FOXP3 wild-type immune dysregulation-polyendocrinopathy-enteropathy-X-linked-like syndrome. *J. Allergy Clin. Immunol.* **131**, 1611–23 (2013).
260. Liu, L. *et al.* Gain-of-function human STAT1 mutations impair IL-17 immunity and underlie chronic mucocutaneous candidiasis. *J. Exp. Med.* **208**, 1635–48 (2011).

261. Toubiana, J. *et al.* Heterozygous STAT1 gain-of-function mutations underlie an unexpectedly broad clinical phenotype. *Blood* **127**, 3154–64 (2016).
262. Boisson-Dupuis, S. *et al.* Inborn errors of human STAT1: allelic heterogeneity governs the diversity of immunological and infectious phenotypes. *Curr. Opin. Immunol.* **24**, 364–378 (2012).
263. Morita, H., Moro, K. & Koyasu, S. Innate lymphoid cells in allergic and nonallergic inflammation. *J. Allergy Clin. Immunol.* **138**, 1253–1264 (2016).
264. Vély, F. *et al.* Evidence of innate lymphoid cell redundancy in humans. *Nat. Immunol.* **17**, 1291–1299 (2016).
265. Zook, E. C. & Kee, B. L. Development of innate lymphoid cells. *Nat. Immunol.* **17**, 775–782 (2016).
266. Townsend, M. J., Fallon, P. G., Matthews, D. J., Jolin, H. E. & McKenzie, A. N. T1/ST2-deficient mice demonstrate the importance of T1/ST2 in developing primary T helper cell type 2 responses. *J. Exp. Med.* **191**, 1069–76 (2000).
267. Oboki, K. *et al.* IL-33 is a crucial amplifier of innate rather than acquired immunity. *Proc. Natl. Acad. Sci. U. S. A.* **107**, 18581–6 (2010).
268. Vandesompele, J. *et al.* Accurate normalization of real-time quantitative RT-PCR data by geometric averaging of multiple internal control genes. *Genome Biol.* **3**, RESEARCH0034 (2002).
269. Ghaedi, M. *et al.* Common-Lymphoid-Progenitor-Independent Pathways of Innate and T Lymphocyte Development. *Cell Rep.* **15**, 471–480 (2016).
270. Griffith, J. W., Sokol, C. L. & Luster, A. D. Chemokines and Chemokine Receptors: Positioning Cells for Host Defense and Immunity. *Annu. Rev. Immunol.* **32**, 659–702 (2014).
271. Miller, A. M. Role of IL-33 in inflammation and disease. *J. Inflamm.* **8**, 22 (2011).
272. Salo, P. M. *et al.* Exposure to *Alternaria alternata* in US homes is associated with asthma symptoms. *J. Allergy Clin. Immunol.* **118**, 892–8 (2006).
273. Brestoff, J. R. *et al.* Group 2 innate lymphoid cells promote beiging of white adipose tissue and limit obesity. *Nature* **519**, 242–246 (2014).
274. Bonig, H., Watts, K. L., Chang, K.-H., Kiem, H.-P. & Papayannopoulou, T. Concurrent Blockade of α 4-Integrin and CXCR4 in Hematopoietic Stem/Progenitor Cell Mobilization. *Stem Cells* **27**, 836–837 (2009).
275. Petty, J. M., Lenox, C. C., Weiss, D. J., Poynter, M. E. & Suratt, B. T. Crosstalk between CXCR4/stromal derived factor-1 and VLA-4/VCAM-1 pathways regulates neutrophil retention in the bone marrow. *J. Immunol.* **182**, 604–12 (2009).
276. Kawai, T. & Malech, H. L. WHIM syndrome: congenital immune deficiency disease. *Curr. Opin. Hematol.* **16**, 20–26 (2009).
277. Chauhan, A., Singh, M., Agarwal, A. & Paul, N. Correlation of TSLP, IL-33, and CD4 + CD25 + FOXP3 + T regulatory (Treg) in pediatric asthma. *J. Asthma* **52**, 868–872 (2015).

278. Bahrami Mahneh, S. *et al.* Serum IL-33 Is Elevated in Children with Asthma and Is Associated with Disease Severity. *Int. Arch. Allergy Immunol.* **168**, 193–196 (2016).
279. Bonanno, A. *et al.* 25-Hydroxyvitamin D, IL-31, and IL-33 in Children with Allergic Disease of the Airways. *Mediators Inflamm.* **2014**, 1–10 (2014).
280. Tamagawa-Mineoka, R., Okuzawa, Y., Masuda, K. & Katoh, N. Increased serum levels of interleukin 33 in patients with atopic dermatitis. *J. Am. Acad. Dermatol.* **70**, 882–888 (2014).
281. Glück, J., Rymarczyk, B. & Rogala, B. Serum IL-33 but not ST2 level is elevated in intermittent allergic rhinitis and is a marker of the disease severity. *Inflamm. Res.* **61**, 547–550 (2012).
282. Pastorelli, L. *et al.* Epithelial-derived IL-33 and its receptor ST2 are dysregulated in ulcerative colitis and in experimental Th1/Th2 driven enteritis. *Proc. Natl. Acad. Sci. U. S. A.* **107**, 8017–22 (2010).
283. Saadah, O. I., Al-Harthi, S. E., Al-Mughales, J. A., Bin-Taleb, Y. Y. & Baeshen, R. S. Serum Interleukin-33 level in Saudi children with inflammatory bowel disease. *Int. J. Clin. Exp. Pathol.* **8**, 16000–6 (2015).
284. Mu, R. *et al.* Elevated serum interleukin 33 is associated with autoantibody production in patients with rheumatoid arthritis. *J. Rheumatol.* **37**, 2006–13 (2010).
285. Matsuyama, Y. *et al.* Increased levels of interleukin 33 in sera and synovial fluid from patients with active rheumatoid arthritis. *J. Rheumatol.* **37**, 18–25 (2010).
286. Mitsui, A. *et al.* Serum IL-33 levels are increased in patients with psoriasis. *Clin. Exp. Dermatol.* **41**, 183–189 (2016).
287. Gold, M. J. *et al.* Group 2 innate lymphoid cells facilitate sensitization to local, but not systemic, TH2-inducing allergen exposures. *J. Allergy Clin. Immunol.* **133**, 1142–1148.e5 (2014).
288. Mirchandani, A. S. *et al.* Type 2 Innate Lymphoid Cells Drive CD4+ Th2 Cell Responses. *J. Immunol.* **192**, 2442–2448 (2014).
289. Huang, Y. *et al.* IL-25-responsive, lineage-negative KLRG1(hi) cells are multipotential ‘inflammatory’ type 2 innate lymphoid cells. *Nat. Immunol.* **16**, 161–9 (2015).
290. Laffont, S. *et al.* Androgen signaling negatively controls group 2 innate lymphoid cells. *J. Exp. Med.* **214**, 1581–1592 (2017).
291. Cormier, S. A., You, D. & Honnegowda, S. The use of a neonatal mouse model to study respiratory syncytial virus infections. *Expert Rev. Anti. Infect. Ther.* **8**, 1371–1380 (2010).
292. Beura, L. K. *et al.* Normalizing the environment recapitulates adult human immune traits in laboratory mice. *Nature* **532**, 512–516 (2016).
293. Yang, X. O. *et al.* T helper 17 lineage differentiation is programmed by orphan nuclear receptors ROR alpha and ROR gamma. *Immunity* **28**, 29–39 (2008).
294. Chung, K. F. *et al.* International ERS/ATS guidelines on definition, evaluation and treatment of severe asthma. *Eur. Respir. J.* **43**, 343–373 (2014).

295. Vannella, K. M. *et al.* Combinatorial targeting of TSLP, IL-25, and IL-33 in type 2 cytokine-driven inflammation and fibrosis. *Sci. Transl. Med.* **8**, 337ra65-337ra65 (2016).
296. Choy, D. F. *et al.* TH2 and TH17 inflammatory pathways are reciprocally regulated in asthma. *Sci. Transl. Med.* **7**, 301ra129-301ra129 (2015).
297. Raundhal, M. *et al.* High IFN- γ and low SLPI mark severe asthma in mice and humans. *J. Clin. Invest.* **125**, 3037–50 (2015).
298. Zhang, Y. *et al.* PARP9-DTX3L ubiquitin ligase targets host histone H2BJ and viral 3C protease to enhance interferon signaling and control viral infection. *Nat. Immunol.* **16**, 1215–1227 (2015).
299. Burzyn, D. *et al.* A Special Population of Regulatory T Cells Potentiates Muscle Repair. *Cell* **155**, 1282–1295 (2013).
300. Zaiss, D. M. *et al.* Amphiregulin, a TH2 Cytokine Enhancing Resistance to Nematodes. *Science (80-.)*. **314**, 1746–1746 (2006).
301. Shih, H.-Y. *et al.* Developmental Acquisition of Regulomes Underlies Innate Lymphoid Cell Functionality. *Cell* **165**, 1120–1133 (2016).
302. Koues, O. *et al.* Distinct Gene Regulatory Pathways for Human Innate versus Adaptive Lymphoid Cells. *Cell* **165**, 1134–1146 (2016).